Surface Modification of Porous Graphite for Liquid Chromatography

Qian-Hong Wan

A thesis submitted in fulfilment of the requirements

for the degree of PhD

to the

University of Edinburgh

1992

Declaration

This thesis has been composed by myself and it has not been submitted in any previous application for a degree. The work reported within was executed by myself, unless otherwise stated.

October 1992

Acknowledgements

I would like to thank my supervisor, Prof. J.H. Knox for his help and encouragement throughout the last four years.

I would also like to thank the British Council and the State Education Commission of China for providing me with a studentship at the University of Edinburgh, and Shandon Scientific Ltd., for providing financial support in the third year when I was joined by my family.

The technical staff in the department were always helpful, and for that I am grateful.

Thanks to members of the chromatography group, in particular Kathleen, Masami and Madge, for their friendship and support.

Abstract

Surface modification of porous graphite has been studied in detail by liquid chromatography. The non-polar nature of the graphite provides the basis for adsorptive modification by which the graphite surface is either deactivated or functionized. While the elimination of geometric heterogeneity is achieved by adsorption of trace polyaromatic compounds, the specialist in selectivity is conferred to the graphite by a monolayer coating of modifiers. A number of strategies are used for different purposes. These include dynamic coating, insoluble coating and cross-linked coating. The chromatographic properties of the modified materials are evaluated in terms of efficiency, selectivity and stability. With the excption for cross-linked coating, the modified materials show performance better than those of the original graphite. Applications to adsorption, ion exchange, chiral and exclusion chromatography are demonstrated. These new packings are found particularly useful in the separation of inorganic anions, amino acid and hydroxy acid enantiomers. They give excellent peak symmetry and long term stability. The mechanisms of retention on the graphite based materials are characterised and discussed.

To my parents

Contents

List of Figures

List of Tables

Chapter 1

Theoretical Background

1.1 Introduction

Liquid chromatography is a type of separation method in which liquid is employed as a mobile phase. Apart from its original form known as column chromatography, several modifications have been developed over the past few decades, including planar chromatography, countercurrent chromatography, open-tubular chromatography and electrochromatography. In this thesis we confine our discussions to liquid chromatography in its original form, that is chromatography carried out in a packed column with a liquid eluent driven by gravity or pressure.

Liquid chromatography is known by a variety of names such as adsorption chromatography, ion exchange chromatography, exclusion chromatography and chiral chromatogrphy, they are used to emphasize the retention mechanism underlying the separation. Despite the difference they appear to bear, all these liquid chromatographic methods operate on the same principle, that is, separation is based on difference in the partition coefficients of solutes distributed between a stationary and a mobile phase.

This chapter is intended to provide a brief account of theoretical background

of liquid chromatography, with particular reference to the mechanisms of solute retention and the dynamics of chromatographic process. Before proceeding with these specific topics the historical development of chromatography is briefly reviewed.

1.2 History

Chromatography is a term first coined by Tswett [1, 29] in referring to the technique he invented at the turn of the century. By passing a solution through a glass column of a solid adsorbent, he succeeded in separating plant pigments into their components, which appeared as coloured zones on the column. This technique is known as classical adsorption chromatography which is largely superseded by other chromatographic techniques nowadays. Nevertheless Tswett's invention was a landmark in the history of chromatography because his method by which chromatograms are developed from narrow initial zones of mixtures to produce discrete bands of separated components, contrasts with earlier methods using continuous flow of mixtures which did not result in complete separation. Tswett is generally accredited with the first scientific investigation of the chromatographic process although some other scientists [2] in his day's had applied analogous technique to different separation problems.

Unfortunately, Tswett's work was not significantly advanced nor was the value of his invention appreciated until 1931 when the historical separation of carotene isomers was achieved by Kuhn, Winterstein and Lederer [3]. This work was followed by an enormous growth of the application of adsorption chromatography but the essential feature of the technique remained at the level Tswett had attained. Clearly there was great room for further improvement particularly in the direction of producing sharper bands of solute and increasing column efficiency.

Around twenty years later in 1952, James and Martin [4] described the first successful experiments on gas liquid chromatography and the technique was rapidly developed into a high efficiency method in the following decade. Liquid chromatography remained relatively neglected during this period, although in 1960 Hamilton et al [5] reported that column efficiency could be improved by reducing particle size in the ion exchange chromatography.

Another ten years elapsed before the potential of small particles in improving the efficiency of liquid chromatography was thoroughly established in later 1960's when the instrumental obstacles to the use of small particles were basically overcome by the work of Horvath et al [22], of Kirkland [24] and of Huber [23]. Their works marked the beginning of a new era of chromatography — high performance liquid chromagraphy(HPLC).

The principles governing the separation in HPLC are virtually the same as in the classical chromatography. However, the speed and efficiency of the separation have been improved dramatically. This is largely due to the use of microparticles as packing material and high pressure as driving force.

The idea of using small particles and high pressures in chromatography was by no means novel by that time. In fact it originated in 1941 in a paper by Martin and Synge [25]. Realising the similarity between the processes occurring in distillation and chromatography, they introduced the concept of the theoretical plate into chromatography in an effort to find a method of expressing quantitatively the efficiency of a column. In analogy to distillation column,a chromatographic column is envisaged as consisting of a number of identical volume elements within each of which equilibration of solute between a moving and stationary phase is assumed to occur. Thus the column efficiency can be expressed either in terms of the number of theoretical plates or the height equivalent to a theoretical plate (HETP), which is the thickness of a theoretical plate within the column. Using

intuitive arguments, Martin and Synge predicted that the smallest HETP should be obtainable using very small particle size and a high pressure difference along the column. It should be pointed out that the plate theory, by itself, does not provide any explicit account how the HETP might depend upon such parameters.

It was Glueckauf [20, 21, 60] who first showed how such factors as particle size, particle diffusion and diffusion in the film around the particle could be related to the HETP. Unfortunately his theory was too complex to be readily applicable and it was left to van Deemter et al [26] to develop a more practical approach.

The plate theory is acknowledged to be oversimplified as it was elaborated on a number of unrealistic assumptions such as negligible diffusion and instantaneous equilibration. In reality, a solute in a chromatographic column must spread longitudinally while the partition equilibration will not be attained instantly because of finite rate of diffusion in the stationary phase. Further spreading can arise from the variations in flow velocity across the column due to the inhomogeneity of the column packing. Taking account of these facts and combining the theorem that for a group of independent statistical processes occurring simultaneously the total variance is the sum of the individual variances while the mean is the sum of the individual means, van Deemter et al [26] were able to show how the overall HETP could be constructed from the individual contributions from longitudinal molecular diffusion, flow dispersion and the finite rate of mass transfer between two phases. Thus for the first time the relationship between HETP and various experimental parameters was established on the ground of a sound physical model and rigorous mathematical treatment.

Detailed study of the flow dispersion in chromatography led Giddings [27] to conclude that band spreading due to flow velocity inequalities is counteracted by the lateral diffusion of solute from one streamline to other, therefore the flow term and diffusion term should be coupled with respect to their effects on HETP. The

non-equilibrium theory, again initiated by Giddings [27], represented a significant advancement of our understanding of the mass transfer mechanism. Due to the thermodynamic nature of the partitioning process, the solute in the two phases tends to reach equilibrium. However, the flow of the mobile phase tends to prevent the equilibrium occurring. Therefore the departure from equilibrium caused by flow can be taken as a measure of the band spreading due to the mass transfer between the two phases. It is essential to operate a chromatographic system under near-equilibrium conditions so as to achieve high efficiency.

Up to this point the way in which particle size influences the column efficiency could be described unambiguously. Briefly, it contributes to the HETP by increasing flow inequality and diffusion length. In gas chromatography, relatively large particle size is allowable for high efficiency separation to be achieved because the diffusivity in gases is approximately 10^5 times larger than that in liquids. In 1963, Giddings [6] predicted, from his comparative study on separation efficiency limits in gas and liquid chromatography, that efficiency comparable to gas chromatography could be achieved in liquid chromatography if the particle diameter were reduced to about 1/30 of that for gas chromatography. This particle size is very close to the present values of 3-10 μm in diameter. Thus, the theoretical framework for liquid chromatography was generally completed early in the 1960's, which paved the way to the modernization of liquid chromatography.

The key to high performance separation in all forms of chromatography lies in the proper control of migration rates and band spreading. For most practical systems, the two processes can be treated almost independently, provided that the departure from equilibrium is not too great and the distribution of solutes is in linear range. The control of migration rates is related to thermodynamic equilibrium while the control of band spreading is mainly achieved by dynamic

considerations.

1.3 Solute Retention

1.3.1 Thermodynamics of Distribution

Consider the distribution of a solute, i, between a mobile phase, x, and a stationary phase, y, at constant temperature and pressure. At equilibrium the net change in free energy for transfer of solute, i, between two phases must be zero. Therefore, equation 1.1 is readily derived:

$$\Delta G^o = -RT\ln K^o \qquad (1.1)$$

where ΔG^o is the difference of the standard free energies of solute in the two phases and K^o is the thermodynamic distribution constant which is the ratio of solute activity in the stationary phase to that in the mobile phase.

In linear elution chromatography, the solute concentrations in two phases are normally very low, K^o may be approximated by the concentration distribution coefficient K_c, which is the ratio of the solute concentrations in the two phases. The free energy difference is then expressed as

$$\Delta G^o = -RT\ln K_c \qquad (1.2)$$

The temperature dependence of K_c can be derived from the standard thermodynamic relationship ($\Delta G = \Delta H - T\Delta S$), which is equivalent to the van't Hoff equation

$$\frac{d\ln K_c}{dT} = \frac{\Delta H}{RT^2} \qquad (1.3)$$

where ΔH is the enthalpy difference between two standard states or the transfer heat of solute between the two phases.

For a distribution system involving a solute which may be present in a number of different forms, a new term is introduced to take account of the influence of chemical equilibria on the overall distribution. This is the distribution ratio D, which is defined as the ratio of total solute concentration in the stationary phase C_s, to that in the mobile phase C_m, or

$$D = \frac{\sum C_s}{\sum C_m} \tag{1.4}$$

In linear chromotography the concentrations of solute species are virtually interchangeble with the activities, thus equation 1.4 can also be written as

$$D = \frac{\sum a_s}{\sum a_m} \tag{1.5}$$

1.3.2 Molecular Interactions

Distribution of a solute between two phases will be at equilibrium when the forces exerting on them by the molecules of each phase are balanced. A proper understanding of the nature of these molecular interactions is therefore essential in order to estimate the relative importance of these interactions and further to control the distribution equilibrium between the two phases.

However complex the molecular interactions involved in a given chromatographic system, the intermolecular forces operating are all from one origin – electromagnetic, arising from the charges on the electrons and nuclei of the atoms and molecules. Five types of electromagnetic interaction may be distinguished [19]:

- Repulsive forces arising from the overlap of the charge clouds in the molecules.

- Dispersion forces due to instantaneous dipoles in the molecules.

- Electrostatic forces arising from unsymmetrical charge distribution.

- Induction forces due to the influence of the electrical field exerting by neighbouring molecules.

- Coulombic forces between charged molecules(i.e. 'ions').

For a general idea on the magnitudes and features of component forces it is adequate to consider the interactions between two similar polarizable dipole molecules in the gas phase. Following Davies [7], we can write the expression for the total interaction energy between two neutral molecules, U(r), as

$$U(r) \;=\; \underbrace{\frac{b}{r^n}}_{U_{repulsive}} - \underbrace{\frac{2\mu^4}{3kTr^6}}_{U_{electrostatic}} - \underbrace{\frac{2\mu^2\alpha}{r^6}}_{U_{inductive}} - \underbrace{\frac{3I\alpha^2}{4r^6}}_{U_{dispersion}} \tag{1.6}$$

$$= \frac{b}{r^n} - \frac{1}{r^6}[\frac{2\mu^4}{3kT} + 2\mu^2\alpha + \frac{3}{4}I\alpha^2] \tag{1.7}$$

$$= \frac{b}{r^n} - \frac{C_1}{r^6} \tag{1.8}$$

In this equation the following notation is used:

b, n = Empirical factors;

r = Distance between the centres of two molecules;

μ = Dipole moment;

k = Boltzman constant;

α = Polarizability;

I = Ionization potential;

T = Absolute temperature.

Figure 1.1 shows how the total energy changes with the centre to centre intermolecular separation. When two molecules approach one another, energy of
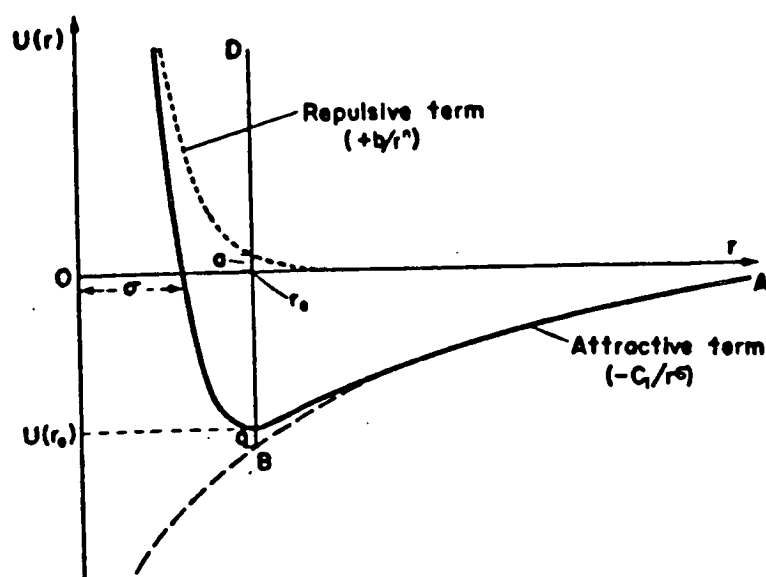
Figure 1.1. The general form of an intermolecular potential energy curve. At long range the interaction is attractive, but at close range the repulsions dominate.

attraction increases until reaching a maximum. Beyond this point, the energy of repulsion comes into play and rapidly becomes predominant.

The factors in equation 1.7 allow us to compare the component items in some typical cases. London first conducted such an evaluation of the coefficients in equation 1.7 which shows the main contribution to the total interaction energy is from the dispersion term for non-polar molecules. This is a characteristic of interactions between non-polar molecules in gas phase. In liquids or solids where molecules are at much closer distances, the random orientation which reduces the electrostatic term to dependence upon r^{-6} is less likely to be maintained, it thus can be expected that equations given above are no longer applicable to these cases unless the electrostatic term is corrected accordingly. If dipolar molecules assume fixed orientation with respect to one another, a great increase in the energy of attraction occurs since the electrostatic term in this case is characterized by the dependence upon r^{-3} instead of r^{-6} as in the gaseous state. Thus the electrostatic interaction is of the key importance and offers more interaction energy than the dispersion term.

In liquid chromatographic systems where either polar solvent or polar stationary phase are employed, some specific types of molecular interaction are frequently invoked and deserve a brief discussion. Of particular interst are hydrogen bonding, charge transfer interactions, and hydrophobic interactions.

Hydrogen bonding is largely electrostatic in origin. In a proton-donor group like $O - H$, the H atom being small in size permits a proton-acceptor to approach closely to it, leading to a smaller value of r and a larger interaction energy (see equation 1.6).

Charge transfer process can be thought of as partial transfer of an electron originally located on a 'donor' molecule to an 'acceptor' molecule. It is obvious that charge transfer energy is an effect of major importance when a molecule

with a low ionization potential interacts with one having a high electron affinity. The formation of copper complex with amines is a good example of such kind of interaction.

Hydrophobic interaction has been invoked to explain the very strong attractive interactions between non-polar molecules in water. It arises from the net changes in energy and entropy required to disrupt the local water structure when two hydrophobic species approach one another. The hydrophobic interaction energy is about one order of magnitude larger than the dispersion energy for non-aqueous systems.

Molecular interactions in the liquid chromatographic system are highly cooperative, a number of interactions between solute-solvent, solute-surface, solvent-surface, solvent-solvent can be attributed to a single solute molecule. Owing to the complex nature of interactions, it is not yet possible to calculate the total energy for any pratical systems at present. However, the analysis of relatively important interactions involved in a given system will help to identify the main factors controlling the distribution equilibrium.

1.3.3 Band Migration

The prerequisite for components to separate is that they have different migration rates in a given chromatographic system. The component molecules travel along the column only at a fraction, R, of the mobile phase velocity because of the partition of the individual components into the stationary phase. Using a statistical argument, R may be expressed as a fraction of the solute in the mobile phase at equilibrium, that is

$$R = \frac{q_m}{q_m + q_s} \tag{1.9}$$

where q is the quantity of solute, and subscripts m and s denote the mobile and stationary phase respectively.

Alternatively, equation 1.9 can be written in terms of time spent in the two phases, as

$$R = \frac{t_m}{t_m + t_s} \tag{1.10}$$

Since the phase capacity ratio k' is defined as the ratio of the solute in the stationary phase to that in the mobile phase, it follows

$$k' = \frac{q_s}{q_m} \tag{1.11}$$
$$= \frac{t_s}{t_m} \tag{1.12}$$

k' is related to R through the relationship

$$R = \frac{1}{1 + k'} \tag{1.13}$$

In referring to the condition of the linear distribution isotherm, k' can be related to the distribution coefficient K_c as follows,

$$k' = \frac{q_s}{q_m} \tag{1.14}$$
$$= \frac{C_s V_s}{C_m V_m} \tag{1.15}$$
$$= K_c \frac{V_s}{V_m} \tag{1.16}$$
$$= K_c \phi \tag{1.17}$$

The quotient V_s/V_m, denoted by ϕ, is often referred to as phase ratio.

As will be shown later, in handling slow equilibration in the mobile phase, it is necessary to distinguish the mobile phase in the stagnant state from that in the flowing state. The mobile zone is the flowing mobile phase while the stationary zone is composed of everything else in the column, including the stationary phase

and the stagnant eluent held in and between the particles. Accordingly, a zone capacity ratio k'' is introduced, which is related to the phase capacity ratio by the geometrical relationship

$$k'' = \frac{k' + \varphi}{1 - \varphi} \tag{1.18}$$

where φ is the fraction of the mobile phase which is stagnant.

1.4 Band Spreading

1.4.1 Transport Phenomena

Band spreading arises from a number of basic phenomena including flow, slow equilibration and axial diffusion. The process of molecular diffusion is a key component of the last two. Accordingly some elemental knowledge of diffusion and flow is therefore essential in order to understand the theories of band spreading in chromatography.

Consider the diffusion of solute in a liquid which is static. The concentraton profile due to diffusion may be obtained by solving an equation derived from the Fick's second law. If only one dimension (z) is concerned, as is often the case in chromatography, the equation can be written as

$$\frac{\partial c}{\partial t} = D\frac{\partial^2 c}{\partial z^2} \tag{1.19}$$

where D is the effective diffusion coefficient and $\frac{\partial c}{\partial z}$ is the concentration gradient.

If the initial profile is a sharp spike, the solution to this equation has a Gaussian form

$$C = \frac{M}{t^{0.5}}exp(-\frac{z^2}{4Dt}) \tag{1.20}$$

where M is a constant proportional to the total mass of diffusing solute.

Gaussian profiles are usually written in a form involving the standard deviation σ:

$$C \propto exp(-\frac{z^2}{2\sigma^2})$$ (1.21)

A direct comparison of the last two equations gives that

$$\sigma^2 = 2Dt$$ (1.22)

This is the well known Einstein's equation. To calculate the effective diffusion coefficient for small and medium size molecules in solvent, a number of empirical expressions are available. Among these, the Wilke-Chang equation [8] is the one most widely used so far:

$$D = \frac{7.4 \times 10^{-12}(\Psi_2 M_2)^{0.5}T}{\eta V_1'^{0.6}}$$ (1.23)

where D is the effective diffusion coefficient in $m^2 s^{-1}$, M_2 is the molecular weight of solvent and Ψ_2 is an association factor — unity for non-polar solvent, 1.5 for ethanol, 1.9 for methanol and 2.6 for water. V_1 is the solute molar volume in $cm^3 mol^{-1}$ and η viscosity of the solvent in $mNsm^{-2}$.

The effective diffusion coefficient is smaller in porous media than in bulk solution because of obstructive effects of the pore structure. There are two major factors which hinder diffusion [15]. One is the tortuosity of the pores which results in an increased diffusion path length and the other is the constriction of the pores which gives rise to nonuniform concentration gradients. Combining these two effects gives the total obstructive factor, γ. For a densely packed column of nonporous spheres with a column porosity of about 40%, γ is approximately 0.6 whereas for a column of porous particles γ is larger and may approach unity.

Diffusion in a chromatographic column is complicated by the presence of the stationary phase in which the diffusion rate can be different from that in the mobile phase. Further, the column packing is hardly homogeneous, thus in

different region of the column different diffusion coefficient, D_i, prevails. Since the diffusion occurring in different regions is effectively independent process, by the theorem of additive variances, the effective diffusion coefficient in the column, D_{col}, can be written as

$$D_{col} = \frac{\sum D_i t_i}{\sum t_i} \qquad (1.24)$$

where t_i represents the mean residence time of solute in the different region.

The velocity profile in laminar flow through circular tubes can be expressed mathematically in a simple form, which is parabolic. The maximum velocity, u_{max}, occurs at the centre of the tube and has the value

$$u_{max} = 2u \qquad (1.25)$$

u is the mean velocity given by Poiseuille's equation

$$u = \frac{r^2}{8\eta} \frac{\Delta P}{L} \qquad (1.26)$$

ΔP is the pressure drop across the length of the tube L, and r is the radius of the tube.

Flow through a packed column is governed by Darcy's law. The mean velocity u is then given by

$$u = \frac{B_o}{\eta \epsilon} \frac{\Delta P}{L} \qquad (1.27)$$

where B_o is the specific permeability with dimensions of length squared, and ϵ is the interparticle porosity of the packed column. The values of ϵ is typically about 0.4 for a well-packed column of spherical materials. A comparison of equation 1.26 and 1.27 yields the specific permeability for open tubes $\epsilon = 1$ with the value of $r^2/8$.

Several equations have been derived to relate the specific permeability to the particle diameter and the column porosity. The best known expression is the

Kozeny-Carman equation [9], which gives the specific permeability as

$$B_o = \frac{d_p^2}{180} \frac{\epsilon^3}{(1-\epsilon)^2}$$ (1.28)

where d_p is the particle diameter.

1.4.2 Band Spreading

It has been established that the major contributions to band spreading are resistance to mass transfer between phases, flow and axial molecular diffusion. Before proceeding to detailed examinations of each of these, several basic terms must be defined. As stated earlier, the plate height initiated by Martin and Synge is a widely accepted parameter for the characterizaton of column efficiency . In practice, the plate height concept is expanded from their original assumptions and used to describe all band spreading phenom.na, provided that they lead to Gaussian distribution of solute molecules along the column.

For a uniform column,free from concentration and velocity gradients,the plate height H may be defined as

$$H = \frac{\sigma^2}{L}$$ (1.29)

where L is the distance migrated by the centre of the zone and σ the standard deviation of the Gaussian distribution, the value of which is usually taken as the quarter of the band width at baseline.

The plate number N is defined as

$$N = \frac{L}{H}$$ (1.30)

Axial Molecular Diffusion   The variance of the concentration distribution due to axial molecular diffusion can be calculated directly from the Einstein

equation,

$$\sigma^2 \;=\; 2Dt_R \tag{1.31}$$

$$\;=\; 2D(1+k')t_m \tag{1.32}$$

$$\;=\; 2D(1+k'')t_{mz} \tag{1.33}$$

Where D is the effective diffusion coefficient of the solute and t_R is the residence time of the solute in the column and subscripts, m and mz, denote the mobile phase and mobile zone respectively.

For the diffusion of an unretained solute in a packed column, the variance can be given as

$$\sigma^2 = 2\gamma_m D_m t_m \tag{1.34}$$

where m denotes mobile phase.

If the solute is retained, however, the diffusion in the stationary phase must be taken into account. By equation 1.24, the effective diffusion coefficient in this case, D_{col}, is given as

$$D_{col} \;=\; \frac{\gamma_m D_m t_m + \gamma_s D_s t_s}{t_m + t_s} \tag{1.35}$$

$$\;=\; \frac{\gamma_m D_m + k'\gamma_s D_s}{1 + k'} \tag{1.36}$$

On substituting equation 1.36 for D in equation 1.32 and combining with equation 1.29, we obtain plate height arising from longitudinal molecular diffusion for the retained solute

$$H = \frac{2(\gamma_m D_m + k'\gamma_s D_s)}{u} \tag{1.37}$$

where u is linear velocity of mobile phase, given by $u = L/t_m$.

Mass Transfer in Stationary Zone   Band spreading due to slow equilibration
has been treated thoroughly by the nonequilibrium theory [27]. Since the band
dispersion is determined by the magnitude of the departure from equilibrium, it
is possible to calculate the variance for the nonequilibrium term. Qualitatively
this can be done in four steps. First, the mass transfer rate for the mobile
phase s_m is related to the equilibrium departure term ϵ_m by noting the fact that
the value of ϵ_m is zero when the complete equilibrium is attained. Second, the
mass transfer rate s_m is related to flow via mass conservation equation. Third,
the non-equilibrium term c_m is found by equating the two expressions for s_m
obtained from step one and step two respectively. Finally, using the appropriate
mathematical manipulation, an equation similar to Fick's first law is obtained.
The effective diffusion coefficient responsible for band spreading is found, thus
the plate height contribution from slow equilibration is obtained by applying the
familiar relationship $H = 2D/u$.

Because the mathematics involved in the nonequilibrium approach is almost
formidable to general chromatographers the theory will not be discussed in detail
here. Instead we turn to the random walk model [27] for the derivation of equa-
tions for the plate height contribution from mass transer within the stationary
zone, since this approach is relatively simple and straightforward while providing
considerable insight into the origin of the band spreading.

The process by which solute molecules diffuse in and out of the stationary
zone can be envisaged as the molecules walking axially in random fashion, with
a number of steps, n, of equal length, l. According to the theory, the variance
arising from this process is simply

$$\sigma^2 = l^2 n \tag{1.38}$$

A diffusion-out process is equivalent to a random step forward because it

releases the molecule to the mobile zone where it can migrate forward at the velocity of the mobile zone, u_{mz}. The distance covered in such a random step or the segment length is thus $u_{mz}t_{out}$, where t_{out} is the mean time spent in the mobile zone. A diffusion-in process is, however, a step backward because it leads to the molecule to be captured by the stationary zone where it begins to fall behind the band centre as the latter continues its forward motion. The total number of random steps, as the band migrates the distance L along the column, is the number of forward steps plus the number of backward steps executed during this period. Since a diffusion-out step must be followed by a diffusion-in step, the total number of steps is just twice the number of diffusion-out steps occurring, thus

$$n \;=\; 2\frac{t_{mz}}{t_{out}} \tag{1.39}$$

$$=\; 2L/u_{mz}t_{out} \tag{1.40}$$

$$=\; 2L(1 - \varphi)/u t_{out} \tag{1.41}$$

where the relationship $u_{mz} = u/(1 - \varphi)$ is employed.

At this point it should be made clear that the segment length is not equivalent to the step length. The reason for this is that while the released molecule is moving a distance $u_{mz}t_{out}$ in the time t_{out}, the band centre is also moving . The step length of the free molecule relative to the band as a whole is thus the segment length $u_{mz}t_{out}$ minus the advance made by the band in the same period, that is

$$l = \frac{1}{1 + k'}u_{mz}t_{out} \tag{1.42}$$

or

$$l = \frac{k''}{1 + k''}u_{mz}t_{out} \tag{1.43}$$

Inserting n and l into equation 1.38 yields

$$\sigma^2 = 2L\left(\frac{k''}{1+k''}\right)^2 \frac{u}{1-\varphi} t_{out} \tag{1.44}$$

Since the mean time taken for one random step is the mean time spent in the mobile or stationary zone divided by the number of random steps, t_{out} can be related to t_{in}, time taken for one random step in the stationary zone, by the relationship

$$k'' = \frac{t_{sz}}{t_{mz}} = \frac{t_{in}}{t_{out}} \tag{1.45}$$

Inserting this equation in equation 1.44 for t_{out} yields

$$\sigma^2 = 2L\frac{k''}{(1+k'')^2} \frac{u}{1-\varphi} t_{in} \tag{1.46}$$

Using the Einstein equation, $t_{in} = d^2/2D_{sz}$, again, we obtain

$$\sigma^2 = L\frac{k''}{(1+k'')^2} \frac{u}{1-\varphi} \frac{d^2}{D_{sz}} \tag{1.47}$$

where D_{sz} is the effective diffusion coefficient of solute and d the distance required to diffuse in the time of one random walk step in the stationary zone. The distance d may be related to the particle diameter d_p by relationship $d = qd_p$, where q is a configurational factor, which, according to Giddings, is 1/30 for liquid spheres and a value smaller than 1/48 for liquid held at the contact points between the particles.

Combining equations 1.29 and 1.47 gives

$$H = q\frac{k''}{(1+k'')^2} \frac{u}{1-\varphi} \frac{d_p^2}{D_{sz}} \tag{1.48}$$

As discussed above, the diffusion coefficient in the stationary zone, D_{sz}, may be found by making use of equation 1.24 , thus we have

$$D_{sz} = \frac{\gamma_{sm}D_m t_{sm} + \gamma_s D_s t_s}{t_{sm} + t_s} \tag{1.49}$$

where subscripts m, sm, s, sz denote the mobile phase, stagnant mobile phase, stationary phase and stationary zone, respectively.

Two limiting cases of equation 1.49 exist. First, if $\gamma_{sm} D_m = \gamma_s D_s$, this means that the effective diffusion in the stationary phase is the same as in the stagnant mobile phase. D_{sz} is thus simplified

$$D_{sz} = \gamma_{sm} D_m \qquad (1.50)$$

Second, if $\gamma_s D_s \ll \gamma_{sm} D_m$, this means that the diffusion in the stationary phase is negligible compared to that in the stagnant mobile phase, D_{sz} becomes

$$D_{sz} = \frac{\gamma_{sm} D_m \varphi}{k''(1 - \varphi)} \qquad (1.51)$$

Accordingly we have two plate height expressions corresponding to the limiting cases discussed above:

$$H = q \frac{k''}{(1 + k'')^2} \frac{u}{1 - \varphi} \frac{d_p^2}{\gamma_{sm} D_m} \qquad (1.52)$$

and

$$H = q \left(\frac{k''}{1 + k''} \right)^2 \frac{u}{\varphi} \frac{d_p^2}{\gamma_{sm} D_m} \qquad (1.53)$$

These equations are readily transformed into Giddings forms [27] by noting that different parameters are used. For instance, $\left(\frac{k''}{1+k''} \right)$ is equivalent to $(1 - \Phi R)$ in the Giddings form, $(1 - \varphi)$ is equal to Φ and so on.

Flow Dispersion   Solute bands in the mobile phase are dispersed not only by diffusion but also by flow. Band spreading is therefore greatly influenced by the detailed flow profile and the rates of flow and diffusion.

In open tubular columns the equation for the plate height contributions from the flowing mobile phase was obtained by Golay [10] . Because the exact flow

profile is known and the lateral exchange takes place by diffusion only, the plate height contribution can be calculated exactly and is given by

$$H = \frac{1 + 6k' + 11k'^2}{96(1+k')^2} \frac{d_c^2 u}{D_m} \tag{1.54}$$

where d_c is the inner diameter of the column.

In a randomly packed column, the tortuous and uneven nature of the packing gives rise to flow velocity variations. According to Giddings [27], these velocity inequalities can be classified into five categories: transchannel, transparticle, short range interchannel, large-range interchannel and transcolumn. Since the magnitudes of these effects vary with the quality of the packing material and the bed structure, the precise numerical values are not available. Nevertherless, an approximate evaluation of each category by Giddings points to the predominance of the short-range interchannel effect around the optimum velocity, that is, $\nu = 3$ (ν will be defined later). The velocity inequality due to this effect is likely to occur in the packed regions where tightly packed 'islands' are joined by loosely fitted particles, thus leaving channels of various diameters.

It is well known that a solute molecule in the flowing mobile zone will acquire intermittent velocity depending upon which streampath it occupies. The molecule in a fast streampath, for instance, may end up in a slow streampath after migrating one or so particle diameters. This velocity exchange can be achieved in two ways. First, if the molecule is locked into the streampath it will be soon carried into a new velocity regime with a velocity unrelated to the preceding. This type of exchange is usually referred to as eddy diffusion, attributed to the flow splitting and recombining due to the presence of the packing. The second means of the velocity exchange is the lateral molecular diffusion by which the molecule moves into a new streampath, new flow channel or new velocity regime.

Following Giddings [27], we apply the random walk model to the treatment

of these two effects. The calculation of the step length and the step number is relatively simple in this case. The step length, l, as defined before, is the distance gained or lost by the molecules in the velocity extreme, S_e, with respect to the mean distance covered by the band as a whole, S, that is

$$l = S_e - S \tag{1.55}$$

In order to determine the step length it is necessary to define an average time, t_e, as the time needed to transfer a molecule from one velocity extreme to another, or simply time spent in one random step. Since the distance between velocity extremes is proportional to the particle diameter, t_e may be obtained from the Einstein equation as

$$t_e = \frac{\omega_\alpha d_p^2}{2D_{col}} \tag{1.56}$$

where ω_α is a structural factor, d_p particle diameter and D_{col} the effective diffusion coefficient in a column, given by equation 1.24.

The mean distance, S, is then

$$S = u_{mz} t_e \tag{1.57}$$

and the extreme distance, S_e, is given by

$$S_e = u_e t_e \tag{1.58}$$

where u_e is the extreme velocity.

On substitution for S and S_e we have

$$l = (u_e - u_{mz})t_e \tag{1.59}$$

$$= \Delta u t_e \tag{1.60}$$

Since Δu is usually a fraction of the mean velocity, equation 1.60 can also be

written as

$$l = \omega_\beta u_{mz} t_e \tag{1.61}$$

$$= \omega_\beta S \tag{1.62}$$

where ω_β, like ω_α, is a structural factor, depending upon the uniformity of the packing structure. Ideally ω_β should approach zero when velocity differential is insignificant.

The number of random steps is simply the number given by the residence time of a solute in the column, t_R, divided by the transfer time, t_e; that is

$$n = \frac{t_R}{t_e} \tag{1.63}$$

$$= \frac{(1+k'')t_{mz}}{t_e} \tag{1.64}$$

$$= \frac{(1+k'')L}{u_{mz}t_e} \tag{1.65}$$

$$= \frac{(1+k'')(1-\varphi)L}{ut_e} \tag{1.66}$$

On combining these expressions with $\sigma^2 = l^2 n$ and $H = \sigma^2/L$, we arrive at

$$H = \omega_\beta^2 \frac{1+k''}{1-\varphi} u t_e \tag{1.67}$$

Inserting equation 1.56 for t_e gives

$$H = \omega \frac{1+k''}{1-\varphi} \frac{d_p^2 u}{D_{col}} \tag{1.68}$$

where $\omega = \omega_\alpha^2 \omega_\beta^2$.

In comparison with Golay expression for flow dispersion in open-tubular chromatography where lateral diffusion is the only means of velocity exchange, equation 1.68 appears to have the similar features with respect to the plate height dependence upon the flow velocity and the retention of solute.

This conclusion is in sharply contrast to that drawn by van Deemter et al [26] from their original investigation of flow dispersion. Their theory is based on the assumption that flow dispersion is solely flow phenomenon where molecular diffusion has no role to play in transferring molecules from one flow streampath to another. Therefore during migration through a column, molecules stay in their streampaths and do not diffuse away until they are carried into a new flow regime due to flow splitting and recombining. The transfer time in this case, t_e, can be taken as the time needed for a molecule to move a distance, S, before change its velocity. Since this distance is proportional to particle diameter, it follows that

$$S = u_{mz}t_e = \omega_\lambda d_p \qquad (1.69)$$

where ω_λ is a structural factor, near unity in most cases.

Inserting S in equation 1.62 gives

$$l = \omega_\beta\omega_\lambda d_p \qquad (1.70)$$

Since molecular diffusion is not taken into account in this treatment, the number of the random steps is redefined accordingly as

$$n = \frac{t_{mz}}{t_e} = \frac{L}{u_{mz}t_e} = \frac{L}{S} \qquad (1.71)$$

Upon appropriate substitution and combination we obtain the plate height expression of the form as derived by van Deemter et al:

$$H = 2\lambda d_p \qquad (1.72)$$

where $\lambda = \omega_\beta^2\omega_\lambda/2$.

If the band spreading arising from eddy diffusion and lateral diffusion can be regarded as independent processes, using the theorem of additive variances, we obtain an plate height expression for the flow dispersion

$$H = 2\lambda d_p + \omega\frac{1 + k''}{1 - \varphi}\frac{d_p^2 u}{D_{col}} \qquad (1.73)$$

or more simply

$$H = H_{eddy} + H_{lateral} \qquad (1.74)$$

However the legitimacy of applying the theorem to the flow dispersion has been questionable. As Giddings pointed out, eddy diffusion and lateral diffusion effects cannot be taken as to operate independently since they may act cooperatively so as to reduce the dispersion solely produced by each of these effects. Accordingly Giddings theory gives

$$H = \frac{1}{\frac{1}{H_{eddy}} + \frac{1}{H_{lateral}}} \qquad (1.75)$$

Although the general concept of coupling eddy diffusion term with lateral diffusion term has been accepted the exact mechanism of interacations between two processes has not been worked out. It is therefore not surprising that theoretical expressions developed for the flow dispersion have all failed to reproduce experimental data [18, 14]. This disatisfaction is largely ascribed to the extreme complexity of the geometry and flow profile within the column bed.

Since science of flow in porous media is not advanced far enough to allow precise numerical evaluation, a number of empirical expressions have been proposed [28]. By far the most popular is due to Knox [11], it states

$$H = Ad_p \left(\frac{ud_p}{D_m}\right)^{0.33} \qquad (1.76)$$

where A is an empirical coefficient.

Overall Plate Height Expressions   Since each dispersion process takes place almost independently, the overall plat height, H, can be expressed as a sum of all the individual contributions:

$$H = H_l + H_f + H_n \qquad (1.77)$$

where subscripts l, f, n refer to longitudinal diffusion, flow dispersion and slow mass transfer in stationary zone, respectively.

In view of the uncertainty over the way the plate height arising from flow dispersion should be represented, we use a function, $f(k', u)$, to denote this term. In combination with the theoretical expressions for the other two terms we obtain an overall plate height equation:

$$ H = \frac{2(1 + k')D_{col}}{u} + f(k', u) + q\frac{k''}{(1 + k'')^2}\frac{u}{1 - \varphi}\frac{d_p^2}{D_{sz}} \qquad (1.78) $$

A number of other well-known plate height equations are listed below for comparision:

1. van Deemter Equation, originally for gas liquid chromatography [26]:

$$ H = 2\lambda d_p + \frac{2\gamma_m D_m}{u} + \frac{2}{3}\frac{k'}{(1 + k')^2}\frac{d_f^2 u}{D_s} \qquad (1.79) $$

where d_f is the thickness of stationary phase.

2. Golay Equation for open-tubular chromatography [10]:

$$ H = \frac{2D_m}{u} + \frac{1 + 6k' + 11k'^2}{96(1 + k')^2}\frac{d_c^2 u}{D_m} + \frac{2}{3}\frac{k'}{(1 + k')^2}\frac{d_f^2 u}{D_s} \qquad (1.80) $$

3. Giddings Equation for chromatography in a column of spherical particles [27]:

$$ H = \sum \frac{1}{\frac{1}{2\lambda_i d_p} + \frac{D_m}{\omega_i d_p^2 u}} + \frac{2(1 + k')D_{col}}{u} + \frac{k'}{30(1 + k')^2}\frac{d_p^2 u}{D_s} \qquad (1.81) $$

where i denotes the velocity inequality category.

1.4.3   Reduced parameters

To evaluate the performance of a packing material or to compare the performance in different chromatographic systems, it is found most convenient to use so called 'reduced parameters', originated by Giddings [27].

The reduced plate height h is defined as

$$h = \frac{H}{d_p} \tag{1.82}$$

and the reduced velocity ν is defined as

$$\nu = \frac{ud_p}{D_m} \tag{1.83}$$

Accordingly, the general equation for the plate height can be cast into the reduced or dimensionless form:

$$h = B/\nu + f(k', \nu) + C\nu \tag{1.84}$$

If the flow term is substituted with the empirical expression proposed by Knox, the equation becomes

$$h = B/\nu + A\nu^{0.33} + C\nu \tag{1.85}$$

This is the very popular Knox equation. The constants A, B and C are dimensionless, and for a good column have the approximate values $A = 1, B = 2$, and $C < 0.1$ [12]. B reflects the geometry of the eluent in the column and the extent to which diffusion of solute is obstructed by the presence of the packing. Ideally, B should approach 2 when obstructive effects are negligibly small. This means that solute molecules are free to diffuse in a packed bed as in bulk solution. A is a weak function of k' but depends mainly upon the uniformity of the packing structure: a poorly packed column will have a high value of A, say 2 to 5 while a well packed column should have A in the range 0.5 to 1. C reflects the efficiency of mass transfer in the stationary zone [13, 17]. Theoretically, from dependence of C upon k', one should be able to identify whether the rate determining process is mass transfer in the stationary phase or diffusion in the stagnant mobile phase. If C reaches a maximum when k' is near unity, this probably indicates the former process is predominant, otherwise C would rise gradually to a maximum with

k' when the latter prevails. Obviously, no matter which rate determining process predominates, a minimum value of C should be obtained for an unretained solute.

If h is plotted against ν according to Knox equation with the constants as given above, the optimum reduced velocity is found to be around 3 at which maximum efficiency corresponding to lowest h occurs.

An important feature of the reduced parameter approach is that identical (h, ν) curves are expected from chromatographic systems which differ in geometrical size of the column and in the nature of the eluent used. Thus plots of reduced plate height against reduced velocity provide the most appropriate means to evaluate or to compare the performance of different chromatographic packing materials.

Chapter 2

Porous Graphite

2.1 Introducton

With the development of the column technology, it becomes clear that several basic requirements must be satisfied for a packing material to be applicable in high performance liquid chromatography (HPLC). Of these the foremost desirable characteristics that the packing should possess are the following: (1) availability in small particle size (viz 3-10 μm); (2) adequate mechanical strength to withstand high pressures; (3) surface homogeneity to ensure symmetric peaks at low coverage; (4) uniform porosity, free from micropores to permit rapid mass transfer to occur. It is therefore not surprising that in the early days of HPLC silica gels were adopted as preferred packing materials because they appear to have all those favourable characteritics.

In contrast to silica gels, carbons seemed to have been completely neglected during this period of time. Attention did not turn to them until in the mid 1970's when interest in carbons was revived in the search for a packing material showing superior pH stability and selectivity over the silica gels.

From the early chromatographic experiments on carbon, it was realized that

none of the existing carbons including synthetic carbons could be used in HPLC without special treatment. Active carbon, being widely used as an adsorbent in displacement and frontal chromatography, is useless for elution chromatography mainly because of its heterogeneous surface giving rise to extremely non-linear adsorption isotherms [86].

Diamond and graphite are crystalline forms of carbon, therefore they are expected to have the most homogeneous surface. But being nonporous and of low specific surface area, they are unlikely to be useful in chromatography. Graphitized carbon black has adequate porosity and homogeneous surface, this property makes it very popular non-polar adsorbent in gas chromatography. However, being made of aggregated colloid particles, this material is extremely fragile and therefore unsuitable for routine HPLC, despite the fact that symmetric peaks have been shown [41]. An effort was made to strenghthen the graphitized carbon black by deposition of a layer of pyrocarbon [36, 37, 38], however once again the modified material gave poor chromatographic performance, probably because the pyrocarbon surface is not as uniform as that of true graphite.

Graphitization of porous carbons appears to be promising to turn carbons into a useful HPLC packing. Unger et al [32] employed purified active carbons and cokes as starting materials. On heating at 2070K and above, the micropores in the initial materials were effectively removed to give a low specific surface area. The resulting packing showed good mechanical strength but poor chromatographic performance and low adsorptive capacities.

Knox and Gilbert [39] introduced in 1979 a novel method for making a porous graphite using a mesoporous silica gel as a template to provide the controlled pore size. The material prepared by this method was substantially advantageous over previous carbons in terms of peak shape but only marginally superior to pyrolytic carbon deposited on graphitized carbon black. Later the production

procedures were improved, which provides the carbon packing with column efficiency comparable to other HPLC packings [51].

2.2 Preparation

According to Knox et al [52], four consecutive stages may be distinguished, principally, in the formation of graphite from naturally occurring or synthetic precursors: homogenization, carbonization, volatilizaton of inorganic impurities and graphitization.

(1) Homogenization covers all operations which lead to an improved ordering of the structure of any solid or liquid carbonacious starting material, usually consisting of a thermal treatment up to about 1000K. It is well known that the degree of graphitizaton of any carbon brought about by high temperature treatment depends strongly on its initial source and the order of the structure.

(2) Carbonization covers processes leading to increases in percentage of carbon content and porosity, which is usually carried out between 1000 and 1500K.

(3) Volatization of inorganic impurities such as sulphur and silica occurs at 1500 to 2000K. Such a treatment gives rise to a large number of structural defect sites and disordering of the mutual arrangement of layers.

(4) Graphitization covers the subsequent heat treatment in an inert atmosphere up to 3200K. This process brings about densification with concurrent removal of structural defects and formation of graphitic structure of various degrees, depending upon the initial source.

In accordance with these four stages, the improved process for making porous graphite, which is based on the 'template method' invented by Knox and Gilbert may be described as follows. The material is produced by impregnating a silica gel of high porosity with a melt of phenol and hexamine in a 6:1 weight ratio. The

impregnated material is heated gradually to 420K to form phenol-formaldehyde resin within the pores of the silica gel. This silica-polymer is then heated slowly to 1200K in a stream of nitrogen. Approximately 50% of the weight of the polymer is thereby lost, and the density of which is increased to about 2 $g\,cm^{-3}$. This effectively completes stages 1 and 2 of the above process. The silica-carbon particles are then treated with hot aqueous potassium hydroxide to dissolve the silica template. The resulting porous glassy carbon has a BET surface area of 450-600 m^2g^{-1} and a pore volume of 2.0 cm^3g^{-1}, corresponding to a particle porosity of about 80%. This carbon is then heated to about 2800K in oxygen free argon to fulfil the requirement of graphitization, thereby completing stages 3 and 4. The end product has a surface area of about 100 to 150 m^2g^{-1} and a pore volume similar to that of the carbon before high temperature treatment. It is thus established that the original mesostructure imposed by the silica template remains intact under graphitization conditions. In the process of heating from 1200 to 2800K the micropores in the porous glassy carbon formed after dissolution of the silica close up as the structural reorganization prevails but the mesopores (10-50 nm pore diameter on average) remain and indeed expand somewhat as the carbon structure densifies to 2-dimensional graphite.

While the particle size, shape, porosity and pore size are determined by the choice of the template material, the surface chemistry is mainly determined by the final heat treatment and any subsequent chemical treatments. It is thus possible in principle to produce porous graphite with a range of pore and surface properties tailored to specific requirements.

2.3 Properties and Characterization

2.3.1 Crystal structure

It is well known that during graphitization crystal development takes place with the formation of the typical layer structure of graphite. However, the degree of such a structural change strongly depends upon the conditions employed. It is also acknowledged that so called 'graphitized' carbons can range from almost amorphous materials to perfect three-dimensional crystalline graphites. In fact, there are two distinct forms of graphitized carbon of particular interest to chromatographers: two-dimensional and three-dimensional graphites.

The crystal structure of the three-dimensional graphite was first deduced by Bernal [40] from X-ray diffractograms. Essentially graphite consists of layers of hexagonal arrays of closely packed carbon atoms, the layers being stacked in such a way that alternate ones lie immediately above or below one another, thus giving a stacking sequence of ab, ab etc, or alternatively abc, abc etc. This form of graphite is not readily obtained from the conversion of amorphous solid carbon to graphite, presumably due to the fact that an extremely high activation energy is required to reorganize the initially randomly oriented graphitic sheets into ordered three-dimensional graphite. Thus most synthetic carbons, when heated to about 3200K assume the second form, that is, two-dimensional graphite in which graphitic sheets remain randomly ordered relative to each other. The essential feature of such a material is that it possesses a truly graphite surface while resembling a glassy carbon in terms of mechanical strength. The rigidity of porous graphite arises from its unique bulk structure: interwined graphitic ribbons which make impossible for the graphitic sheets to move relatively to each other.

The X-ray deffraction study of some porous graphite samples by Knox et
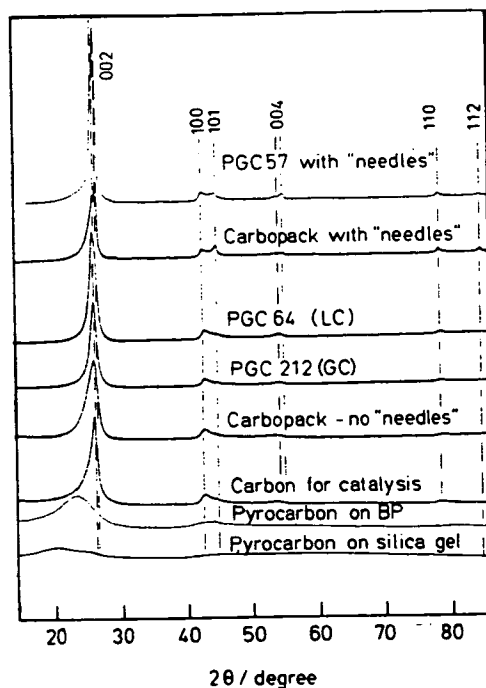
Figure 2.1. X-ray diffractograms of carbons. From Ref. [51].

al [51] has established that porous gaphite produced by heating the precurser carbon to above 2300K has the molecular structure of a two-dimensional graphite which is essentially indistinguishable from that of graphitized carbon black in crystallographic terms, see Figure 2.1.

However the high resolution electron micrography study has revealed the striking difference between two materials. As shown in Figure 2.2, graphitized carbon black is made up of colloidal particles which are not interconnected whereas porous graphite is shown in the form of continuous structure.
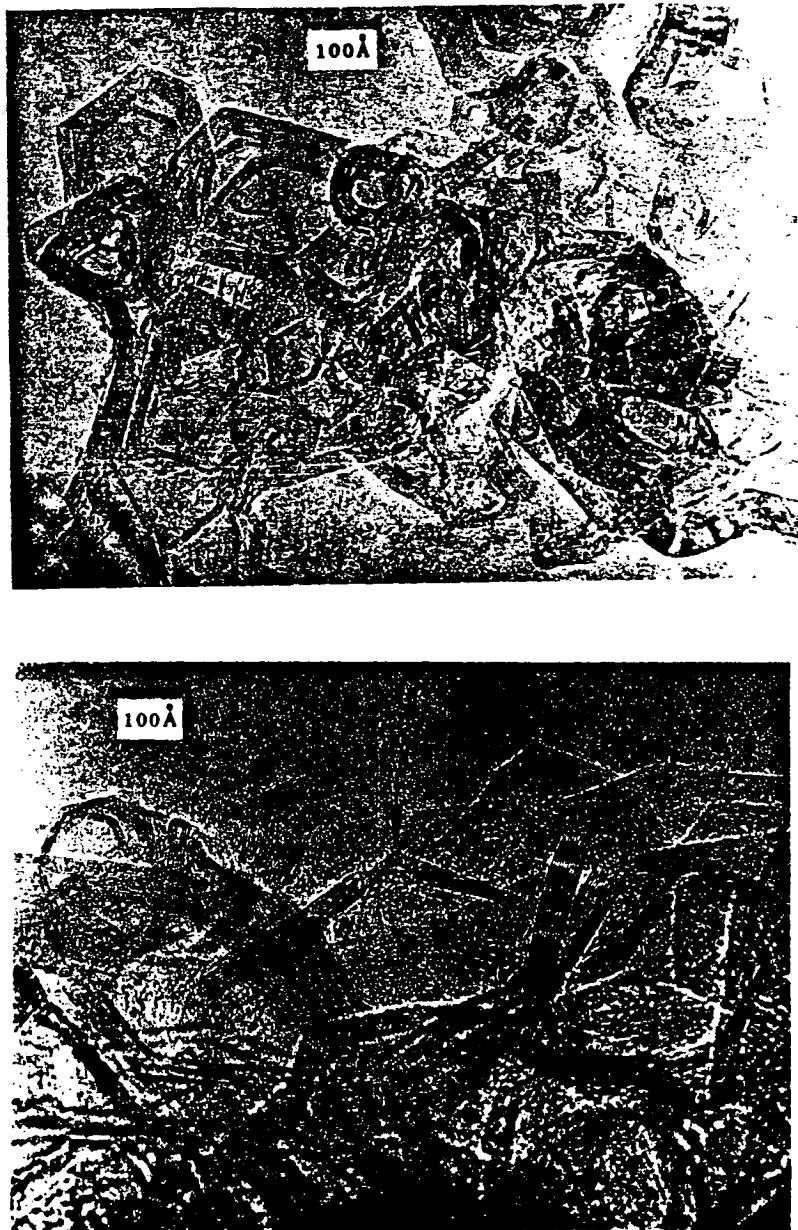
Figure 2.2. Electron micrograms of graphitized carbon black and porous graphite. Upper: Carbopak B, a typical graphitized carbon black. Lower: porous graphite prepared at 2340°C. From Ref. [51].

2.3.2 Pore structure

The pore structure of a graphitized carbon covers a wide range depending upon the degree of graphitization. Isotropic and amorphous carbons are extremely microporous whereas anisotropic graphites exibit little porosity. Between these two extreme limits a considerable variation in pore structue can be expected for the materials of various degrees of graphitization. With respect to graphitized carbon prepared by the template method, the origin of porosity may be visualized as follows:

In the process of homogenization or the early stages of carbonization, the mixture of phenol and hexamine is developed into a heavily cross-linked polymer within the pores of the template silica. The rigidity of this three-dimensionally cross-linked structure prevents large scale re-ordering of the material during carbonization, and therefore the micropores are introduced as a result of loss of volatile small molecules and oxygen-containing linkages. After dissolution of the silica template, the remaining carbon exhibits high porosity, which consists of meso-pores left behind by the template and micro-pores due to carbonization. During graphitization crystal growth occurs with alignment of the layer planes but the final size of the crystallite is limited by the connecting bridges in the sponge-like structure of the porous carbon so that most of the meso-pores remain together with small proportion of the micropores. Apparently, the dimensions of this porosity are dependent upon the original polymer source, the pore structure of the template and the conditions of carbonization and final heat treatment temperature.

The foregoing postulation regarding the formation of pore structure was substatiated by the experimental observations. The pore structure of the material experiences a dramatic change upon heating from 1200 to about 2800K as the
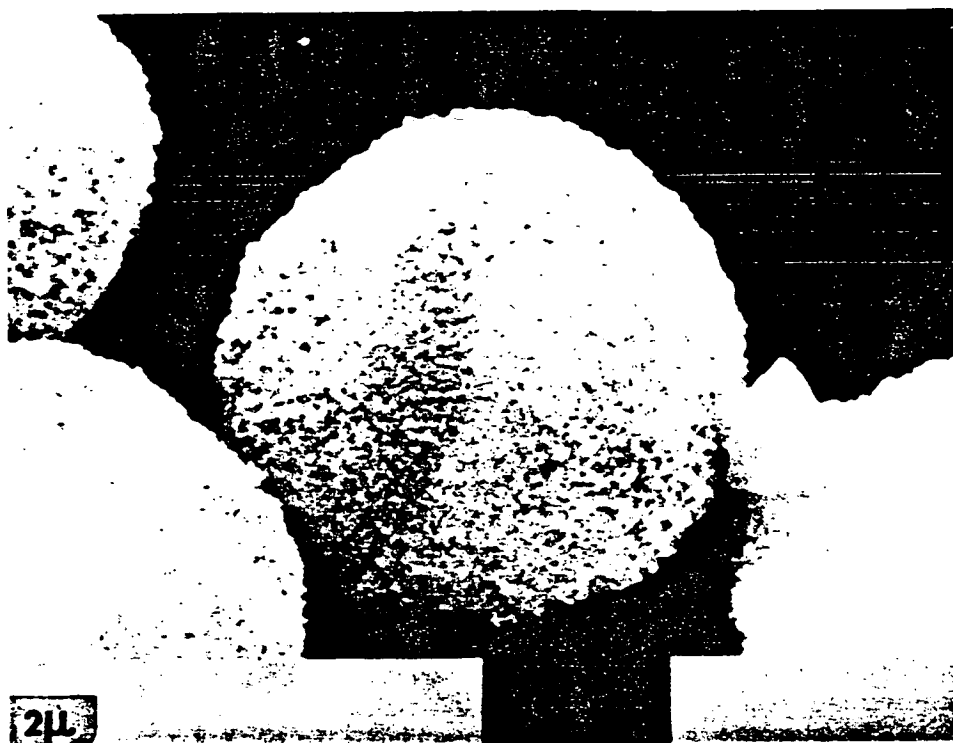
Figure 2.3. Scanning electron micrograms of porous graphite. From Ref. [51].

specific surface area is reduced significantly, from 450-600 to 100-150 m^2g^{-1}. Since the mean pore diameter is inversely proportional to the surface area when the pore volume is held constant [45], the reduction in surface area indicates the elimination of the micropores while preservation of the mesopores. The pore volume as a whole is hardly changed during the process of graphitization since the end product retains the spherical form and the particle size of the original silica template. The scanning electron micrograms in Figure 2.3 clearly show the spherical shape of the particles and their sponge like structure.

Typical values for the surface area, pore volume, particle porosity, and mean

Table 2.1. Physical properties of silica gels and graphitic carbons

Materails	Surface area, $m^2 g^{-1}$	Pore volume, $ml\, g^{-1}$	Porosity, %	Mean pore diameter, nm
Hypersil	170	0.68	60	10
Silica template	50	1.4	75	30
PGC 1000°C	350	1.4	75	30 + *micropores*
PGC 2500°C	120	1.4	75	30
Carbopack B	80	0.6	60	20

pore diameters of graphitic carbons are summerized in Table 2.1, together with those of silica gels used as templates [43].

2.3.3 Surface Composition

Although the pore structure parameters and the specific surface area have been extensively studied, the surface compositon of the porous graphite remains ill-defined [54]. It is generally accepted that apart from its primarily aromatic character, the graphite surface carries a variety of functional groups. The majority are acidic groups such as carbonyl, carboxyl and phenolic hydroxy but some basic groups may present as well. These functional groups are thought to locate at defects sites which occur randomly at the edges of crystallites. Thus the less crystalline the product the higher will be the concentration of polar surface functional groups.

A number of methods have been proposed for eliminating the polar surface functional groups, including heat treatment and chemical reduction. Of these, hydrogen treatment at 1300K is claimed to be most effective in removing trace amounts of surface oxides [42, 50, 48, 49].

2.4 Chromatographic Properties

2.4.1 Performance

The performance of a packing material may be evaluated by analysing the plot of the reduced plate height (h) against the reduced fluid velocity (ν) according to the equation:

$$h = A\nu^{0.33} + B/\nu + C\nu \tag{2.1}$$

As discussed in the preceding chapter, the coefficients A, B and C can be taken as a measure for the bed structure of the column and the quality of the packing material. The minimum h can be expected for unretained solute since the kinetics of adsorption and desorption is not involved. Rapid increase in h with k' is generally attributed to thermodynamic band broadening caused by the surface heterogeneity. Since chromatographic peaks are often asymmetric in this case, the plate height cannot be interpreted in terms of the above equation but serves to indicate how well the packing material is prepared.

The performance of the ungraphitized carbon packings have proved to be disappointing. Colin et al [36] determined the reduced plate height for their pyrocarbon modified carbon black, the optimum values of 3-7 were found for solutes with k'-values up to 1.1. However, for solutes of $k' > 2$, column efficiency deteriorated drastically, indicating high degree of the surface inhomogeneity.

In contrast to these carbons, graphitized carbon black, studied by Ciccioli et al [41], gave symmetrical peaks up to high k' values with negligible dependence of h upon k'. The optimum values of reduced plate height are all around 4 for various particle sizes. Similar values were obtained for microparticulate porous graphite. These two-dimensional graphites are therefore superior to ungraphitized carbons in terms of column efficiency, especially for strongly retained

solutes.

2.4.2 Retention and Selectivity

Both porous graphite and reversed phase silica are non-polar adsorbents, characterized by solute retention being controlled by dispersion interactions, however, there are a number of principal differences arising from their different surface characteristics. The surface of graphite consists essentially of gigantic aromatic molecules which possess no funtional groups except possibly at their edges. On the other hand, the surface of reversed phase silica is composed of a highly open framework of solvated and mobile alkyl chains with a large population of unreacted hydroxyl groups at the matrix surface. At the same eluent composition stronger retention for non-polar sulutes is observed with porous graphite than on reversed phase silica. This increased retention is mainly attributed to the great free energy change upon adsorption onto graphite surface relative to partition into liquid organic phase. This may be understood by referring to the interaction energy curve illustrated in Figure 1.1. The rigidity of solid surface allows solute molecules to have a closer access, thus giving rise to higher interaction energy.

These retentive characteristics can be quantitatively expressed by plotting the logarithm of k' for members of a homologous series against the number of carbon atoms, n, in the molecule or alkyl chain. A linear relationship is often found with the slopes indicating the retention per carbon atom of the solute. The values of the slope obtained on graphite are substantially greater than those on reversed phase silica, both being measured with the same solutes under comparable conditions. For example, Unger [33] quoted the slope of 0.28 for polynuclear aromatics eluted with methanol from graphitized coke, compared to the value of 0.12 for LiChrosorb RP-18.

Although both of graphite and reversed phase silicas act as non-polar adsorbents, graphite behaves distinctly differently from reversed phase silicas in relation to selectivity. It has been observed that polar derivatives of benzene, especially those having large dipole are much strongly retained by carbons than benzene itself whereas the opposite is true with reversed phase silicas. Another important example in this regard is the reversal of the elution order of xylenes when separated on graphite. As pointed out by Kiselev and Yashin [53], this distinct stereoselectivity is likely to arise from the flat surface of graphite. When o-xylene and p-xylene are adsorbed onto the graphite, four carbon atoms contact the surface (two from the methyl groups and two from the ring) whereas with m-xylene only three atoms contact (two from the methyl groups and one from the ring), thus m-xylene is eluted before o-and p-xylenes. Charge transfer interactions between graphite surface and aromatic compounds are also invoked to explain the retention behaviour of phenol isomers, steroid analogues, natural products isomers and antibiotics [35, 46].

2.5 Applications

A continuously growing number of separations using porous graphites have been reported since they became commercially available under the trade name of Hypercarb in 1988. Some of these separations might be achieved with reversed phase silicas as well, however, the unique properties of graphite offer the best chance to solve those problems difficult or even impossible with conventional packings. The work in this direction proves to be fruitful. Unlike reversed phase silica, the true graphite surface contains no acidic groups and can be used directly for the separation of amines without the need to add blocking agents to eluents. Anilines were separated on porous graphite, showing no significant peak

tailing [51]. Graphite is totally unreactive and unaffected by aggresive solvents, therefore it is an ideal packing for HPLC with eluents of extreme pH's. This is demonstrated by the ion-pairing separation of phenols using an eluent of pH 12.6 [34, 43]. Owing to its superior stereoselectivity, the material has been applied to the separations of diastereomers, geometrical isomers [44].

Chapter 3

Experimental work

3.1 Introduction

As noted above, a packing suited for HPLC must meet three basic requirements: rigidity of particles, uniformity of pore structure and homogeneity of surface. These requirements are often found conflicting with respect to carboneous materials. For instance, high degree of graphitization is desirable to aquire a uniform surface and to eliminate micropores, however the materials obtained in this way may be of no use because of lack of mechanical strength. For this reason compromises must be made between particle rigidity, surface homogeneity and pore size uniformity. So far the template method of Knox and Gilbert is the only means by which all those desired features can be combined to a single carboneceous material.

Porous graphite prepared by this method has highly homogeneous surface and this is confirmed by chromatographic studies which show good peak symmetry for a variety of solutes which are eluted within a relatively short period of time. However, for stongly retained compounds the material appears not so ideal in terms of column efficiency as asymmetry of the peaks is noticeably increased

with retention of solutes. This drawback of graphite can only be attributed to undesirable surface characteristics. And indeed, by no means can the graphite surface be made completely energetically homgeneous unless defective sites such as steps, recessions and terrces can be masked. A look at the origin of surface heterogeneities is nececessary before going on to consider deactivation of high energy sites on the graphite surface.

According to Graham [47], there are two types of heterogeneity distinguishble on the surface of graphite. One is the chemical or polar variety characterized by hydrophilic sites most likely on the peripheries of the aromatic sheets. Their effects and removal have been briefly discussed in the preceding chapter. The other is of geometric character typified by steps and recesses. It is likely that two types of heterogeneity can occur on a single active site, however, the geometric heterogeneity is believed to be predominent in causing peak tailing of non-polar solutes. This point can be made clearer by considering the surface of reversed phase silica gels where non-polar groups (alkyl chains) and polar-groups (silanol) co-exist but high efficiency is still attainable provided that no chemical reaction occurs between the solute and the silanol groups on the matrix. The concentration of defect sites is expected to be dependent strongly upon the conditions of graphitization or how well the aromatic sheets are reorganized to form a continuous surface. In view of the fact that a perfectly homogeneous surface is not available even with native graphites, one would accept that a minor proportion of strong adsorption sites is likely to be present on the surface of the synthetic product, which is presumably responsible for observed asymmetric peaks. It is obvious that this type of heterogeneity cannot be eliminated by chemical reduction like hydrogen treatment. Contrary to what one might expect, the removal of chemisorbed substance could actually increase the potential of the strong sites and contribute more to the total heterogeneity.

Given the high chemical potential on the strong active sites, they might be masked by adsorption of high molecular weight compounds (modifiers) onto the graphite surface. As a consequence of deactivation, it is expected that retention would be reduced and concomitantly peakshape improved. The effect of modifiers was demonstrated by Gilbert et al [31] who obtained improved symmetry of elution peaks for the more retained alkyl benzenes and polynuclear aromatics by adding a small proportion of terphenyl into the eluent.

Apart from the prelimenary work of Gilbert et al on the deactivation of PGC with modifiers, no further investigation has been reported in this respect. We felt deactivation of this type deserved more detailed investigation in view of the ubiquitous nature of the geometrical heterogeneity on the surface of a porous solid. With aromatic compounds as modifiers, a thorough study has been undertaken in an effort to establish whether or not the adsorption appoach is effective in reducing the detrimental effects of surface nonuniformity on chromatographic efficiency. The results will be presented in the following chapter.

The majority of HPLC separations to date have been achieved with reversed phase columns. However, in recent years the demand for specialist columns is markedly growing, especially in the field of pharmaceuticals and biotechnology where the separations of enantiomers and biopolymers are of primary interest. With regard to the unique properties of graphite the material would be expected to play more important role if it could be modified to provide functional groups required for specific separations. With a wealth of binding chemistry, silica gels have exihibited a great versatility and wide range of applications [64], it is logical to ask whether the modification of graphite could follow the same route as by chemical bonding.

Graphite is well known for its chemical inertness, nevertherless two kinds of reaction may be classified according to its structural $\pi - \sigma$ anisotropy [83, 84].

In the first type of reaction the molecular weight of the graphite macromolecules is increased by intercalation of guest species which are bonded through the π-electron system, thereby causing the macromolecules to swell in a direction perpendicular to the basal plane. The reaction of graphite with fluorine is an example of this type of reaction, and results in a stable monofluoride. The second type of reaction involves rupture of σ-bonds with concurrent breakdown of the lattice into smaller fragments. So called graphite oxide is prepared by oxidizing graphite with concentrated nitric and sulphuric acids containing some potassium chlorate [55]. The exact nature of the carbon-oxygen linkages is not well defined in spite of a century of effort. Both kinds of reaction are of little value in surface modification because of their massive destructive effects. Thus, a physical approach rather than chemical bonding must be sought to functionize the unreactive surface of graphite.

We turn to adsorption modification as this is the only way in which the functional groups may be introduced as a submonolayer, monolayer and multilayer coating onto the graphite surface. Three methods have been adapted for this purpose. They are dynamic coating, insoluble coating, and cross-linked polymer coating. The surface coated graphites have been employed in various modes of HPLC, including ion exchange, chiral and size exclusion chromatographies.

3.2 Methods of Characterization

3.2.1 BET Method

Of numerous parameters used to characterize a porous solid, specific surface area is perhaps the most important one as it provides a basis for calculating the surface coverage of a modifier.

The most common method for determining the surface area is the well known BET method [57, 58], based on the two parameter equation 3.1

$$\frac{P}{Q(P_o - P)} = \frac{1}{Q^o c} + \frac{c-1}{Q^o c}\frac{P}{P_o}$$ (3.1)

where,

P, P_o = Equilibrium gas pressure of adsorbate and vapour pressure of the liquid adsorbate, respectively;

Q = Amount adsorbed in moles of adsorbate per gram of adsorbent;

Q^o = Specific monolayer capacity in moles of adsorbate per gram of adsorbent;

c = Constant.

Nitrogen is generally employed as adsorbate and consequently adsorption measurements are carried out at the temperature of liquid nitrogen (77K). Data on the nitrogen isotherm between relative pressure (P/P_o) of about 0.05 and 0.35 are plotted in terms of the BET equation, which should result in a straight line. From the slope (S) and the intercept (I), the specific monolayer capacity (Q^o) can be calculated. Finally, the specific surface area, S_{BET} , is obtained by multiplying Q^o by the cross-sectional area of a nitrogen molecule, A_m:

$$S_{BET} = Q^o A_m N$$ (3.2)

where N is Avogradro's constant (6.02×10^{23} molecules per mole) and A_m is taken to be 0.162 nm^2 per molecule.

A programme in BASIC language is available for processing the adsorption data in terms of BET equation, which is used in the present work.

3.2.2 Breakthrough Method

The dynamic adsorption isotherm on a stationary phase can be derived by chromatography either from an elution or a breakthrough curve. A number of methods have been available for this purpose, which include those of Glueckauf's [60] and Cremer and Huber's [61]. All these methods take into account the fact that the quantity adsorbed onto the adsorbent is a product of the retention volume and the solute concentration in the mobile phase, it is thus possible to determine the isotherm from a single breakthrough or elution curve if the solute concentration in the mobile phase at each point of the isotherm is accurately known. This requires calibration of the instrument prior to any experimental determination.

The breakthrough method introduced by James and Philips [59] becomes the method of choice because this simple method provides reliable data without the necessity of calibrating the instrument and the involvement of complex mathematical analysis. The method is briefly described as follows:

A stream of solution containing the compound under study, at concentration C_a, is continuously pumped through a column until equilibration is attained. This may be indicated by an abrupt rise in the record baseline as illustrated in Figure 3.1. When the baseline is stable the stream is replaced by another one, at the same flow rate but with a higher concentration, C_b. For concave isotherms, the resulting breakthrough curve is a self-sharpening front [60]. If a volume V_i of the solution flows when the breakthrough occurs, a mass balance equation can be written to relate the amount Q of the solute adsorbed to the concentration C_i in the stream:

$$Q = \sum (V_i - V_{i-1})C_i \tag{3.3}$$

The adsorption isothem is constructed using a series of adsorption data Q
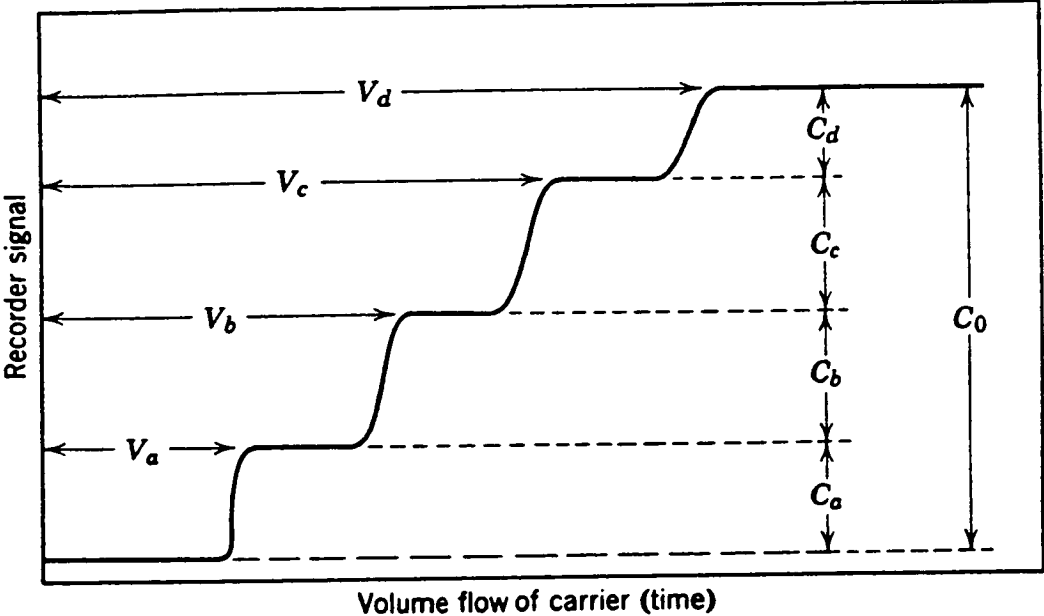
Figure 3.1. Idealised breakthrough curves.

obtained from the breakthrough curves for a number of successive concentration steps. The elution volume V_e, measured from the breakthrough curve, is corrected to the volume V_i by subtracting the void volume of a column V_o.

3.3 Equipment and Materials

3.3.1 Equipment

Liquid chromatographic systems used in this work were assembled in the laboratory with components from a variety of sources: Altex Model 110A pump (Beckman, High Wycombe, U.K.) and Kontron Model 410 pump (Krontron Intertechnique, St. Albans, U.K.); Rheodyne injector valves (Shandon Southern Products, Runcorn, U.K.); Shandon LC column oven; Cecil Model 2012 UV spectrophotometer (Cecil Instruments, Cambridge, U.K.) and Kratos Model 773 UV spectrophotometer (Spectros International, Urmiston, Manchester, U.K.); Hewlett Packard 3390A reporting integrator (Hewlett Packard, Palo Alto, California, U.S.A.) and BBC Model SE120 recorder.

Porous graphite samples were obtained from Chromatographite (Department of Chemistry, University of Edinburgh, U.K.) as spherical particles with a mean diameter of 5 μm and a particle porosity of 75%. Except for the work on adsorption chromatography where the packings were supplied as prepacked columns, the graphite samples were all fractionated to remove fines which might be present as a by-product. The procedures are described as follows.

10.0 g of graphite particles is added to 1000 ml of aqueous solution of sodium dodecylbenzenesulfonic acid (0.5%, w/v). The solution is stirred continuously until the particles are well dispersed. The dispersion obtained is then allowed to stand for 4-5 hours or so for larger particles to settle while the fines remain

Table 3.1. Particle properties and column dimensions

LC mode	Graphite sample	Particle size, μm	Particle porosity, %	Surface area, m^2g	Column dimension, mm
Adsorption	PGC A2	5	75	150	100×4.6
	PGC A3	5	75	150	100×4.6
	PGC A4	5	75	150	100×4.6
	PGC A5	5	75	150	100×4.6
Ion exchange	PGC 94F	5	75	107	50×4.6
Chiral					
a. chiral SP	PGC 94F	5	75	107	50×4.6
b.chiral MP	PGC 94F	5	75	107	100×4.6
Exclusion	PGC 94F	5	75	107	50×4.6

in the solution. The supernatant is then discarded, the remaining particles are further fractionated by repeating the above procedure at least five times. Finally, the particles are filtered and washed successively with water (5 × 100 ml) and acetone (5 × 100 ml) and dried overnight in an oven at 100°C.

BET surface areas of the graphite samples were measured with nitrogen using a laboratory constructed instrument, which is fully described elsewhere [62].

The particles were slurry packed into a column using a Shandon Packing Pump at 6000 psi. The slurry liquid was isopropanol and the displacer was a mixture of isopropanol and ethanol (1:4, v/v), unless otherwise stated. The performance of a column packed with uncoated graphite was checked with a standard test mixture containing phenol, anisole, p-cresol, phenetole and 3, 5-xylenol.

UV spectra of amino acids and their copper complexes were recorded by a Perkin Elmer Model 402 spectrophotometer (Perkin-Elmer, Beaconsfield, UK).

The particle properties and column dimensions used for different modes of liquid chromatography are summarized in Table 3.3.1.

3.3.2 Chemicals

Chemicals used as eluent components, solute analytes or modifiers were purchased from a variety of sources. They were of 'Analar' or similar high purity grades and used as received.

3.4 Procedures

Experimental methods for modifying porous grahite fall into three types according to the nature of the coating obtained. A general description of each is given briefly in this section. Fuller details may be found under appropriate headings.

Dynamic coating is achieved by the passage of an eluent containing dissolved modifiers through a column. The column is ready for use when an equilibration is attained. This can often be observed by the appearance of a breakthrough front and a subsequent steady baseline. This method offers great flexibility, it is particularly useful for modifiers of low molecular weight. Because of their weak adsorption, they can be readily stripped off to give a fresh graphite surface. When operating a column coated in this way the eluent must contain the modifier.

Insoluble coating is accomplished by applying an eluent to replace the solution of modifier which is at equilibrium with the column. The modifier, being insoluble in the eluent, is held on the surface so strongly that no bleeding occurs.

Cross-linked coating, different from the previous two methods, is carried out on the packing material before the column is packed. A polymeric modifier is adsorbed onto the surface of graphite from a static solution and followed by cross-linking to render it insoluble in all solvents. The coated particles are then dispersed in a suitable solvent (water in this work) and slurry packed into a column.

3.4.1 Adsorption Chromatography

Deactivation of strong sites on the graphite surface was achieved by the insoluble coating method. Modifiers such as dibenzenefluene and dibenzanthraquinone dissolved in chloroform were adsorbed onto the graphite by passing the solution through the column. Equilibration was indicated by the breakthrough method with UV wavelength set at 280 nm. Methanol predominant eluents were then applied to displace the solution of modifiers.

The removal of excess adsorption of modifers was then carried out by exhaustive elution of the column with eluotropically strong solvents such as benzene and toluene.

3.4.2 Ion Exchange Chromatography

Each of three methods for preparing an ion exchange coating on the graphite surface was examined with polyethyleneimine (PEI) as a modifier.

Dynamic coating was accomplished by continuously pumping an aqueous solution of PEI (0.05%, w/v, pH 7.0) through a column (50×4.6 mm) at 0.5 $ml\,min^{-1}$. As PEI is UV transparent the equilibration is indicated by constant retention of analytes instead of breakthrough curve.

Coating with an insoluble monolayer of PEI was achieved using a phosphate buffer ($0.1M$ $NaH_2PO_4 - 0.1M$ Na_2HPO_4) to displace the PEI solution with which the column was at equilibrium, PEI being insoluble in this buffer.

Coating of cross-linked PEI involved reaction of PEI with naphthalenesulphonyl chloride previously adsorbed on the graphite surface, followed by cross-linking with 1,4-butanediol diglycidyl ether. The detailed procedures are as follows: 0.6 g of porous graphite is added to an ethereal solution of 0.06 g of 2-naphthalenesulphonyl chloride and the suspension is allowed to stand for three

to four hours before the solution is filtered off. To 20 *ml* of an aqueous solution of PEI (1%, *w/v*) is added the coated graphite and the suspension is shaken mechanically overnight. The adsorbed coating of PEI is cross-linked by reaction with 1,4-butanediol diglycidyl ether in 5 *ml* of dioxane solution (5%, *w/v*) for three or four hours at room temperature. The coated graphite particls are collected on a filter, washed exhaustively with methanol and water, and packed at 6000 *psi* with water as slurry liquid.

The ion exchange capacity of the column is calculated from the breakthrough volume of an aqueous solution of sodium benzene sulphate (10 *mM*, pH 2.0 with phosphate acid) at flow rate 0.5 $ml\,min^{-1}$, and UV wavelength at 254 *nm*.

3.4.3   Chiral Chromatography

Chiral selectors are attached to the surface of graphite either as dynamic coating or insoluble coating.

Dynamic Coating

An eluent containing chiral selectors was prepared as follows:

Appropriate quantities of L-phenylalanine and copper sulphate are carefully weighed and separately dissolved in double distilled water. The solutions are then mixed to give a molar ratio of ligand to metal ion of 2 to 1 before addition of a phosphate buffer solution. Acetonitrile is added in volume percentage as required. The pH is adjusted with aqueous sodium hydroxide or orthophosphate acid. Before use, the eluent thus prepared is degassed in an ultrasonic bath under reduced pressure. It is important to check that no precipitation occurs by leaving eluent overnight whenever a new composition is prepared.

Insoluble Coating

Chiral selectors in this case are D and L-isomers of N-2-naphthalenesulphonyl phenylalanine, denoted as NS-D-Phe and NS-L-Phe, respectively. They were synthesized following Fischer and Bergell [82, 56]. 1.65 g (0.01 mole) of L-phenylalanine is dissolved in 20 ml of 1 N sodium hydroxide, an ethereal solution of 2.27 g (0.01 mole) of 2-naphthalenesulphonyl chloride is added and the mixture is shaken electromagnetically for three to four hours.

The sodium salt of the derivative is sparingly soluble in water and separates out during the reaction. The semiemulsion which results is acidified to congo red, whereupon the sodium salt goes into aqueous solution and the mixture separates into two layers. The derivative passes into the ethereal layer from which it begins to crystallize spontaneously in a few minutes. The crystals are collected on a filter and are recrystallized from a very small amount usually 5 ml or less of 60% ethanol. Several recrystallizations may be required to give a constant melting point. The product is vacuum dried. The yield of 50% can be easily achieved.

D-isomer of phenylalanine derivative is prepared in the same procedures except that D-phenylalanine is used in place of L-phenylalanine.

The calculated value for $C_{19}H_{17}NO_4S$ are C, 64.2; H, 4.82; N, 3.94%. Elemental analysis found: C, 64.3; H, 4.84; N, 4.00% for NS-L-Phe and C, 64.3; H, 4.83; N, 3.99% for NS-D-Phe.

The chiral selector, NS-L-Phe or NS-D-Phe, was adsorbed onto the graphite from a methanolic solution of varying concentration, the amount adsorbed being determined by the breakthrough method at UV wavelength of 320 nm.

Aqueous solution of copper acetate were used as eluents for the separations of amino acid enantiomers.

In selecting an ideal chiral selector some other amino acid derivatives have

been synthesized and tested. These compounds including benzenesulphonyl-L-phenylalanine, naphthalenecarbonyl-L-phenylalanine, and naphthalene-L-alanine were prepared following the analogous procedures as described above.

3.4.4 Exclusion Chromatography

Either monolayer or multilayer coating was attempted by impregnating porous graphite with an aqueous solution of polyvinyl alcohol (PVA). 0.6 g of porous graphite is dispersed in 5 ml of aqueous solution of PVA (0.5%) and the suspension is allowed to stand for four hours. The excess solution is filtered off to produce a monolayer coating whereas for the formation of a multilayer coating the solvent is evaporated to dryness under the controlled temperature, usually 120°C. The polymeric coatings adsorbed on the graphite surface are then cross-linked by reaction for four hours with 1,4-butanediol diglycidyl ether in 5 ml of dioxane solution (5%, w/v) in the presence of boron trifluoride etherate (0.5%, w/v) as base catalyst.

The coated material is then washed with ethanol (3 × 10 ml) and water(3 × 10 ml), successively and packed with water into columns under the pressure of 6000 psi.

Chapter 4

Adsorption Chromatography

4.1 Introduction

Adsorption chromatography is the oldest of all liquid chromatographic methods
as it was the original form of chromatography invented by Tswett about ninety
years ago. In contrast to its classical form, modern adsorption chromatography is
a rapid, efficient method and is still playing active role in separation of a variety
of compounds. The unique applicability of this technique is best represented
by the separation of C_{60} and C_{70} since these carbon clusters, being insoluble in
most of common polar solvents, pose a serious challenge to many other separation
methods [63].

In adsorption chromatography separation is based upon the selective adsorp-
tion of the solutes onto the surface of an adsorbent. The eluent used to displace
the adsorbed solutes can be polar or non-polar, depending upon the nature of the
adsorbent used. For instance, for the separation of polar or fairly polar organic
solutes, silicas are often employed in conjunction with non-polar solvents such as
hexane as eluents.

Unfortunately amorphous silicas, though widely used in chromatography,

have extremely heterogeneous surfaces [64]. At least two types of main active sites which have different adsorption strengths have been identified. The first type is free hydroxyl groups which are predominant species on the surface and the second type is hydrogen bonded hydroxyl groups which are considered to be 'tailing producing' sites. Accordingly, deactivation of silica adsorbent is generally required and this can be done by adsorption of a partial monolayer of modifier such as water or other polar compounds to those strong sites.

As discussed previously, porous graphite is a strong non-polar adsorbent and is commonly used with a polar eluent to effect the separation of polar solutes. In this context, the graphitic surface is responsible for the adsorption of the solutes whereas polar functional groups on the surface are expected to have negligible effects because they are deactivated by a layer of adsorbed eluent molecules. Following this we have some reason to believe that the poor chromatographic performance of some graphite adsorbents may be attributable to non-polar or dispersion interactions with the solutes rather than the ionic or hydrogen bonding interactions as found in adsorption chromatography with silica adsorbents.

4.2 Adsorption Isotherms

Adsorption of a solute from a dilute solution onto a homogeneous surface may be described in terms of the Langmuir equation [65]:

$$\theta = \frac{K^\circ C}{1 + K^\circ C} \tag{4.1}$$

where θ is the fractional coverage of the adsorbent surface by adsorbate, the value is equivalent to Q/Q°, the ratio of the quantity adsorbed, Q, to that when the surface is completely covered, Q°. K° is the thermodynamic equilibrium constant for the adsorption process, and C the concentration of the adsorbate.

Two limiting forms of the Langmuir isotherm are of particular interst to chromatographers. At low solute concentrations, the Langmuir equation reduces to a linear isotherm or Henry's equation ($Q = Q^{\circ}K^{\circ}C$). Thus the solute distribution coefficient becomes constant. At high solute concentrations the Langmuir equation shows θ approaching unity, i.e., the total solute concentration in the adsorbent phase becomes constant, corresponding to the completion of an adsorbed monolayer. The monolayer capacity Q° may be obtained by rearranging equation 4.1:

$$\frac{1}{Q} = \frac{1}{Q^{\circ}} + \frac{1}{KQ^{\circ}C}$$ (4.2)

For a Langmuir adsorption a plot of $1/Q$ versus $1/C$ should produce a straight line with the intercept of $1/Q^{\circ}$. This provides a simple test of whether a practical adsorption system obeys the Langmuir equation so as to permit the determination of the monolayer capacity.

The Langmuir equation is derived on the assumption that the surface of an adsorbent is homogeneous and no interaction occurs between the neighbouring adsorbed molecules [65]. It is obvious that not all systems conform to the Langmuir model. Deviations can occur due to either heterogeneity of the surface or interactions between adsorbed molecules.

As a first type of deviation from the Langmuir model one may consider ideal adsorption on a set of localized sites with weak interaction between adsorbed molecules on neighbouring sites. According to Fowler and Guggenheim [66], if the interaction is sufficiently weak that the random distribution of the adsorbed molecules is not significantly affected, the resulting expression for the isotherm is

$$\frac{\theta}{C(1-\theta)} = K^{\circ}exp(\frac{-2w\theta}{RT})$$ (4.3)

where $2w$ is the pair interaction energy (negative for attraction, positive for repulsion). For $w \to 0$ equation 4.3 reverts to the Langmuir expression. According to this model a plot of $\ln \frac{\theta}{(1-\theta)C}$ versus surface coverage θ should be linear with a slope proportional to w.

The second type of deviation arsing from surface hererogeneity has been studied by Graham [47] and Snyder [86]. Consider sorption on two sets of independent nonequivalent sites with no interaction between adsorbed molecules. It can be predicted that the Langmuir equation is not applicable to this case as the assumption of homogeneous surface is broken down. However the adsorption may be described as a superimposition of two independent Langmuir isotherms:

$$Q = \frac{Q_1^o K_1^o C}{1 + K_1^o C} + \frac{Q_2^o K_2^o C}{1 + K_2^o C} \tag{4.4}$$

where subscripts 1 and 2 refer to normal adsorption sites and strong adsorption sites, respectively.

For the equation to reduce to linear form, C should approach a low value as in the case of the Langmuir adsorption. Howerver, a comparison of equation 4.1 with equation 4.4 reveals that for the same low value of C, equation 4.1 may be approximated by a linear eqation $Q = KC$ but not equation 4.4 owing to the fact that K_2 for the adsorption on the strong sites is higher than K_1 for the adsorption on the normal sites. Thus reduction of solute concentrations is required to retain the isotherm linearity on the heterogeneous surface.

If C is sufficiently low, equation 4.4 reverts to Henry's equation as shown below by equation 4.5

$$Q = (Q_1^o K_1^o + Q_2^o K_2^o)C \tag{4.5}$$

This equation shows that in the presence of strong active sites the distribution constant is higher than that on the homogeneous surface consisting of solely normal adsorption sites. It is also clear that even if the capacity of the strongly

adsorbing sites Q_2^o is low but K_2^o is high the concentration at which the isotherm becomes non-linear can be very low. However if C is high enough that these sites become saturated then the isotherm can again become linear.

Peak Tailing

To a chromatographer who is mainly concerned with analytical rather than preparative separations, peak tailing is an annoyance, not only because it can ruin otherwise satisfactory separations but also because it complicates the evaluation of the column efficiency since the dynamic theories are no longer applicable in this case.

There are two primary sources of tailing: extracolumn and isotherm non-linearity. Tailing due to extracolumn effects such as poor sample injection and large dead volume in a chromatographic system has been treated in some detail by Sternberg [67]. Ideally, the sample should be introduced into the system as a narrow symmetric band. However inadequate injection may give rise to an exponential distribution of the solute, thus leading to tailing on elution. Large dead volume tends to cause tailing simply because it serves as an inadequate 'injector' in which the solute molecules diffuse into slow streamlines and thus fall behind those in the main stream. Fortunately this type of tailing can be easily identified by the experience based on routine observations [16] and therefore will not be pursued further.

The second type of tailing originates in the thermodynamics of adsorption process. The first attempt to relate the peakshape to the adsorption isotherm in terms of rigorous mathematical language is due to de Vault [85].

Under the assumptions of a plug flow and negligible mass transfer resistance, we have a differential mass balance equation for a trace of an adsorbable species

in a packed column:

$$u_m \frac{\partial C}{\partial z} + \frac{\partial C}{\partial t} + \phi \frac{\partial Q}{\partial t} = 0 \qquad (4.6)$$

where u_m is a linear velocity of the solvent, ϕ a ratio of the volume of the adsorbent to that of the interparticle space within the column.

If we assume adsorption equilibrium and mass transfer equilibrium can be represented, respectively, by

$$Q = f(C) \qquad (4.7)$$

and

$$(\frac{\partial Q}{\partial t})_z = \frac{dQ}{dC}(\frac{\partial C}{\partial t})_z = f'(C)(\frac{\partial C}{\partial t})_z \qquad (4.8)$$

the resulting mass balance equation becomes

$$\partial C \partial t)_z + \frac{u_m}{1 + \phi f'(C)}(\frac{\partial C}{\partial z})_t = 0 \qquad (4.9)$$

The linear velocity, $u(c)$, with which the solute band migrates through the column is given by

$$u(c) = (\frac{\partial z}{\partial t})_c = -\frac{(\frac{\partial C}{\partial t})_z}{(\frac{\partial C}{\partial z})_t} = \frac{u_m}{1 + \phi f'(C)} \qquad (4.10)$$

and the mean retention time is given by

$$t = \frac{L}{u(c)}[1 + \phi f'(C)] \qquad (4.11)$$

Figure 4.1 shows how isotherm linearity affects the chromatographic peaks. If the isotherm is linear $(f''(C) = 0)$, then there is no dispersion under equilibrium conditions. All concentration levels travel at the same velocity and the outlet response replicates the input with a time delay corresponding to the hold-up in the column. However for a nonlinear system the different concentration levels travel at different velocities since the slope of the isotherm $(f'(C))$ is concentration dependent. With a concave isotherm, typical in adsorption chromatography,
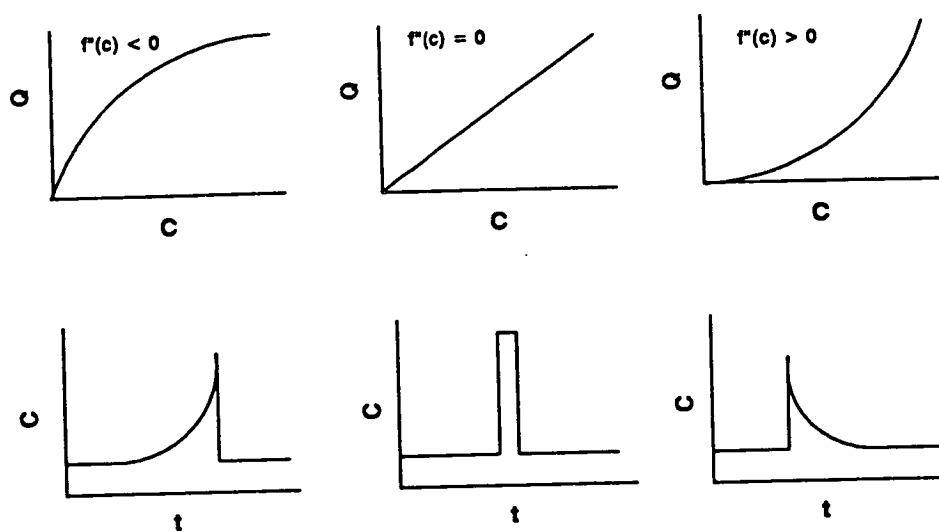
Figure 4.1. Schematic diagrams showing peakshapes under some typical equilibrium conditions.

the leading concentration front will tend to be sharp and the trailing front 'diffuse' during the development in the column. The initial spike like sample pulse therefore is eluted along the column as a peak with a sharp front, followed by a broadening tail. The tailed peak as recorded on elution is the image of the peak in the column.

In a linear system both the retention time and the peak shape are independent of sample size, but with a non-linear isotherm the retention time decreases and the peak becomes more and more dispersed and asymmetric with increasing sample size. Variation of sample size thus provides a simple test for system linearity.

Although such effects as diffusion and finite mass transfer rate are not allowed for, the theory can provide meaningful insight into the origin of peak tailing for more complex systems because the general pattern with respect to peak symmetry is not affected by these factors.

4.3 Heterogeneity of Graphite

It has been observed during the development of porous graphite that some batches of product are not acceptable in terms of column efficiency as badly peak tailing is produced for all types of solute. This was initially attributed to the residue oxides left behind by the heating processes [51]. A few examples are shown in Figure 4.2. For the reasons given in the preceding section, the peak tailing can be related to the nonlinearity of adsorption isotherm. At low solute concentrations, nonlinearity can be caused either by heterogeneity of the surface or by interactions between solute molecules on the neighbouring sites. As the latter is less likely given the fact that only trace amount of solute is introduced, the heterogeneity of the surface is likely to be the root cause and is accordingly
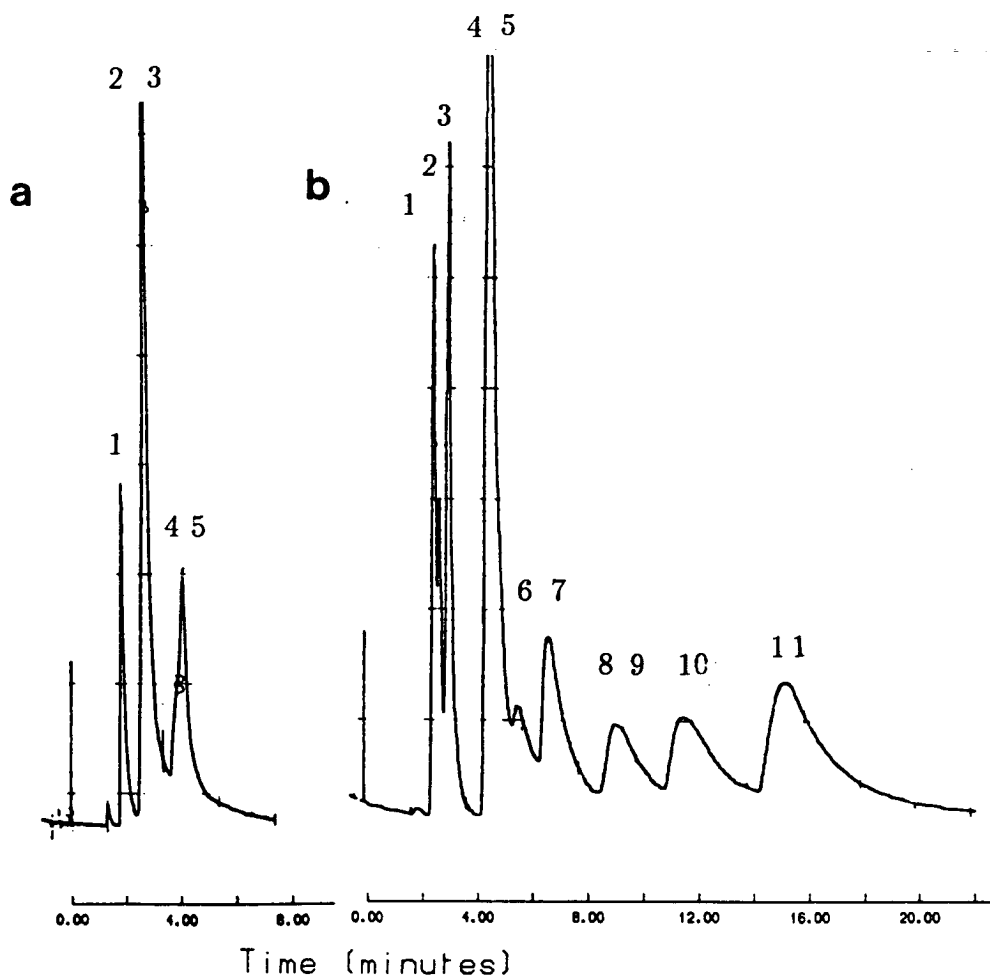
Figure 4.2. Separations on 'bad' batches of porous graphite. (a) Column, PGC A3, 100×4.6mm; eluent, methanol; flow rate, 1 ml/min, detection, UV 254 nm. Solutes: 1 = phenol, 2 = anisole, 3 = p-cresol, 4 = phenetole, 5=3, 5-xylenol. (b) Column, PGC A2, 100 × 4.6; eluent, methanol-water (80:20); flow rate, 0.87 ml/min, detection, UV 254 nm. Solutes: $1 = PhNH_2$, $2 = PhH$, $3 = PhOH$, $4 = PhMe$, $5 = PhCN$, $6 = PhOMe$, $7 = PhBr$, $8 = PhCOMe$, $9 = PhI$, $10 = PhNO_2$, $11 = PhCOOMe$.

examined.

The adsorption of dibenzanthrequinone (DBAQ) from chloroform solution onto a sample of graphite, PGC A2, has been studied by the breakthrough method. The adsorption isotherm is-shown in Figure 4.3 (a). It appears to follow the Langmuir adsorption but with H-type character at low concentration region. This becomes obvious by casting the isotherm equation in a reciprocal form where a straight line is found except in low concentration region, where $1/Q$ is smaller than it should be according to the Langmuir isotherm for low values of C, as shown in Figure 4.3 (b). The deviation from the Langmuir adsorption is thus attributed to the heterogeneities on the surface of graphite.

4.4   Deactivation of Graphite

The peak tailing and the deviation from the Langmuir adsorption highlight the presence of strong adsorption sites on the surface of the graphite samples. The proportion of these strong sites is expected to be very small compared to the prevailing normal adsorption sites. Perhaps this is why deviations occur in low concentration region and disappear with increase in concentration as the strong sites are saturated. The concentrations of strong sites vary from batch to batch, depending upon the conditions of graphitization. For example, two types of graphitized carbon sample studied by Graham [47], Graphon and P-33 (heat treated at 3000K), were found to contain 1.25% and 0.15% strong sites, respectively. With respect to the relative strength of adsorption sites, the adsorption heats of strong site were estimated to be twice in magnitute that for the normal sites. Because of these energetic differences, it is reasonable to expect that strong sites can be deactivated by preferential adsorption of high molecular weight compounds. This situation mirrors the deactivation of silica by adding a
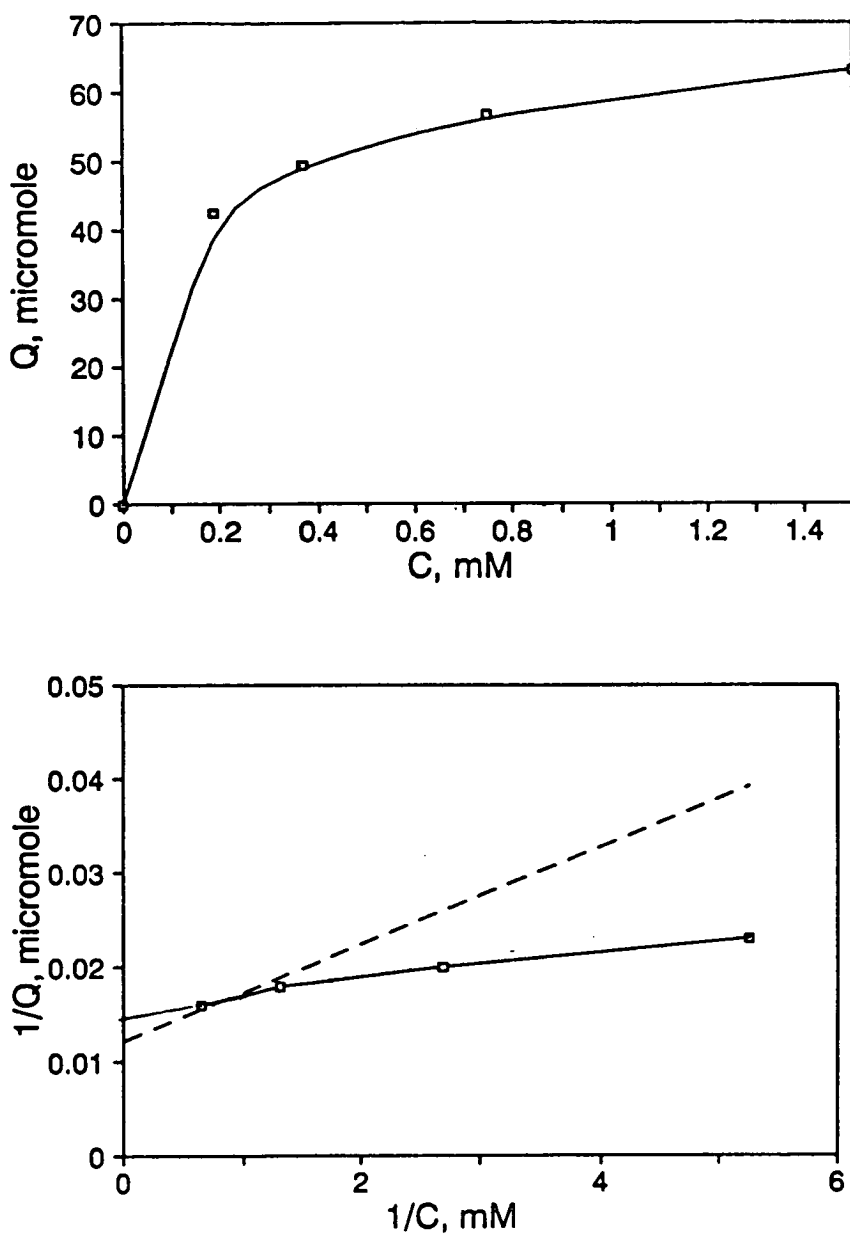
Figure 4.3. Isotherms for adsorption of dibenzanthrequinone from chloroform onto graphite, PGC A2. (a) Normal adsorption isotherm. (b) Reciprocal form of adsorption isotherm.

small amount of water in hexane-predominant eluents.

Two aromatic compounds, dibenzofluorene(DBF) and dibenzanthrequinone (DBAQ), were used as modifiers since their planar configurations, well matched with the graphite surface, are expected to offer the best chance to achieve 'permanent' deactivation.

The graphite sample PGC A3 was deactivated by adsorption of DBF from a chloroform solution, and about 13 mg of DBF were adsorbed as determined by the breakthrough method. An improvement in column efficiency is indeed obtained as shown in Figure 4.4. There are five distinct sharp peaks obtained for the standard test mixture, however under the same elution condition, only three peaks with severe tailing could be identified before the column was treated (see Figure 4.2). Thus the adsorptive modification proves to be effective in improving the chromatographic properties of a packing owing to the masking of strong sites.

In an attempt to restore the original surface character, the DBF-coated column was subject to the elution of a large quantity of toluene, which is classified into the strongest solvents in eluotropic strength on the graphite [68]. After the adsorbed molecules were washed out , the baseline was brought down to the normal level, the column was then tested with the same mixture under the same chromatographic conditions. Chromatograms obtained as illustrated in Figure 4.4 clearly show that, apart from slight increase in retention, no loss of column efficiency and peak symmetry were observed with the removal of adsorbed modifier molecules. It is likely that the treatment of toluene removes the modifier molecules adsorbed on the normal sites while has little effects on the molecules on the strong sites. Because of large energy change involved, the adsorption on strong sites is so strong that it may be treated as chemisorption. It is almost impossible to remove adsorbed adsorbed modifiers from these strong sites under the usual chromatographic conditions, the intention of permanent
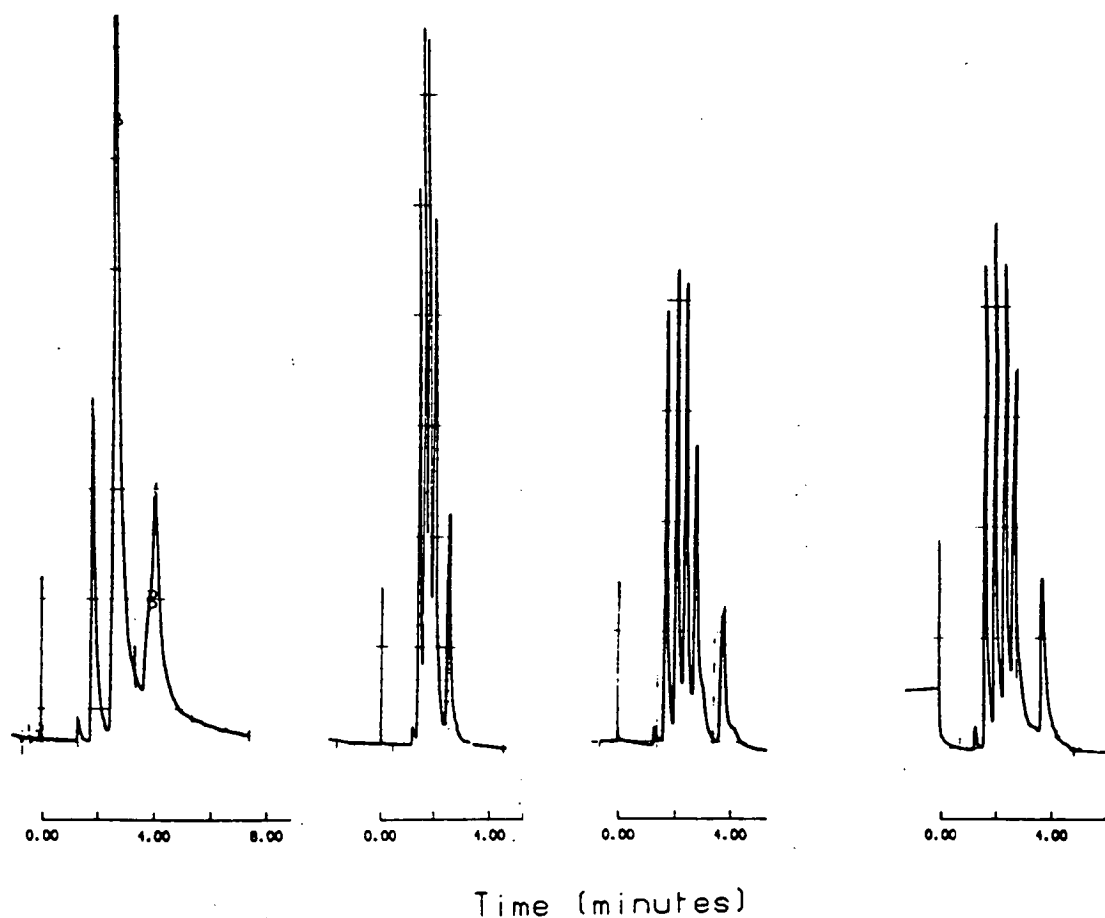
Figure 4.4. Deactivation of graphite. From left to right: column, as originally tested; column, after adsorption of *dibenzofluorene,* after washing with 500 *ml* toluene; column, after washing with 1000 *ml* toluene. Conditions and solutes as for Figure 4.2 (a).
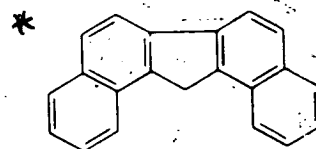
deactivation is therefore fulfilled in this way.

Similar results were obtained for the column PGC A5 with DBAQ as modifier. The column was brought to equilibration with 0.05 $mg\,ml^{-1}$ of chloroform solution, and then subject to washing with 2 litres of benzene by passing the solvent through the column. An improvement both in column efficiency and peak symmetry was observed once again for the same test mixtures as used in previous study. The resulting separations are shown in Figure 4.5.

The effect of modifier coverage on retention and selectivity was investigated with benzene derivatives as solutes. The column of different coverage of DBAQ was obtained by adsorbing different amounts of DBAQ onto the packing of column PGC A2 from chloroform solution of various concentrations. The values of k' for solutes were recorded at each surface coverage. The results are shown in Figure 4.6 as plots of capacity ratio against quantity adsorbed for the mixture of substituted benzenes.

From the figure, it can be seen that decrease in retention and selectivity of solutes was a general trend with increase in the surface coverage, however, at high surface coverage, the reversal of elution order for some solutes was observed. Thus varying the coverage of modifier on the graphite surface is a simple means of controlling the retention and selectivity.

4.5   Conclusions

This work establishes that peak tailing in adsorption chromatograhy as observed with some batches of poorly produced porous graphite is mainly caused by geometric heterogeneity on the surface. As an alternative to heat treatment to promote further graphitization, adsorptive modification is an economic way to
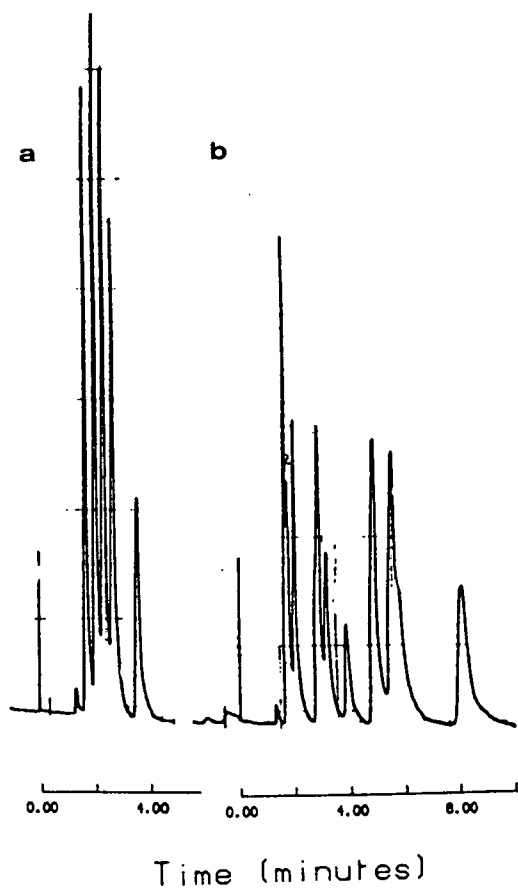
Figure 4.5. Separations on deactivated graphite. Column, PGC A5, treated with DBAQ; others in (a) and (b) as for Figure 4.2 (a) and (b), respectively.
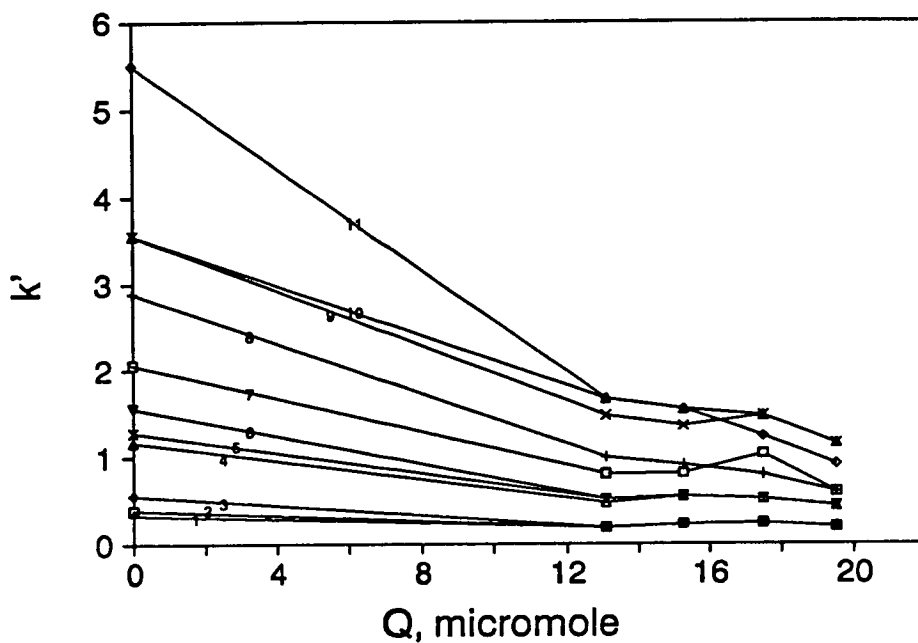
Figure 4.6. Effect of the amount of modifier adsorbed on retention. Solutes: $1 = PhNH_2$, $2 = PhH$, $3 = PhOH$, $4 = PhMe$, $5 = PhCN$, $6 = PhOMe$, $7 = PhBr$, $8 = PhCOMe$, $9 = PhI$, $10 = PhNO_2$, $11 = PhCOOMe$. Conditions as for Figure 4.2 (b).

reduce the effect of the surface heterogeneity and hence to improve the chromatographic properties. Deactivation of graphite by adsorption of polyaromatic compounds is virtually permanent owing to the strong adsorptive strength on the defective sites. Selectivity different from that of bare graphite is attainable by coating the graphite with a layer of modifiers, thus the graphite serves as a support, in analogy with silica in chemically bonded phases.

Chapter 5

Ion Exchange Chromatography

5.1 Introduc tion

Ion exchange chromatography has been a useful technique for the separation of ionic or ionizable compounds which range from inorganic ions to biopolymers such as nucleotides and proteins. Like all other forms of HPLC, the key to success of ion-exchange separations lies in the design of a stationary phase, which is often referred to as ion exchanger. The ion exchanger in general consists of solid support and functional groups on its surface. There are several different types of ion exchanger available. The early materials used in classical chromatography were made by bonding acidic or basic functional groups onto a porous matrix produced by co-polymerization of styrene and divinylbenzene, but were unable to withstand high pressure and tended to swell in solvents. Modern resins have been greatly improved in terms of rigidity by increasing cross-linkages in the matrix. However, the efficiencies obtained with these materials have not equalled those of chemically bonded ion exchangers based on silica gels. This is probably due to the unfavourable mass transfer properties of organic phases.

In an effort to overcome the mass transfer effects Horvath et al [22] introduced,

in 1967, pellicular ion exchangers which were made by coating impervious glass beads with a layer of ion exchange resin. Such materials have been largely superseded by packing materials which consist of porous silica gel with ion exchange functional groups chemically bonded onto the surface [64]. These materials are much more efficient due to their excellent mass transfer properties and their ability to withstand pressure. As with all other silica based packing materials they have limited operating range of pH (2-8). An expansion of pH range is desirable for regeneration of the column and control of exchange capacity.

Being chemically stable and mechanically robust, porous graphite would be an ideal supporting material, particularly for ion exchange chromatography. This chapter is devoted to our efforts to confer ion exchange properties on porous graphite. A theoretical consideration of ion exchange process is presented first, followed by discussions on the mechanism of separations using surface coated graphite as ion exchanger.

5.2   Theory of Ion Exchange

Ion exchangers can adsorb solutes from solution with which they are in contact. The sorption behaviour of electrolytes is quite different from that of non-electrolytes. While the neutral species are sorbed by ion exchangers in the same way as by nonionic adsorbents, the charged species are subject to the electrostatic forces arising from the interactions with the fixed ionic groups in the adsorbents. The result is a so called Donnan-type sorption equilibrium which is unique for ionic sorbents.
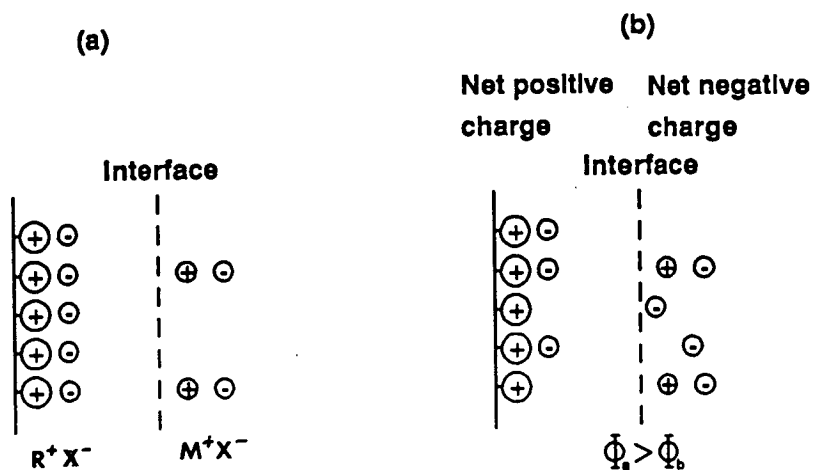
Figure 5.1. The formation of an electric potential (a) There is initially a net migration of anions (in this case) from left to right through the interface and so a small charge imbalance is set up. (b) At equilibrium, when a potential difference between the solutions has been established, the rates of passage of the anions are the same in both directions.

5.2.1   Membrane Potential

The classical theory of sorption of electrolytes by ion exchangers has revolved round the concept of the 'membrane potential' [71]. Consider an anion exchanger R^+, saturated with counterions X^- and let it immerse in a dilute solution of a salt MX. Under thermal agitation the ion X^- in the exchanger tends to diffuse into the more dilute solution but the cation R^+ cannot follow as it is fixed on the solid support. Consequently an electric potential difference is set up across the interface, as shown in Figure 5.1.

The process will not proceed indefinitely because the charge separation it builds retards the further diffusion of anions. At equilibrium the electrochemical

potentials of X^- are the same on either side of the interface. This situation resembles membrane potentials built up between two solutions containing different concentrations of the salt MX and separated by a membrane permeable only to X^- [72].

If the two phases are denoted by s and m the condition of equilibrium is

$$\bar{\mu}_{X^-(s)} = \bar{\mu}_{X^-(m)}. \tag{5.1}$$

where $\bar{\mu}$ is electrochemical potential which includes the chemical potential μ, the electric work $ZF\Phi$, where Z is the number of charge the ionic species carries, F is Faraday constant, and Φ electrical potential.

The sorption equilibrium is then expressed in terms of chemical potential and electric potential as follows:

$$\mu_{X^-(s)} + ZF\Phi_{(s)} = \mu_{X^-(m)} + ZF\Phi_{(m)} \tag{5.2}$$

Rearranging the above equation and inserting activity for μ yields the electric potential difference at equilibrium

$$\Delta\Phi_{(s,m)} = -\frac{1}{ZF}[\Delta G^o_{X^-(s,m)} + RT\ln\frac{a_{X^-(s)}}{a_{X^-(m)}}] \tag{5.3}$$

where $\Delta G^o_{X^-(s,m)}$ is the standard free energy difference for the transfer of anion X^- from the solution to the stationary phase in the absence of the electric potential difference.

By rearranging equation 5.3 the equilibrium constant is given as

$$K^o = exp[-\frac{\Delta G^o_{X^-(s,m)} + ZF\Delta\Phi_{(s,m)}}{RT}] \tag{5.4}$$

It is apparent that the sorption of electrolytes onto a charged surface is controlled by two terms, chemical and electrical potentials. This conceptual separation of the free energy change involved in an ion exchange process is helpful to understand the retention behaviour of some simple ions. For instance, if a series

of ions were known to have the same electrical potential differences in a given system, they would be eluted in the order of their ionic radii with large molecules eluted first. This is because the dispersion forces, as the main component of the chemical potential, diminish rapidly with the distance between species under interaction. Nevertheless, this approach is found unpractical since the $\Delta\Phi$ is a parameter subject to no direct experimental determination, it is thus impossible to relate the individual terms of the free energy change to the properties of the ion exchanger. This problem cannot be solved by routine thermodynamic thinking, but requires the knowledge of the structure of interphase region, i.e. the location and arrangement of charges.

5.2.2   Electric Double Layer

The structure of the interphase region is best understood in terms of Stern's double layer model [87, 70]. The interface between the charged surface and an electrolyte solution can be regarded as consisting of two regions: an inner region known as Helmholtz layer which may include adsorbed ions and a diffuse region in which ions are distributed according to the influence of electrical forces and random thermal motion, see Figure 5.2 (a). The theoretical treatment of the double layer model shows that the potential decreases linearly with distance from the surface in the Hemholtz layer while exponentially in the diffuse region, see Figure 5.2 (b). Thus the potential, Ψ, in the Helmholtz layer and in the diffused region may be estimated from the following respective equations:

$$\Psi = \Psi_o - \frac{\sigma_o d}{\varepsilon_o \varepsilon_r} \qquad (5.5)$$

and

$$\Psi = \Psi_H exp(-\frac{x}{\kappa^{-1}}) \qquad (5.6)$$

in which the following notation is used:
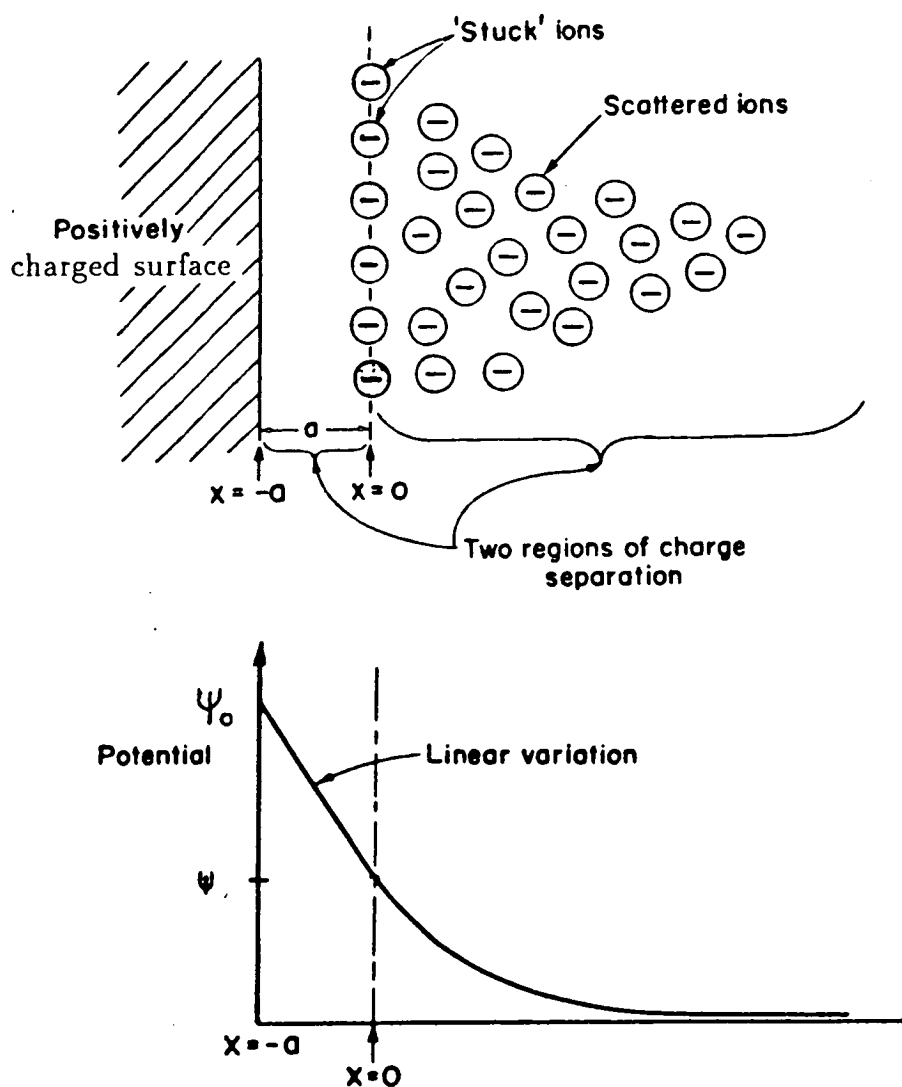
Figure 5.2. Electic double layer. (a) The Stern model with a layer of (-) excess charge fixed to the positively charged surface and the remainder scattered in cloud fashion. The *locus* of centres of the fixed ions is at a distance *a* from the surface. (*Note:* Only the excess charges are shown in the diagram, and the water molecules are omitted. The latter sit on the surface and separate it from the ions.). (b) The potential variation according to the Stern model.
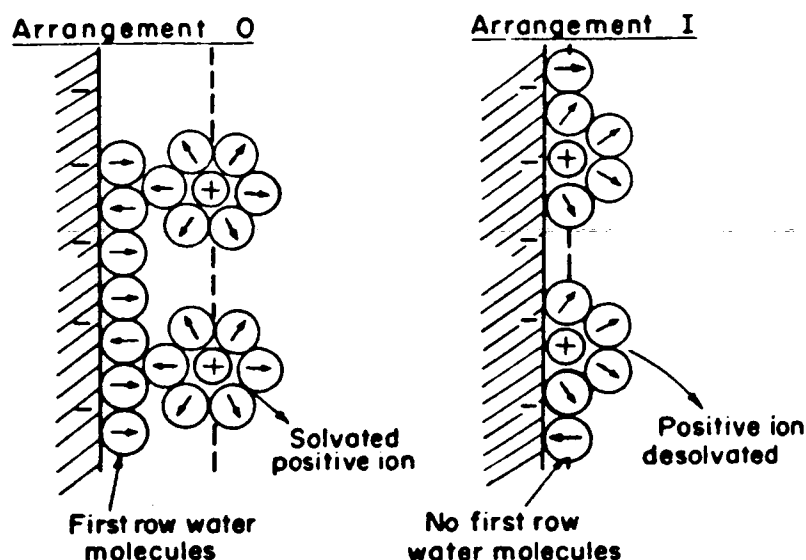
Figure 5.3. Schematic diagrams for arrangement of ions in the Helmholtz layer. (a) Arrangement O and (b) Arrangement I. Conpensating charges in the diffuse layer are not shown.

Ψ, Ψ_o, Ψ_H = Electrical potentials at a distance from the charged surface,

at the surface, and at the Helmholtz plane, respectively;

σ_o = Charge density at the surface;

ε_o = Permittivity in vacuum;

ε_r = Relative permittivity in the medium;

d = Distance from the surface within the Hemholtz plane;

x = Distance from the Helmholtz plane;

κ^{-1} = 'Thichness' of the diffuse charge layer, given by $\left(\frac{\varepsilon_o \varepsilon_r RT}{2CF^2}\right)^{\frac{1}{2}}$

As far as the sorption of ions is concerned the inner part of the double layer is of primary importance. It is therefore necessary to take a close look at the Helmholtz layer. According to Grahame [88], the Helmholtz layer can be further divided into two parts: the inner Helmholtz layer and the outer Helmholtz layer. As shown in Figure 5.3, hydrated ions can take either arrangement O or arrangement I. The plane drawn through the locus of centres of the hydrated ions in the

arrangement O is the OHP (outer Helmholtz plane) and accordingly the locus of centres of dehydrated ions in the arrangement I is defined as the IHP (inner Helmholtz plane).

Whether ions occupy the OHP or quit the OHP and populate the IHP is the matter of the free energy change for ions to move from the OHP to IHP while at the same time displacing the appropriate number of adsorbed water molecules. If the free energy change is negative ions will make move. The study of the forces operative have revealed that interactions which contribute to the total free energy can be classified into three groups: (1) water-surface interaction; (2) water-ion interaction; (3) ion-surface interaction. The first two interactions involving water are considered under the heading of hydration as they act as resisitance to a contact adsorption to occur. The third group of interactions is the only force to draw ions to the charged surface, which may be considered as composed of two main contribution terms: the dispersion interaction and the electrical interaction. Thus the standard free energy change for transfer of a mole of hydrated ions from a bulk solution to the charged surface can be expressed as

$$\Delta G^o_{tot} = \Delta G^o_{dis} + \Delta G^o_{ele} + \Delta G^o_{hyd} \tag{5.7}$$

The expressions available for the estimation of respective interaction energies are as follows:

$$\Delta E_{dis} = -(\frac{3}{2}\alpha_1\alpha_2 \frac{I_1 I_2}{I_1 + I_2})/r^6 \tag{5.8}$$

$$\Delta E_{ele} = Ze\Delta\Phi = Ze(\Psi_o - \frac{\sigma_o}{\varepsilon_o\varepsilon_r}d) \tag{5.9}$$

$$\Delta E_{hyd} = \frac{Z^2 e^2}{8\pi\varepsilon_o R}(1 - \frac{1}{\varepsilon_r}) \tag{5.10}$$

where

α_1, α_2 = Polarizabilities of molecules 1 and 2;

I_1, I_2 = Ionization potentials;

r = Distance between two molecules;

R = Radius of hydrated molecules;

d = Distance from the charged surface within the Helmholtz layer.

As can be seen from the above expressions, a high electrical potential is essential for ions to take the arrangement I. The strong electrical interaction will provide sufficient energy for the ions to overcome the hydration barrier to approach the bare surface. The closer the ions to the surface, the stronger the attractive forces because the energy of dispersion interaction increases in an inverse sixth power of the distance between two molecules under interaction. The dispersion interaction may become predominant when the ions make attachment on the surface. If this is the case the free energy change in magnitude will decrease with the ionic radius.

On the other hand, ions may prefer to stay at the OHP and go no farther to the bare surface than this plane, if the potential on the surface is not sufficiently high for the ions to get rid of the hydration sheaths. Since no change in hydration energy is involved , and dispersion interaction is relatively unimportant at large distance, the electrical interaction is likely to be primarily responsible for the migration of the ions towards the OHP. The energy of this interaction decreases as δ increases, where δ is the distance between the OHP and the surface. The value of δ may be estimated as shown in Figure 5.4. In this case the standard free energy change ΔG^o_{tot} is expressed in terms of the potential at the OHP:

$$\Delta G^o_{tot} = -ZF\Psi_{OHP} = -ZF[\Psi_o - \frac{\sigma_o}{\varepsilon_o\varepsilon_r}(2r_w + \sqrt{3}r_w + r_i)] \qquad (5.11)$$

The above equation shows once again that the free energy change decreases with ionic radius when adsorption occurs solely on the OHP.
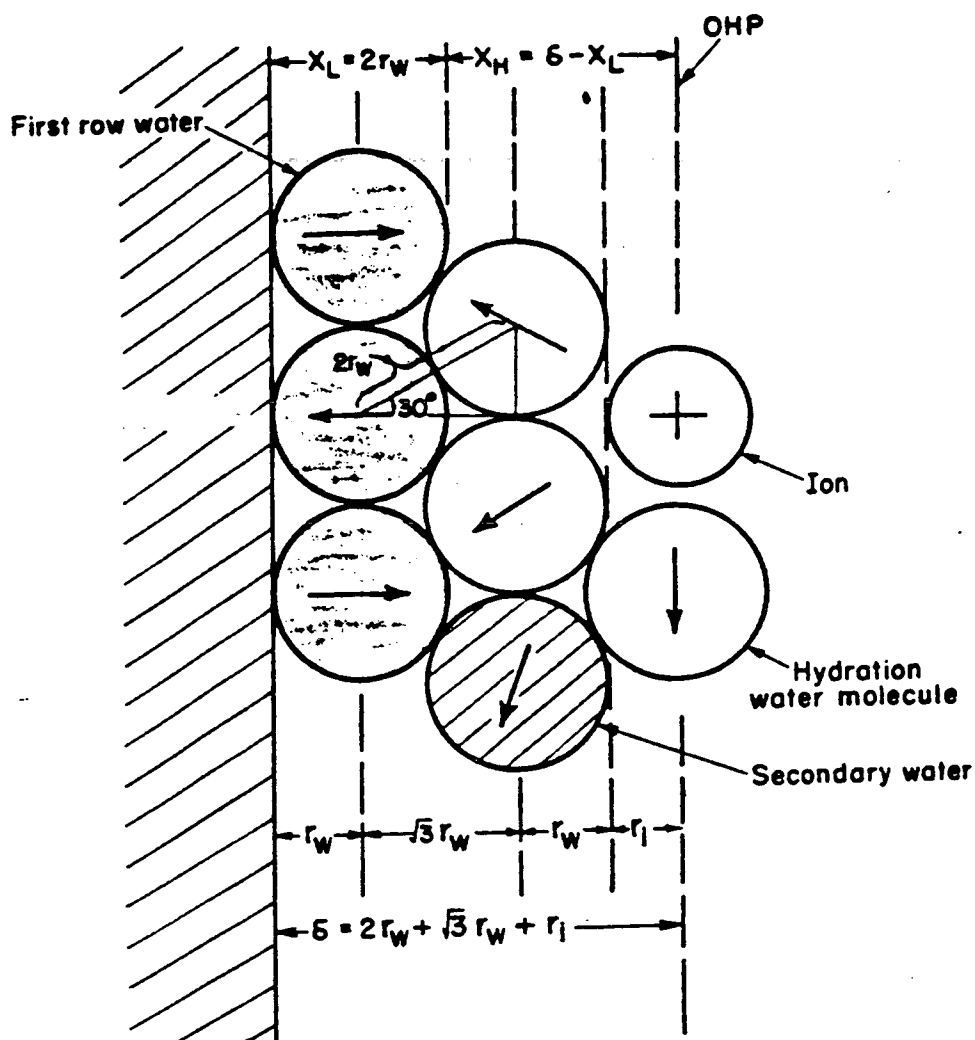
Figure 5.4. Schematic diagram for the calculation of distances between the OHP and the surface. From Ref [87].

Apart from these two extreme cases, there are a great number of intermediate states where partially dehydrated ions adsorb in a plane at a certain distance to the bare surface. Since the distance is determined by the balance of forces exerted on the ion, the ion of low hydration energy will get closer to the surface than that of high hydration energy, thus leading to strong binding. It has been observed in ion exchange chromatography that the order of the alkali metal ions bound to sulfonate ion exchanger is in accordance with their ionic radii. This is often attributed to the fact that the ion of larger ionic radius has lower hydration energy and hence stronger binding [71]. However, when the functional groups of the ion exchanger are replaced with carboxyl or phosphate groups, this order is changed and in part reversed [106]. The reversal of the binding order is likely due to the decrease in the electric potential on the surface, giving rise to weak electric interactions between the adsorbent and the adsorbates. Thus the adsorption on the OHP prevails where the ion of small radius has high binding strength.

5.3 Mechanism of Ion Exchange Chromatography

As noted above, the distribution of an ionic species between two phases can be described in terms of the equation derived from the concept of membrance potential. However it is not convenient for practical applications as the activity coefficient of the adsorbed species is an unknown parameter. As for the adsorption of a neutral species, the Langmuir equation is found adequate to describe the adsorption of the ions on the charged surface, provided that the surface concentration of the fixed charged groups is sufficiently low that repulsive interactions between neighbouring adsorbates are negligible. It is well known that electrolyte

solutions are markedly nonideal even at low concentrations, it is therefore neces-
sary to use activity in place of concentration in the treatment of ion adsorption
equilibria.

Accordingly, the Langmuir equation is written in terms of activity as

$$\theta = \frac{K^\circ a_m}{1 + K^\circ a_m} \tag{5.12}$$

where θ is the fraction of the occupied surface, a_m is the activity of the ionic
species in the bulk of solution and K° is a constant, which as usual is related to
the standard free energy change through equation 5.13

$$\Delta G^\circ = -RT \ln K^\circ \tag{5.13}$$

As has been discussed in the preceding chapter, two limiting forms of the
Langmuir equation can be derived, corresponding to linear isotherm and mono-
layer coverage, respectively. In ion exchange chromatography a monolayer cov-
erage of ion exchanger by eluent components is often assumed and thus variation
of the electrolyte concentrations will not affect the surface coverage [30]. This
assumption may not be fulfilled in some cases, especially when a low concentra-
tion weak electrolyte solution is used as an eluent. According to the theory of
electrical double layer, a complete coverage of the charged surface in contact with
a dilute solution is unlikely to occur unless the components of the solution have
binding strengths strongly enough to overcome the thermal agitation. Applying
the full form of the Langmuir equation to the treatment of ion adsorption in ion
exchange is thus thought to be a more realistic approach.

Let us consider an ion exchange system containing an anion exchanger R^+,
counterion in the buffer solution B^- and an analyte ion A^-. At equilibrium, the
following equations are used to express the distribution and competition for the

adsorptive sites:

$$R^+ + B^- \ \rightleftharpoons \ RB \tag{5.14}$$

$$R^+ + A^- \ \rightleftharpoons \ RA \tag{5.15}$$

$$RB + A^- \ \rightleftharpoons \ RA + B^- \tag{5.16}$$

Equation 5.16 is not independent being obtained by substituting the first two equations.

Applying the multicomponent Langmuir equation to the first two equations gives:

$$\theta_B = \frac{K_B^o a_B}{1 + K_B^o a_B + K_A^o a_A} \tag{5.17}$$

$$\theta_A = \frac{K_A^o a_A}{1 + K_B^o a_B + K_A^o a_A} \tag{5.18}$$

In analytical chromatography, only trace amount of analytes are present, which are usually considered to be negligible relative to the other ionic species in the buffer solution. If this convension is accepted then equations 5.17 and 5.18 can be simplified

$$\theta_B = \frac{K_B^o a_B}{1 + K_B^o a_B} \tag{5.19}$$

$$\theta_A = \frac{K_A^o a_A}{1 + K_B^o a_B} \tag{5.20}$$

The distribution coefficient of the analyte species is then given by

$$D = \frac{Q^o \theta_A}{a_A} = \frac{Q^o K_A^o}{1 + K_B^o a_B} \tag{5.21}$$

where Q^o is the monolayer capacity of an ion exchanger. Rearranging the above equation gives

$$\frac{1}{D} = \frac{1}{Q^o K_A^o} + \frac{K_B^o}{Q^o K_A^o} a_B \tag{5.22}$$

Plotting $1/D$ against a_B should produce a straight line with an intercept of $1/Q^\circ K_A^\circ$ and a slope $K_B^\circ/Q^\circ K_A^\circ$. The same relation should hold if distribution coefficient D is replaced by retention capacity factor k' since $k' = \phi D$. Thus the plot of $1/k'$ versus a_B provides a simple test for the ion exchange mechanism proposed above, which may be termed as 'adsorption machanism' to distinguish from the others.

An alternative mechanism widely accepted in the literature is so called ' displacement mechanism'. This is based on the assumption that the ion exchange sites are fully occupied by the equal number of the counterions and the adsorption of the analyte ions takes place by displacing the adsorbed counterions. This process may be represented by equation 5.16, the equilibrium constant being given by

$$K_{IE} = \frac{a_{RA} a_B}{a_{RB} a_A} \tag{5.23}$$

The distribution coefficient, D, is then given by

$$D = \frac{a_{RA}}{a_A} = \frac{K_{IE} a_{RB}}{a_B} \tag{5.24}$$

By the above mentioned assumption, a_{RB} is a constant, independent of a_B, thus can be combined with K_{IE} to give a new constant, K, equation 5.24 becomes

$$D = \frac{K}{a_B} \tag{5.25}$$

Rearranging the above equation yields

$$\frac{1}{D} = \frac{a_B}{K} \tag{5.26}$$

which shows a plot of $1/D$ versus a_B will produce a straight line . At the first glance one would think this result is the same as expected from the 'adsorption mechanism', however, closer inspection of these two plots reveals a distinct difference. When the plot of $1/D$ versus a_B is extrapolated to $a_B = 0$, the adsorption

mechanism gives an intercept, characterized by the equilibrium constant, K_A; whereas the displacement mechanism predicts the straight line will pass through the origin. Thus whether or not the plot produces an intercept can be taken as to indicate which mechanism is predominent under given conditions.

5.4 Results and Discussion

5.4.1 Separations of Inorganic Anions

A variety of ionizable compounds can be readily adsorbed by porous graphite and hence serve as 'fixed' functional groups which are necessary to carry out ion exchange chromatography with the graphite. Polyethyleneimine(PEI) has been found to be unique in that it possesses properties which allow each of three methods developed for coating graphite to be tested. Firstly, polyethyleneimine is highly hydrophilic and can be mixed with water in all proportion. This is ideal for dynamic coating technique. Secondly, upon the addition of electrolytes, it precipitates out from aqueous solutions, thus an insoluble layer adsorbed on the graphite surface is obtained in a very simple way. The third important property of polyethyleneimine is that it can be readily converted into a cross linked network by a bifunctional group reagent [105]. It is apparent that the adsorbed layer might have insufficient long term stability as a gradual leaching of weakly adsorbed solutes could occur, it is desirable that the adsorbed layer of PEI can be cross-linked to render it insoluble in all solvents.

Dynamic Coating

Figure 5.5 shows the separation of anions on the graphite dynamically coated with PEI. The baseline separation of iodate, bromide, nitrite and nitrate was
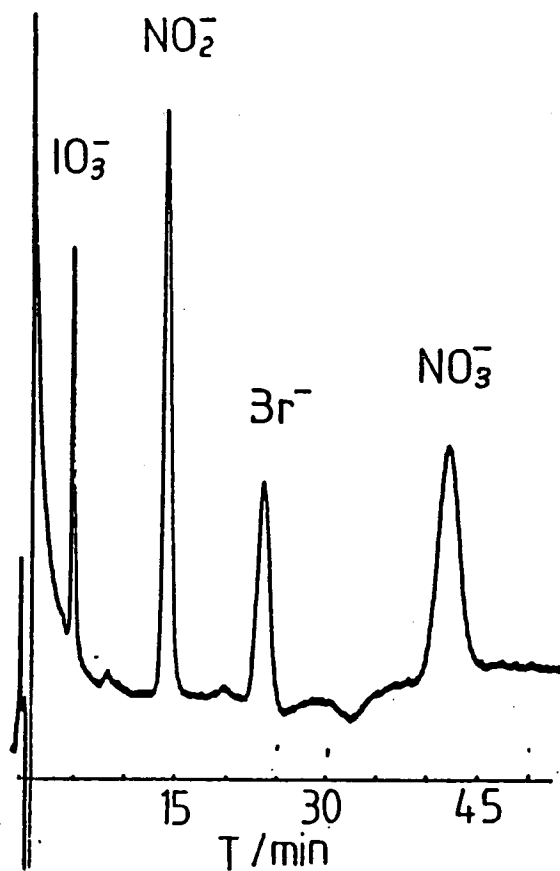
Figure 5.5. Separation of anions on the graphite dynamically coated with PEI. Column, PGC 94F, 50 × 4.6 mm; eluent, 0.1% (w/v) aqueous PEI, pH 7.0; flow rate, 0.5 ml/min; detection, UV 220 nm; temperature, 30^oC.
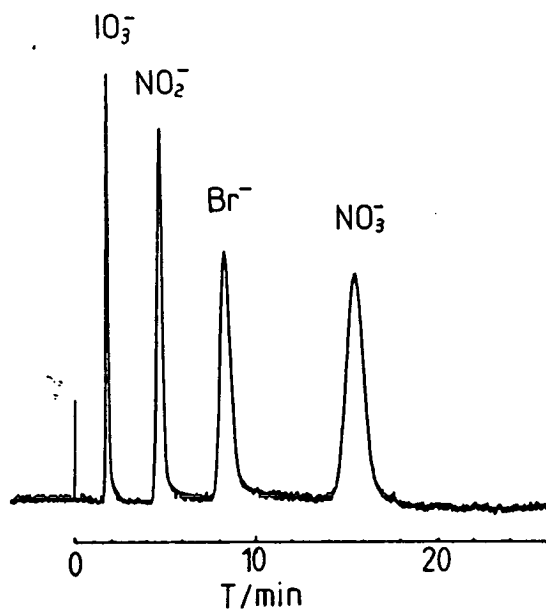
Figure 5.6. Separation of anions on graphite coated with insoluble monolayer of PEI. Column, PEI coated PGC 94F, 50 × 4.6 mm; eluent, $0.02M$ sodium phosphate, pH 7.0; flow rate, 0.5 ml/min; detection, UV 220 nm; temperature, ambient.

readily achieved with the elution order as the same as in conventional anion chromatography [106]. It is noticeable that fairly high efficiency has been achieved with the dynamic coating of PEI even for late eluted epecies. This is presumably attributed to the improvement in the surface characteristics brought about by the coating.

Insoluble Monolayer Coating

Figure 5.6 shows the separation of anions on the graphite coated with an insoluble monolayer of PEI. The analytes were eluted in generally the same order as in Figure 5.5. The retention was less since the eluent contained a higher concentration of counterions.
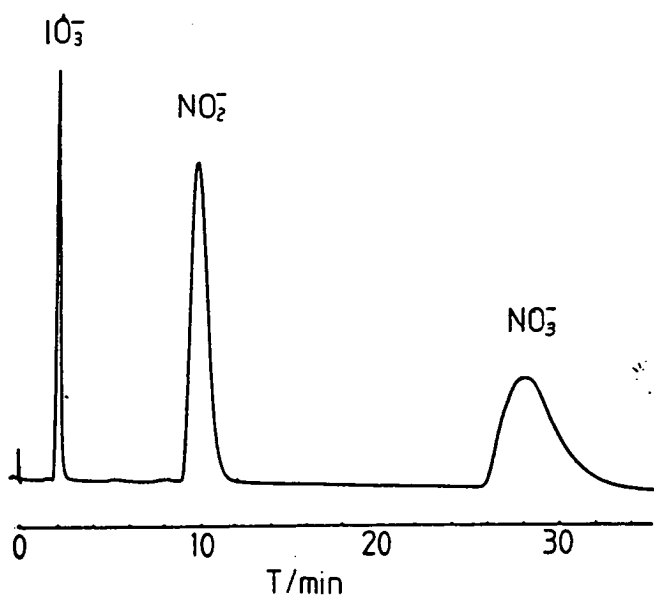
Figure 5.7. Separation of inorganic anions on graphite coated with cross-linked PEI. Conditions as for Figure 5.6. $(Br^- \text{ omitted})$

Cross-linked Network

Figure 5.7 shows the separation of anions on a cross-linked PEI coating. The elution pattern was essentially the same as in Figure 5.5 but the retention was greater due to the increase in ion exchange capacity. It was found that the exchange capacity varies over the range of 2.5 - 3.8 $\mu mol\, m^{-2}$, depending upon the conditions of coating. It may be noted that the column efficiency is inferior to those of the graphites coated in-column. Although it is likely that increased column efficiency would be obtained with the improvement of the packing procedure, we do feel that this low efficiency was due at least in part to the fact that the cross-linked polymer coating impair the pore structure of the original graphite support, thus giving rise to unfavourable mass transfer properties.
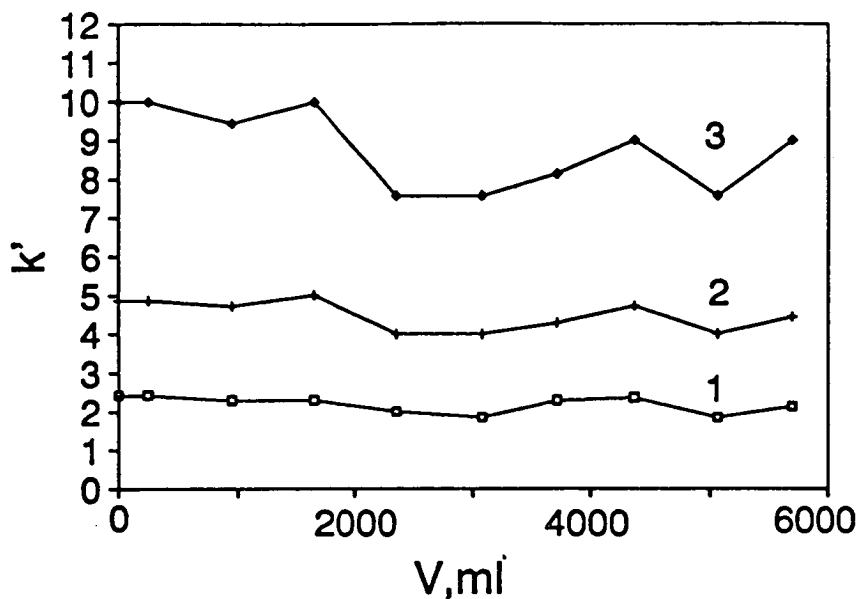
Figure 5.8. Column stability against elution. Solutes: 1 = nitrite, 2 = bromide, 3 = nitrate. Conditions as for Figure 5.6

5.4.2 Stability, Retention and Efficiency

The effects of variation of chromatographic conditions on retention and efficiency were examined using the column obtained by coating graphite with an insoluble layer of PEI because high peak symmetry had been shown.

Since the ion exchange functional groups are attached to the graphite surface by adsorption, it is critical to ensure the coating has sufficient stability to allow reliable data to be collected. Figure 5.8 illustrates the stability of the column. Passage of more than 5 litres of phosphate buffer (about 7,000 column volumes) gave no change in retention, other than those due to the effect of temperature fluctuation during the course of the experiment. It is evident that strict control of temperature is necessary to obtain reproducible results.

As has been pointed out the mechanism of ion exchange chromatography
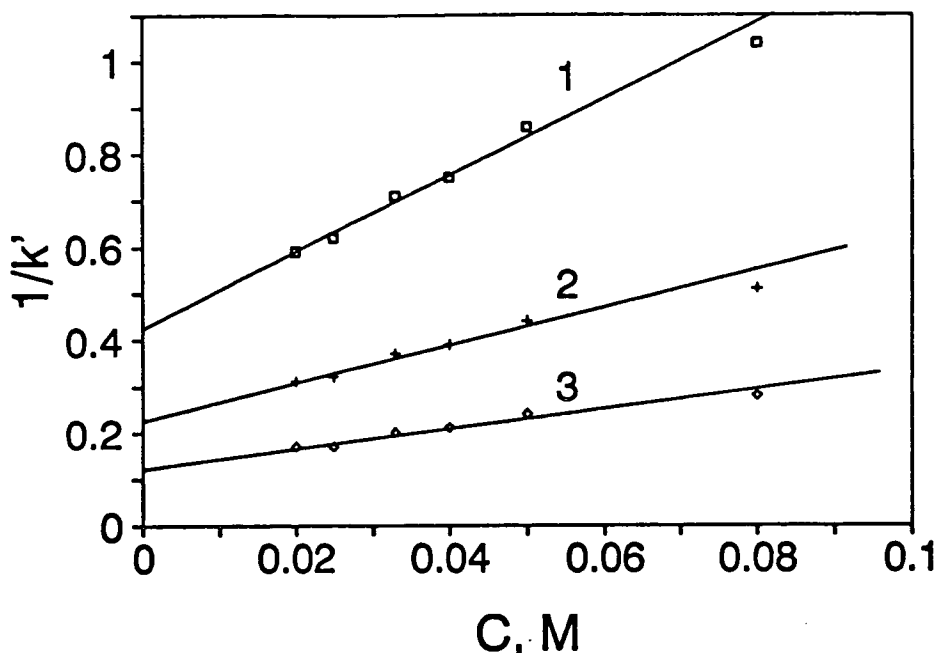
Figure 5.9. Dependence of k' upon phosphate concentration. Except for temperature at 30°C and varying buffer concentrations, others as for Figure 5.8

can be conveniently explored by varying the concentraions of the buffer solution. Figure 5.9 shows when the reciprocal of k' is plotted against the concentration of the phosphate solution a straight line is indeed obtained. If the straight line is extropolated to $C = 0$, the intercept of various values for different solutes is obtained , indicating the predominance of 'adsorption mechanism'.

Figure 5.10 shows that retention was sharply decreased with increase in pH from 5 to 7, then flattened off. This is typical behaviour of a weak anion exchanger composed of a mixture of primary, secondary and tertiary aliphatic amines as they have different basicities.

Figure 5.11 shows that HETP values were generally in the range from 70 to 200 μm at linear velocity of 1.0 $mm\,sec^{-1}$, which are comparable to those for anion exchangers based on silica gels.
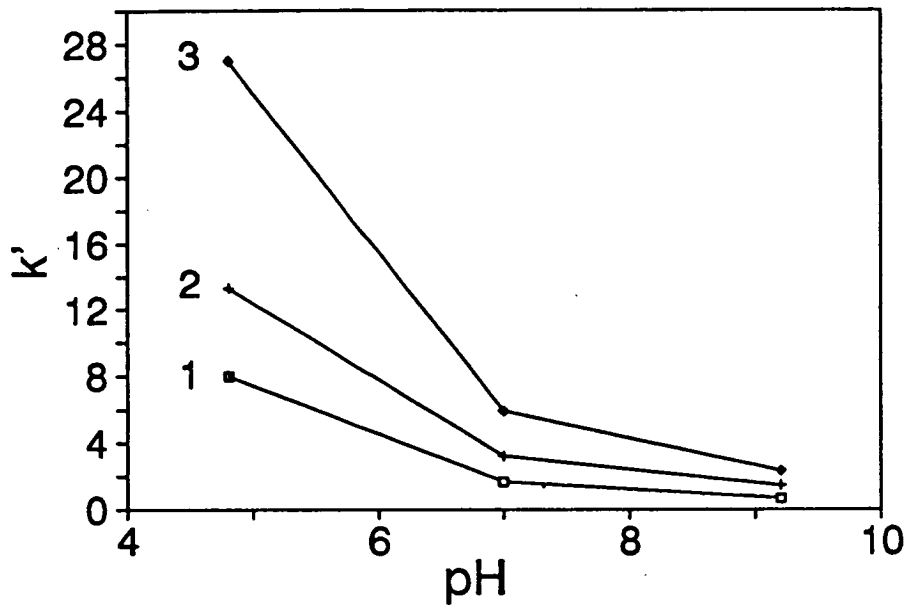
Figure 5.10. pH dependence of k'. Except for temperature at $30°$ and varying pH's, others as for Figure 5.8.
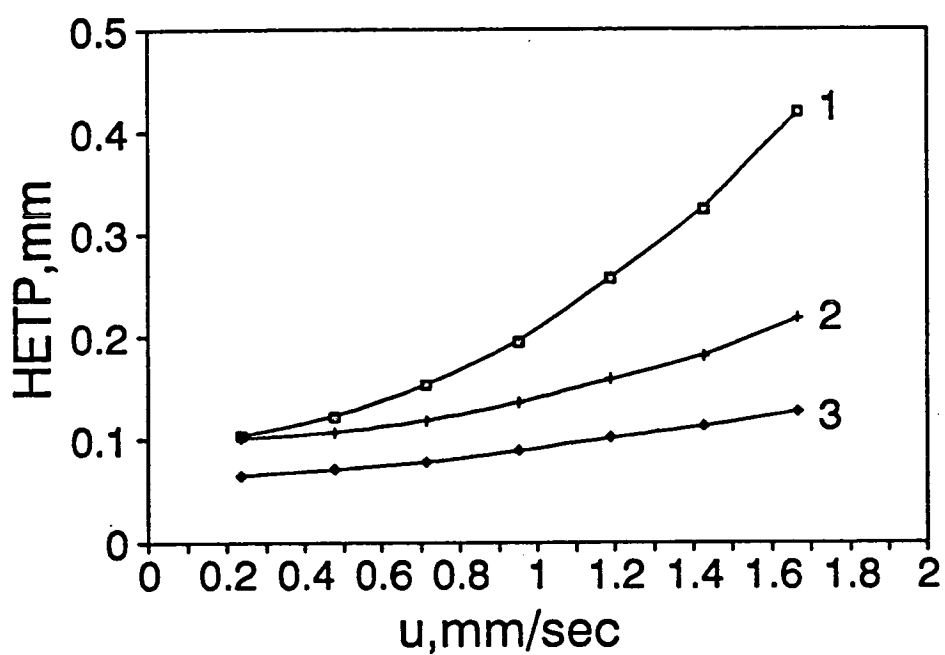
Figure 5.11. Plots of plate height vs. linear velocity. Except for temperature at 30° and varying velocities, others as for Figure 5.8.

5.5 Conclusions

These preliminary results demonstrate how porous graphite can be conferred with the properties of an ion exchanger. The chromatographic behaviours of some inorganic anions confirm that this new ion exchanger is comparable with those silica based materials in terms of column efficiency, peak shape and ion exchange capacity. The dependence of capacity ratio upon buffer concentration verifies the retention mechanism proposed on the assumption that adsorption of counterions onto the binding sites in the ion exchanger obeys the Langmuir equation.

Chapter 6

Chiral Chromatography I

6.1 Introduction

Liquid chromatography offers many options to control the selectivity of the system. One of those possible methods of enhancing the separation is to utilize interactions between added selector and the solutes to be separated. Chiral chromatography provides a best testimony to the power of this approach.

A pair of enantiomers have identical physical and chemical properties with the exception that they rotate plane-polarized light in opposite directions. Since two enantiomers as a pair are nonsuperimposable mirror images of each other much like the left and right hands, they are often referred to as chiral compounds.

The traditional method of resolving enantiomeric compounds is to react them with a chiral reagent to form diastereomers [73]. Unlike enantiomers, diastereomer pairs may have significantly different physical properties which may be the basis for their separation from one another. For instance, the covalently formed diastereomeric compounds may be separated by chromatography provided that they differ in distribution coefficient between two phases.

Although resolution of enantiomers by chromatography can be accomplished

in this way, we reserve the term 'Chiral Chromatography' for those systems in which the diastereomers are formed in the chromatographic column during the separation, the chiral resolving agent being introduced either in the mobile or in the stationary phase. A great number of resolutions have been mediated by dissociable diastereomers between racemic substrates and chiral resolving agents, including metal-ligand complexes, inclusion complexes, charge transfer complexes and acid-base complexes. With the chiral resolving agent incorporated in the stationary phase, known as chiral stationary phase, the chromatographic separations of enantiomers are exclusively based on the difference in formation constant or stability of dissociable diastereomers with chiral selector bonded on the support, rather than the difference in solubility or adsorptive strength as in the case of covalent diastereomers. In this chapter, we explore the use of amino acid derivatives as chiral selector to prepare chiral stationary phases, with emphasis upon the ways in which chiral selectors are attached to the graphite surface and upon the underlying mechanism by which the chiral separations occur.

Before taking up this matter, let us briefly review the theories developed over the past decades to account for the chiral recognition phenomena.

6.2   Theory of Chiral Chromatography

6.2.1   Chiral Recognition

Although the enantiospecific properties of some natural polymers such as wool and cellulose have been observed for long time, the origin and the mechanism of enantiospecificity is still obscure and an area of intensive study. The most widely accepted theory is based on the 'three point interaction' concept. This was first postulated by Ogster [89] in 1948 to account for the distinguishing power of an

enzyme. Three different active points are presumed to be present in the enzyme, which specifically combine with the corresponding three different groups of the substrate. Three point combination is necessary to ensure enantiospecificity in an enzymatic reaction. This model was justified by Dalgliesh's work [91] on the optical resolution of aromatic amino acids by paper chromatography. By varying the functional groups of the aromatic amino acids, he was able to identify molecular interactions responsible for optical resolution. In addition to two hydrogen bonds due to amino and carboxyl groups, the steric interaction of the aromatic ring was found necessary to enable the resolution to occur. The most significant result of this work was the demonstration that rather complex chiral recognition phenomena could be explained in a relatively simple way, and the provision of useful clues in the search for chiral separation systems.

Work by Baczuk et al [92] represents the first successful attempt to extend the three point interaction model to the design of a chiral stationary phase. From the earlier work on optical resolution of amino acids, they realized that a packing for the direct separation of amino acid enantiomers needs to contain 'built in' optically active sites which are available for the solute species to establish a three point interaction. On the basis of structural considerations, Baczuk et al reasoned that L-arginine shows the proper arrangement of ionic sites for three point interaction with complementary sites on dihydroxyphenyalanine (DOPA), therefore it should be most likely to accompolish the resolution of DOPA enantiomers. Upon covalently bonding of L-argine to Sephadex resin, DOPA racemates were indeed separated into their enantiomers with a pure water eluent.

Although the three point interaction model itself is rather simple, confusions regarding interpretation of this model are rather common in the literature. In an attempt to clarify them Pirkle [74] restate this model as 'chiral recognition requires a minimum of three simultaneous interactions between the chiral

stationary phase and the enantiomers to be separated, at least one of these interactions being stereochemically dependent'. The steric interactions can be repulsive. Indeed in many cases, the steric hindrance can enhance the difference in stability between two diasteromers. Pirkle took his arguement further by stating that three point interaction should not be understood as requiring the involved species be conformationally locked, although a degree of conformationally preference at least with one enantiomer is typically involved in instances of observed chiral recognition. From the thermodynamic point of view, this clarification seems unnecessary since at equilibrium only those interactions involved in the formation of conformationally favourable complexes between the chiral selector and enantiomers contribute to the total energy difference required for chiral recognition. It is on this basis that chiral recognition at a given instant can be rationalized and formation constant of diasteromer calculated from the energy change involved.

Up to this point the validity of the three point interaction model applicable to chiral recognition has been established entirely on the basis of experimental considerations. Recently, a theoretical treatment of chiral recognition by Salem et al [90] has lent a solid support to this model. Consider three freely rotating chiral tetrahedral molecules R, R' and S' as shown in Figure 6.2.1. The total interaction energy is expressed as a sum of interaction energies between the substituent atomic centres on both molecules, which includes all terms from two-centre interactions up to simultaneous eight centre interactions. A qualitative analysis of the differential energy between homochiral ($R \longleftrightarrow R'$) and heterochiral ($R \longleftrightarrow S'$) confirms that only simultaneous interactions between three pairs of atoms or two interacting faces are responsible for chiral recognition. In order to calculate the differential energy, all possible atom-atom interactions between two molecules must be taken into account and therefore the calculation inevitably becomes very
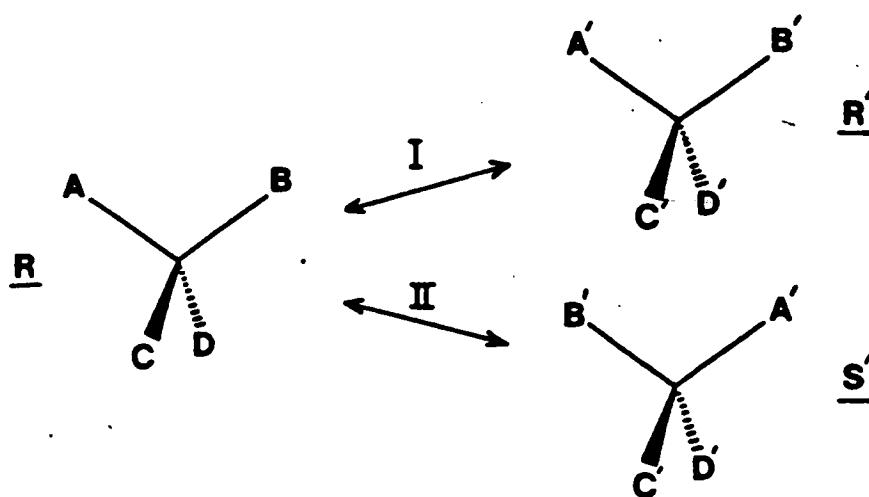
Figure 6.1. The differential energy responsible for chiral recognition is given by interaction I minus interaction II.

tedious, and more seriously, inaccurate because of empirical 'overlap-exchange' functions involved. For the purpose of qualitative understanding, we offer an alternative explanation with respect to the necessity of three point interactions, which is based on classical thermodynamic equilibrium considerations.

As we have mentioined earlier, the homochiral or heterochiral complex tends to take a thermodynamically favourable form at equilibrium so as to maintain the free energy change of the system at minimum. Three possible combinations may be distinquished: point to point, edge to edge and face to face (see Figure 6.2). Let us consider the standard free energy change related to the respective combinations.

Case 1: Point to point combination or single interaction:

$$\Delta G^o_{S'} = -E_{CC'}$$

$$\Delta G^o_{R'} = -E_{CC'}$$

$$\Delta G^o = \Delta G_{R'} - \Delta G^o_{S'} = 0$$
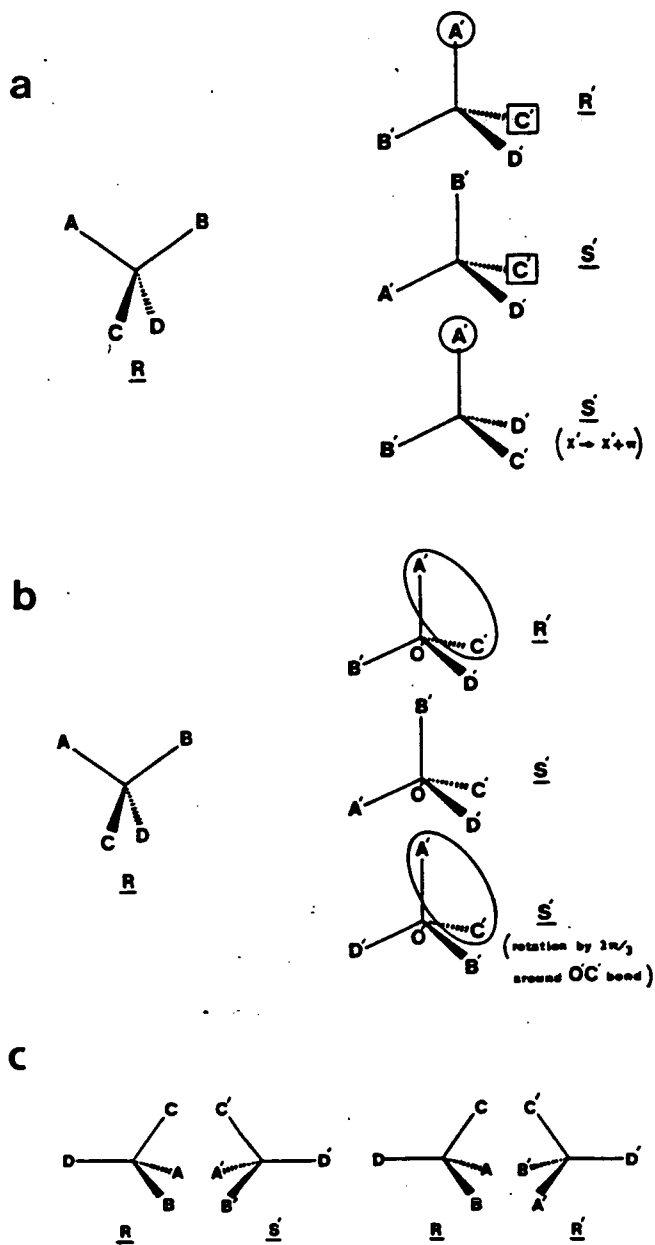
Figure 6.2. Chiral interactions involving single, dual and triple atoms.

Case 2: Edge to edge combination or dual interaction

$$\Delta G^o_{S'} = -(E_{CC'} + E_{AA'})$$

$$\Delta G^o_{R'} = -(E_{CC'} + E_{AA'})$$

$$\Delta G^o = \Delta G^o_{R'} - \Delta G^o_{S'} = 0$$

Case 3: Face to face combination or triple interaction

$$\Delta G^o_{S'} = -(E_{CC'} + E_{BB'} + E_{AA'})$$

$$\Delta G^o_{R'} = -(E_{CC'} + E_{BB'} + E_{AD'})$$

$$\Delta G^o = \Delta G^o_{R'} - \Delta G^o_{S'} = -(E_{AD'} + E_{AA'})$$

where E represents the contribution of individual interactions to the overall standard free energy change ΔG and the negative sign represents the attractive interaction.

It is not surprising that no differential energy is found in the cases of interactions involving solely point to point or edge to edge contact. However face to face or three point interaction yields energy difference between two diastereomeric complexes provided that one of the interactions involved in the formation of complex is different from the other in terms of binding strength. This treatment justifies a widely employed approach to design a chiral recognition system by amplifying the difference in interaction energy between chiral selector and enantiomers to be separated.

The minimum energy difference required to effect a complete separation of a pair of enantiomers can be obtained directly from the relationship

$$\Delta(\Delta G) = -RT \ln \frac{K_D}{K_L} \tag{6.1}$$

Assuming $K_D/K_L = 1.5$ and $T = 298K$, we have $\Delta(\Delta G) = -1kJ$.

6.2.2 Mechanism of Chiral Separation

In order for enantiomers to be resolved on a chiral stationary phase, the transfer free energy changes must differ from one another. If retention of enantiomers is entirely controlled by the formation of transient diastereomers in the stationary phase, the enantioselectivity α_E can be defined as a ratio of formation constant for D-isomer to that for L-isomer, assuming the L-isomer is eluted first:

$$\alpha_E = \frac{K_D}{K_L} \tag{6.2}$$

One might argue that this is not always the case in pratical chiral chromatography since non-chiral interactions may play an important part in controlling the retention. If this is the case, then a chiral stationary phase can be visualized as consisting of chiral sites as well as non-chiral sites, thus the distribution of enantiomers on the stationary phase is somehow analogous to the adsorption on the heterogeneous surface. The capacity factor k' can be expressed as a sum of k'_c, retention due to the chiral sites, and k'_n retention due to the non-chiral sites. In this case the enantioselectivity should be replaced by the separation factor α, which is defined as a ratio of k's for a pair of enantiomers.

$$\alpha = \frac{k'_D}{k'_L} = \frac{k'_{c(D)} + k'_n}{k'_{c(L)} + k'_n} \tag{6.3}$$

It is obvious that separation factor is optimized for enantioselectivity only when non-chiral retention is absent.

Consider another case where a secondary chemical equilibrium is involved in chiral separations and solute retention is entirely due to chiral interactions. For instance, the separation of acid enantiomers, HA, via formation of dissociable diastereomers with a chiral selector, S.

In an aqueous solution, the acid is capable of dissociating as follows:

$$HA \rightleftharpoons H + A \tag{6.4}$$

$$K_a = \frac{a_H a_A}{a_{HA}} \qquad (6.5)$$

Suppose that only the dissociated species A reacts with the chiral selector S to form a complex:

$$A + S \rightleftharpoons AS \qquad (6.6)$$

$$K_c = \frac{a_{AS}}{a_A a_S} \qquad (6.7)$$

At equilibrium, the distribution of the analytes between two phases is represented by the distribution ratio D, which can be written as

$$D = \frac{a_{AS}}{a_A + a_{HA}} \qquad (6.8)$$

Substituting equations 6.5 and 6.7 in equation 6.8 results in

$$D = \frac{K_a K_c a_S}{K_a + a_H} \qquad (6.9)$$

k' is related to D through the equation:

$$k' = \phi D = \phi \frac{K_a K_c a_S}{K_a + a_H} \qquad (6.10)$$

It can be seen that the retention of a weak acid is strongly dependent on the acidity of the solution. In acidic conditions such that $a_H \gg K_a$, no formation of a diastereomer can be expected because in this case the analyte exists predominantly in the form of undissociated acid. In contrast, when $a_H \ll K_a$, maximum retention may be observed.

The separation factor is given as

$$\alpha = \frac{k'_D}{k'_L} = \frac{K_D}{K_L} \qquad (6.11)$$

This result appears surprising that the separation factor, equivalent to the enantioselectivity in this case, is not affected by the pH of the eluent . This is because

we assume at the beginning that the distribution of the analyte is solely determined by the interaction between the dissociated analyte and the chiral selector. The change in retention caused by alteration of the pH of eluent is the same for either L- or D-isomer and thus has no effect on the enantioselectivity.

The potential for separation of enantiomers through the use of a chiral adsorbent has been explored extensively since the first report in 1920s on the observation of induced optical rotation in racemic dye solutions used to dye wool [97, 96]. Most of the earlier investigations were made with natural chiral polymers such as wool, cellulose and other polysaccharides. These materials are of little use in modern liquid chromatrography mainly because of their poor mechanical strength. Instead, synthetic chiral stationary phases have been developed over the last two decades, represented by a variety of silica gels incorporating chiral functional groups. These adsorbents provide the advantage of tailored binding properties for a specific type of enantiomers, thus the mechanisms of chiral chromatography with these functional groups are more readily discerned.

There are a variety of synthetic chiral adsorbents available however only a few can be used with aqueous eluents [74]. Among these, the copper complexing type is unique in that the binding sites in the chiral functional groups are well understood. Investigations with this type of stationary phase will thus yield a wealth of information concerning the mechanism by which enantiomers are separated.

The chemistry of copper complexes have been studied extensively with ligands containing nitrogen , oxygen or sulphur as binding atom. The stability of the complex is thought to be achieved by having only partial donation of electron pairs from the ligand to the metal ion. There are a great number of ligands which have been studied, but only a few of them are found of use in chiral separations. These compounds have a common feature of forming a stable chelate
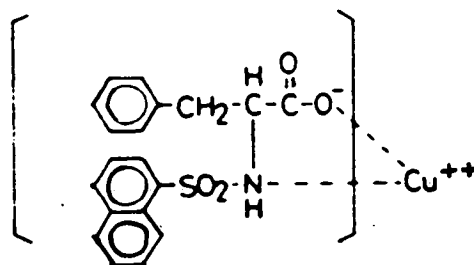
Figure 6.3. Configuration of copper complex of N-2-naphthalenesulphonyl-L (or D) -phenylalanine

ring with copper ion. An representative of this type is amino acids. As shown in Figure 6.3, an amino acid (N-2-naphthalenesulphonyl-phenylalanine in this example) coordinates with a cupric ion through O (carboxyl) and N (amino) atoms to give a complex of five membered rings.

Since the stability of a complex is mainly attributed to the bonds formed between the ligand and cupric ion, it may be said that other things being equal, high polarizability or high basicity of the binding atoms confers high stability on the complex. It is therefore not difficult to understand why derivatization of either carboxyl group or amino group could reduce the chelate complex to an unidentate complex and thus ruin the chiral recognition system because the unidentate complex is no longer able to fulfill the requirment of three point attatchments.

Chiral chromatography by copper complexation was developed by Davankov and Rogozhin [95, 93, 94] in 1970's. The first chiral complexing adsorbent was prepared by bonding L-proline onto a chloromethylated styrene-divinylbenzene copolymer, with which a number of amino acid enantiomers were successfully resolved in conjunction with an eluent containing copper ions. Mechanisms of

this type of separation have been a subject of numerous experimental and theoretical intestigations [104]. Most of these have been focused on the study of ligand exchange equilibria but have failed to appreaciate the adsorption equilibria involved in the interphase region. For similar reasons to that given in the treatment of ion exchange, monolayer coverage of adsorbent by the counterions in the eluent may not be readily achieved when dilute electrolyte solution is used as an eluent, the effect of the electrolyte concentration on the surface coverage should be taken into account. In an attempt to cover separations carried out when the binding sites of chiral stationary phase are not saturated by cupric ions in the eluent, we elaborate a different mechanism of chiral separation by copper complexation.

When an enantiomer analyte A is introdued into a chromatographic system consisting of a chiral adsorbent S and an eluent containing copper ions M, the main equilibria involved are the following (for simplicity, signs of charges have been ommitted):

$$A + M \; \overset{1}{\rightleftharpoons} \; MA$$

$$\underline{S} + M \; \overset{2}{\rightleftharpoons} \; \underline{MS}$$

$$\underline{MS} + MA \; \overset{3}{\rightleftharpoons} \; \underline{MAS} + M$$
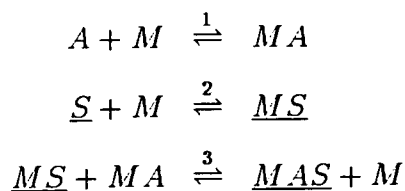
Equilibrium constants for the above equations may be expressed in terms of activities of solutes or fraction of surface coverage, if applicable.

$$K_1 \;\; = \;\; \frac{a_{MA}}{a_A a_M} \tag{6.12}$$

$$K_2 \;\; = \;\; \frac{a_{MS}}{a_S a_M} = \frac{\theta_{MS}}{(1 - \theta_{MS}) a_M} \tag{6.13}$$

$$K_3 \;\; = \;\; \frac{a_{MAS} a_M}{a_{MS} a_{MA}} \tag{6.14}$$

The distribution ratio D for the analyte is written as

$$D = \frac{a_{MAS}}{a_{MA} + a_A} \tag{6.15}$$

To substitue for a_{MAS} in equation 6.15 from equation 6.14, a_{MS} must be known first. This can be obtained from equation 6.13, by noting $a_{MS} = \theta_{MS}Q^o$, where Q^o is the monolayer capacity of the chiral adsorbent. Thus:

$$a_{MS} = \frac{Q^o K_2 a_M}{1 + K_2 a_M} \tag{6.16}$$

Upon substitution the equation 6.15 becomes

$$D = \frac{Q^o K_1 K_2 K_3 a_M}{1 + (K_1 + K_2)a_M + K_1 K_2 a_M^2} \tag{6.17}$$

The dependence of D upon a_M can be made more explicit by writing equation 6.17 in the reciprocal form:

$$\frac{1}{D} = \frac{1}{Q^o K_1 K_2 K_3 a_M} + \frac{K_1 + K_2}{Q^o K_1 K_2 K_3} + \frac{a_M}{Q^o K_3} \tag{6.18}$$

It is interesting to note that there are two limiting forms of equation 6.18 with respect to the activity of copper ions in the eluent. First, at extremely low concentrations where $a_M \to 0$, the third term of the equation is negligible, we have

$$\frac{1}{D} = \frac{1}{Q^o K_1 K_2 K_3 a_M} + \frac{K_1 + K_2}{Q^o K_1 K_2 K_3} \tag{6.19}$$

D increases with a_M. This is because a certain proportion of the chiral compounds remain free from binding with the metal ions, increase in a_M will be favoured by the formation of the metal complexes, thus enhance the distribution of analyte into the stationary phase.

Alternatively, when the concentration of metal ions in the eluent is sufficiently high that the first term in the equation becomes relatively unimportant and thus can be neglected, we have

$$\frac{1}{D} = \frac{K_1 + K_2}{Q^o K_1 K_2 K_3} + \frac{a_M}{Q^o K_3} \tag{6.20}$$

A plot of $1/D$ versus a_M will produce a straight line with a slope of $Q^o K_3$ and an intercept of $\frac{K_1+K_2}{Q^o K_1 K_2 K_3}$. This equation is of the same form as that derived on the assumption that the chiral selectors are completely transformed into the metal complexes upon addition of the metal ions, thus a_{MS} is constant, independent of the concentration of the metal ions in the eluent. In this case, the variation of a_M will shift the exchange equilibrium, as can be seen in equation 6.14, thus affect the distribution of the analyte ions between the two phases.

6.3   Results and Discussion

6.3.1   Characterization of Chiral Stationary Phase

A good chiral selector to be used for preparation of a chiral stationary phase should provide: (1) high enantioselectivity; (2) rapid exchange kinetics; (3) long term stability and (4) adequate adsorbability. With these criteria as guidelines we have examined a series of amino acids and their derivatives for possible use in chiral chromatography. These compounds include phenylalanine, benzenesulphonyl-L-phenylalanine, naphthalenecarbonyl-L-phenylalanine, naphthalenesulphonyl-L-alanine, naphthalenesulphonyl-L-phenylalanine and naphthalenesulphonyl-D-phenylalanine (NS-D-Phe). All of them meet the first three requirements except naphthalene carbonyl-L-phenylalanine, which shows no enantioselectivity. One possible explanation for this is that because of decrease in polarization of nitrogen atom arising from the formation of peptide bond, the compound is unable to form a chelate stable enough to effect retention and separation.

Naphthalenesulphonyl derivatives of phenylalanine became the choice of chiral selector simply because they are the only compounds which offer sufficient adsorbability to avoid being washed away during the chromatography.

Surface Coverage

As can be expected the highest capacity of chiral stationary phase may be generated only when the support surface is completely covered by the chiral resolving agent. The surface coverage is therefore an important parameter to characterize the chiral stationary phase.

The surface coverage can be calculated from an adsorption isotherm determined by the breakthrough method. An isotherm for the adsorption of naphthalenesulphonyl-L-phenylalanine(NS-L-Phe) from methanol onto the graphite column is illustrated in Fugure 6.4 (a).

The concave shape of the isotherm, which covers a concentration range that could be explored conveniently without solubility limitation was thought to obey the Langmuir equation. This is established in the reciprocal plot shown in Figure 6.4 (b), where a straight line is obtained. The monolayer capacity was found to be about 1.4 $\mu mol\, m^{-2}$, taken with the BET surface area of 107 $m^2 g^{-1}$ and the weight of 0.50 g for the packing within the column (50 × 4.6 mm).

In the present work, a 10.0 mM solution of NS-L-Phe was used to give the surface concentration of 1.2 $\mu mol\, m^{-2}$, corresponding to 80% of monolayer coverage. It should be pointed out that the same coverage can not be obtained at the same concentration for adsorption onto the reversed phase silica gels as the latter is much weaker non-polar adsorbent. In fact the purity of the synthetic product may be checked using ODS-Hypersil as the stationary phase and 50% methanol as the mobile phase, in which the retention of phenylalanine derivatives is characterized by the phase capacity ratio being 7.

The surface coverages found in this study show that the chiral resolving agent is strongly adsorbed by graphite from methanol, giving rise to the surface concentrations comparable to those of the chemically bonded phases. When methanol
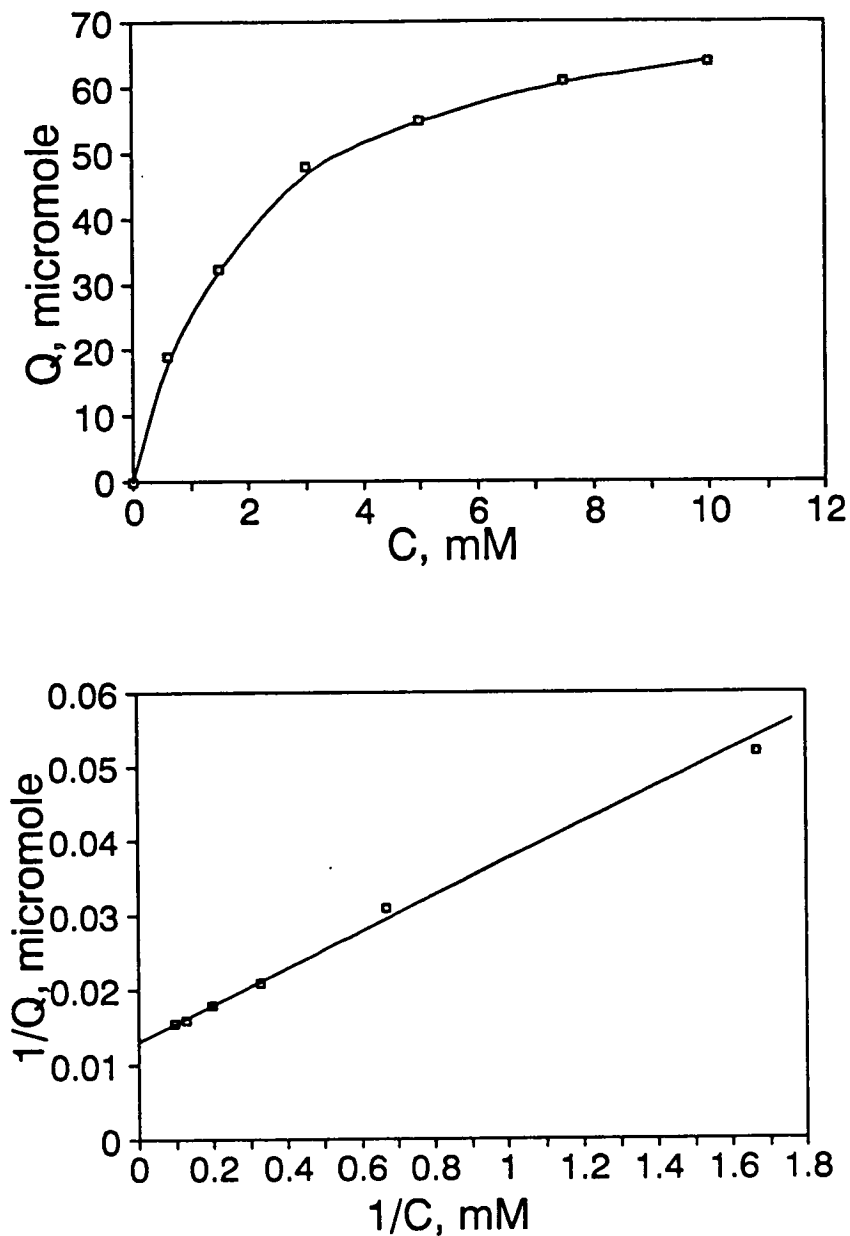
Figure 6.4. Adsorption isotherms of naphthalenesulphonyl-L-phenylalanine on graphite. (a) Plot of quantity of solute adsorbed versus concentration. (b) Reciprocal plot of isotherm.

is replaced by an aqueous eluent NS-L-Phe is more or less permanently adsorbed and acts as if it were chemically bonded.

Enantioseletivity

The stationary phases were prepared by coating the graphite with L- or D-phenylalanine derivatives as mentioned above. The methanol used as coating solvent was replaced with 2.0 mM aqueous solution of copper acetate at pH 5.60. The system was used to separate a wide range of amino acid and hydoxy acid enantiomers in order to establish how effective the chiral stationary phases. The column was equilibrated with an eluent containing cupric ions before introducing analytes into the system. The amounts cupric ions adsorbed onto the stationary phase may be determined by the breakthrough method at 254 nm, which is found varying, depending upon the concentrations employed. The data for retention and selectivity are summarised in Table 6.1, together with the published results obtained on reversed phase silica [112, 75]. Some examples of separation of racemates into enantiomers are shown in Figure 6.5. The enantioselectivity up to 2 is readily obtained for hydrophilic species. It is noted that comparable data have been obtained on the reversed phase silica coated with N,N-dioctyl-L-alanine, using an aqueous solution of copper sulphate (between 0.1 and 2.0 mM) at pH 5.50 as eluent.

It is worth noting that columns containing either D- or L- amino acid derivative are identical in terms of retention, selectivity and efficiency, expect the elution order of D- and L-isomers of analytes opposite to each other. Both stationary phases show preferentially retention of enantiomer with the same configuration as that of the chiral selector with an exception of proline.
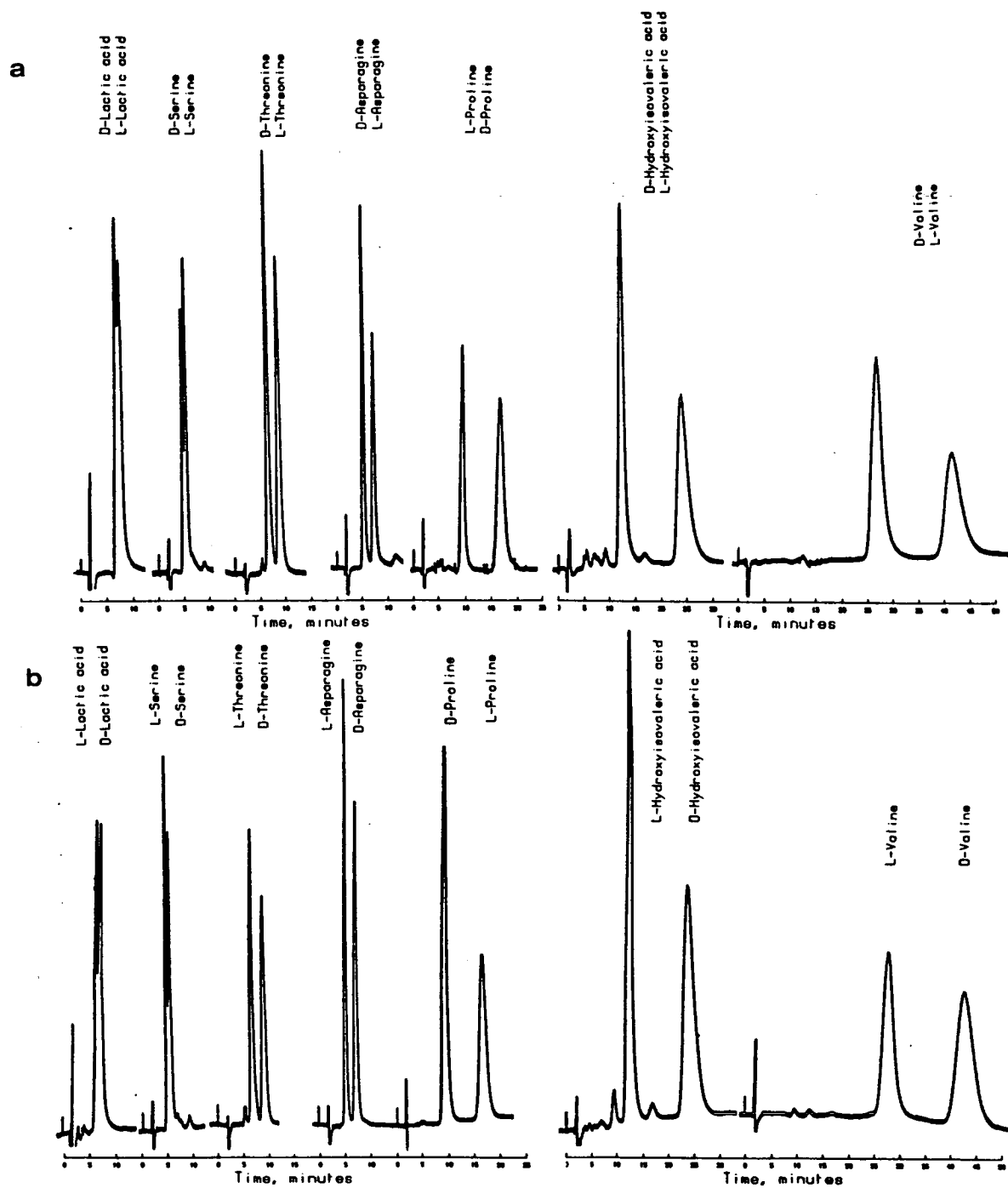
Figure 6.5. Chiral separations of amino and hydroxy acids. Column, PGC 94F coated with L-isomer in (a) and D-isomer in (b) of naphthalenesulphonyl-phenylalanine, 50 × 4.6 *mm*; eluent, 2.0 *mM* copper acetate, pH 5.6; flow rate, 0.5 *ml/min*; detection, UV 254 *nm*, tempreture, 30°.

Table 6.1. Retention and selectivity of chiral chromatography

Amino acid	Porous graphite [a]			Reversed phase silica [b]		
	k'_D	k'_L	α	k'_D	k'_L	α
Serine	1.58	1.91	1.21	6.45	8.04	1.25
Asparagine	1.86	2.92	1.57	-	-	-
Threonine	2.63	3.86	1.47	7.07	9.13	1.29
Proline	7.91	3.96	2.00	5.64	12.04	2.13
Glutamine	5.08	5.78	1.14	-	-	-
Valine	13.36	21.33	1.60	7.32	14.93	2.04
Lactic acid	2.80	3.17	1.13	12.5	15.9	1.27
Hydroxy isovaleric acid	5.04	10.75	2.13	-	-	-
Hydroxy isocaproic acid	18.82	21.67	1.15	-	-	-

[a] Chromatographic conditions as in Figure 6.5.

[b] Chromatographic conditions: column, MCI GEL CRS10W(ODS-silica coated with N, N-diactyl-L-alanine), 50 × 4.6 mm; eluent, 0.1 to 2.0 mM $CuSO_4$, pH 5.50; detection, UV 254 nm.

Durability

A durability test was undertaken by passage of a large volume of eluent through the column. The capacity ratios of tested analytes against the volume of the eluent passed are shown in Figure 6.6. The k' values of proline and threonine enantiomers are almost unaffected after the passage of 5,000 ml, which is equivalent to 7,000 column volumes, of 2 mM copper acetate under the typical conditions. Unchanged retention with passing volumes suggests that the adsorption of chiral reagent on the graphite surface is so strong that no bleeding could occur with aqueous dominant eluents.

6.3.2 Effects of Eluent Variables upon Retention

Effect of concentration of copper acetate
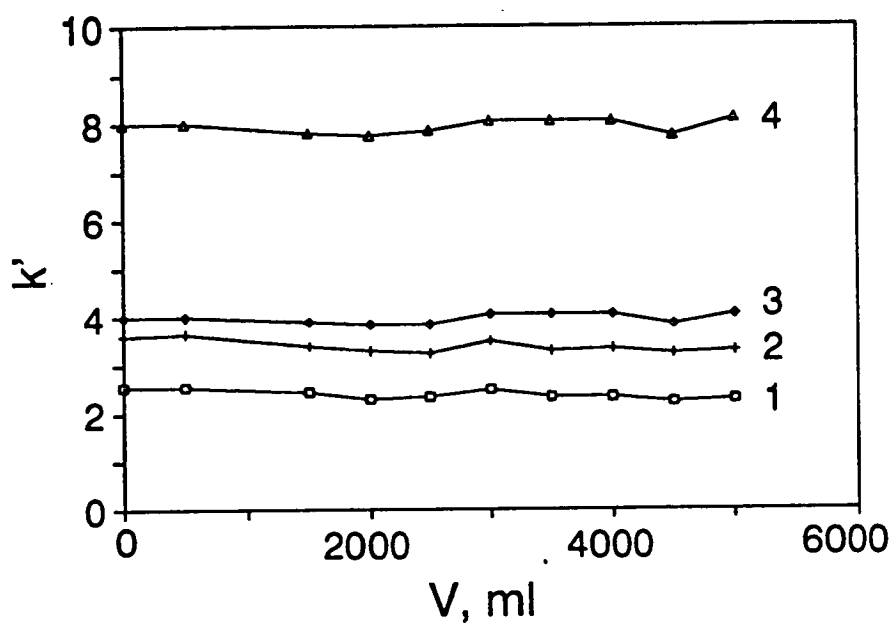
Figure 6.6. Effect of elution volume upon capacity ratio. Solutes: 1 = D-threonine, 2 = L-threonine, 3 = L-proline, 4 = D-proline. Conditions as for Figure 6.5.
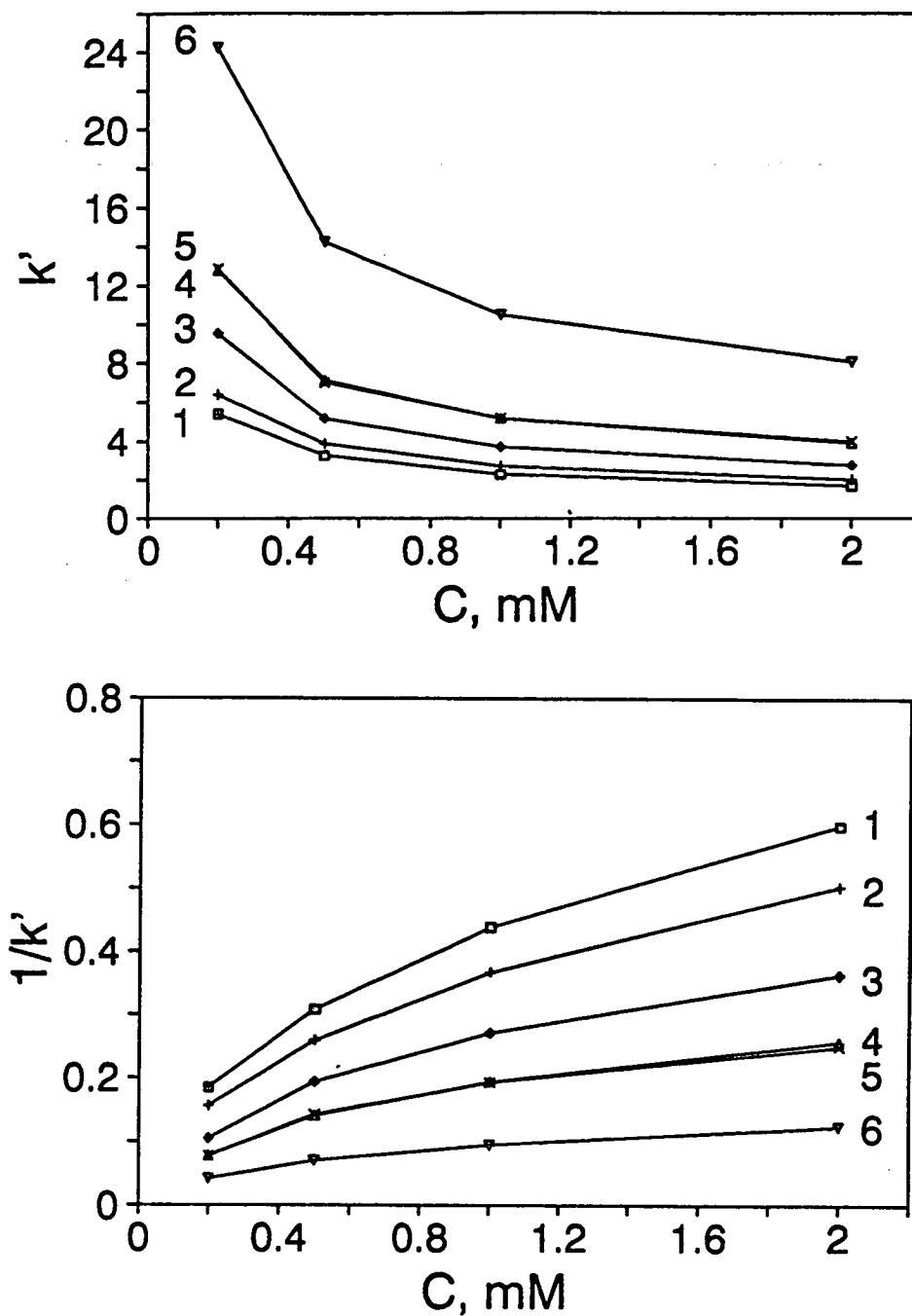
Figure 6.7. Effect of concentration of copper acetate upon capacity ratio. Solutes : 1= D-serine, 2 = L-serine, 3 = D-threonine, 4 = L-threonine, 5 = L-proline, 6 = D-proline. (a) Plots of k' vs C. (b) Plots of $1/k'$ vs C.

Figure 6.7 shows the dependence of k' upon the concentration of the copper acetate in the eluent, where the pH is at 5.6. k' is inversely proportional to the concentration of copper ions in the eluent, pointing to the competition between the cupric ions and the analyte complexes for the binding sites of the ligands anchored on the surface. In low concentration region, the reciprocal of k' is more or less linearly changed with $[Cu(Ac)_2]$ as suggested by equation 6.18, however when $[Cu(Ac)_2]$ is larger than 1.0 mM, deviation from a linear function becomes apparent with a concave towards abscissa. This is presumably attributed to the nonideal properties of the electrolyte solution. The straight line produced over the range of low concentration suggests that the binding sites of the amino acid as the chiral selector have been saturated by the copper ions in the eluent even at relatively low concentrations.

Effect of pH

Figure 6.8 shows plots of k' versus pH of the eluents for a number of amino acid enatiomers. The retention increases with pH in all cases. This can be understood in terms of fraction of amino acid in the form of completely dissociated, $RHC(NH_2)COO^-$, which favours the formation of chelate complexes. High pH will increase this fraction and hence exchange capacity of the column. However, the value of pH above 6 should be avoided because the cupric ions may precipitate out as hydroxides.

From the results presented above we might conclude that retention of amino acids is predominantly controlled by the formation of ternary complexes. However the excess cupric ions in the eluents reduces the retention by influencing the exchange equilibrium.

As predicted from the theoretical considerations the enantioselectivity is entirely determined by the ratio of stability constants for a pair of distereomers and
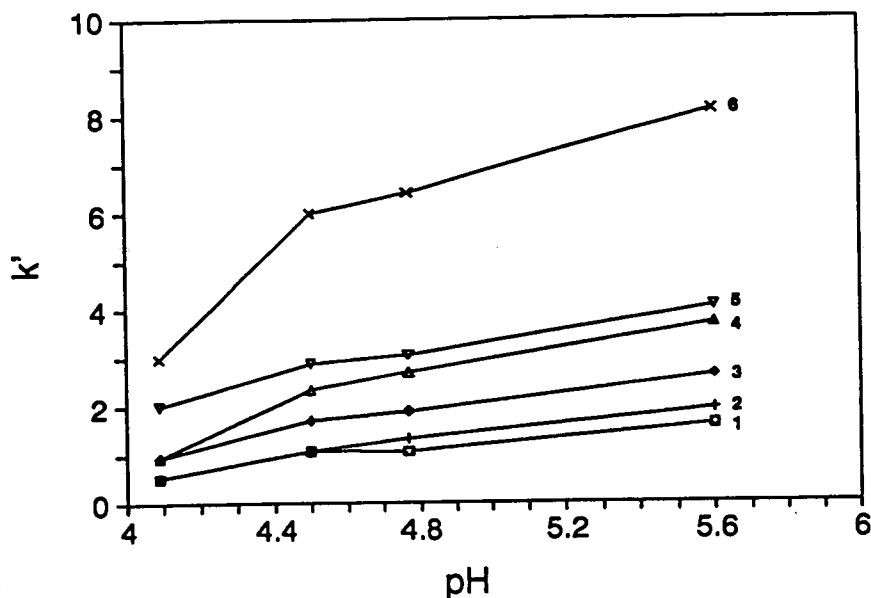
Figure 6.8. pH dependence of retention. Solutes as for Figure 6.7.

unaffected by the composition of eluents. As shown in Figure 6.9, this is indeed the case. This result suggests that non-chiral adsorption is unimportant, otherwise, significant deviations from constant enantioselectivity would be observed.

6.3.3 Thermodynamics of Chiral Recognition

As has been discussed previously, the total standard free energy change may be split into its components. If only three point simultaneous interaction is considered, the total energy change can be written as a sum of free energy changes contributed from each attachment:

$$\Delta G^o = \Delta G_1^o + \Delta G_2^o + \Delta G_3^o \tag{6.21}$$

For the separation of amino acids, which have a general form $RHC(NH_2)COOH$, by copper complexation, it seems reasonable to assume that the chelate interactions between cupric ion and the ligand are roughly the same for amino acids of different R groups, which is justified by the close values of formation constants of
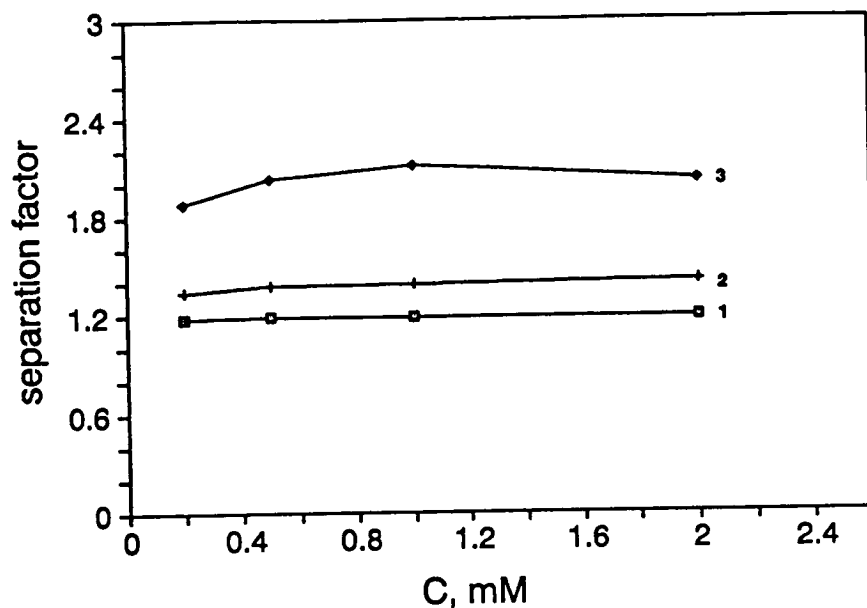
Figure 6.9. Dependence of separation factor upon the concentration of cupper acetate. Solutes: 1=D- and L-serines, 2=D- and L-threonines, 3=D- and L-prolines.

copper complexes in aqueous solution [77]. The difference in retention for various amino acids is, to large extent, ascribed to the interactions between R groups in the chiral selector and the acid analytes.

As shown in Figure 6.3, the chiral selector N-2-naphthalenesulphonyl-L(or D)-phenylalanine, has two major non-polar groups: phenyl and naphthalene. When the chiral selector is allowed to contact the graphite surface, a permanent attachment is thought to occur through the cooperative interactions of phenyl and naphthalene groups with the non-polar surface. Since the energy arising from this type of interaction is relatively high, the adsorption may be regarded as equivalent to chemical bonding. Accordingly, the surface made up of the adsorbed phenyl group (denoted as R' for general discussion) and uncovered graphite can be treated as an expansion of the R' group. The interaction of the R group in the analyte with this surface offers an additional stability to the diastereomer thus formed in relation to that formed in solution. As can be seen from Table 6.1,
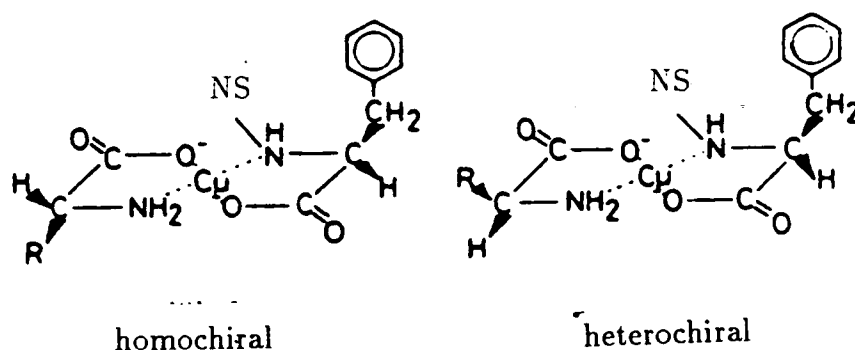
Figure 6.10. Configurations of homochiral and heterochiral complexes

the k' values of D- and L-valine enantiomers in which R is $(CH_3)_2$ are 13.36 and 21.33,respectively, compared to 1.58 and 1.91 for D- and L-serine enantiomers which have $R = HOCH_2$. It is thus evident that the thermodynamics of the adsorption in which the interaction of the R groups between chiral selector and analyte is inevidably involved plays a decisive role in discriminating the amino acids of different R groups during the chiral chromatography. Graphite as a strong non-polar adsorbent turns out to be advantageous for the separation of hydrophilic amino acids as in this case stronger retention is desirable.

The concept of the expanded R' group can be applied to explain why D-isomer is normally eluted before L-isomer when the chiral selector used has L-configuration. In other words, the stability of homochiral diastereomer is higher than that of heterochiral diastereomer. The two diasteomers are depicted in Figure 6.10. These two planar complexes have exactly the same structure but different orientation of R groups of analytes. The R group of the analyte is in the same side as the R' of the selector in the case of homochiral diastereomer while opposite is true for heterochiral diastereomer. In homochiral diastereomer,

Table 6.2. Thermodynamic data for chiral separation of amino acids

Amino acid	ln k' at temperature 298K	$\Delta H^{\circ}, kJ\,mol^{-1}$	$\Delta S^{\circ}/R + \ln \phi$
D-proline	2.17	-11.6	-2.51
L-proline	1.48	-12.5	-3.56
D-threonine	1.02	-11.0	-3.42
L-threonine	1.40	-12.1	-3.48

close contact of R group of the analyte with the expanded R' group of the selector allows strong interaction to occur, thus leading to strong retention. In heterochiral diastereomer, the chelate interactions of cupric ions with amino and carboxyl groups are about the same as in homochiral complex, however, the interactions of R groups with the R' group in a chiral stationary phase are weak because the rigid structure of the copper complex prevents them from engaging full contact.

It has been observed that most of common amino acid enantiomers obey this rule with D-isomer eluted first. However proline enantiomers are found to be an exception that L-isomer is eluted first. In order to understand this phenominum, a thermodynamic study was undertaken. According to the van't Hoff equation, a plot of ln k' against 1/T should give a straight line, whose gradient is $-\Delta H^{\circ}/R$ and intercept at 298K is $(\Delta S^{\circ}/R + \ln \phi)$, where ϕ is phase ratio. Assuming ϕ to be constant and independent of temperarure, the intercept value can be used to indicate the trend of the entropy change.

Plots of ln k' against $1/T$ for proline and threonine enantiomers are given in Figure 6.11.

The thermodynamic data calculated from the above plots are given in Table 6.2.

The values of ΔH° for L-isomers are all larger in magnitude than those for D-isomers. This result provides experimental evidence for our rationale of chiral
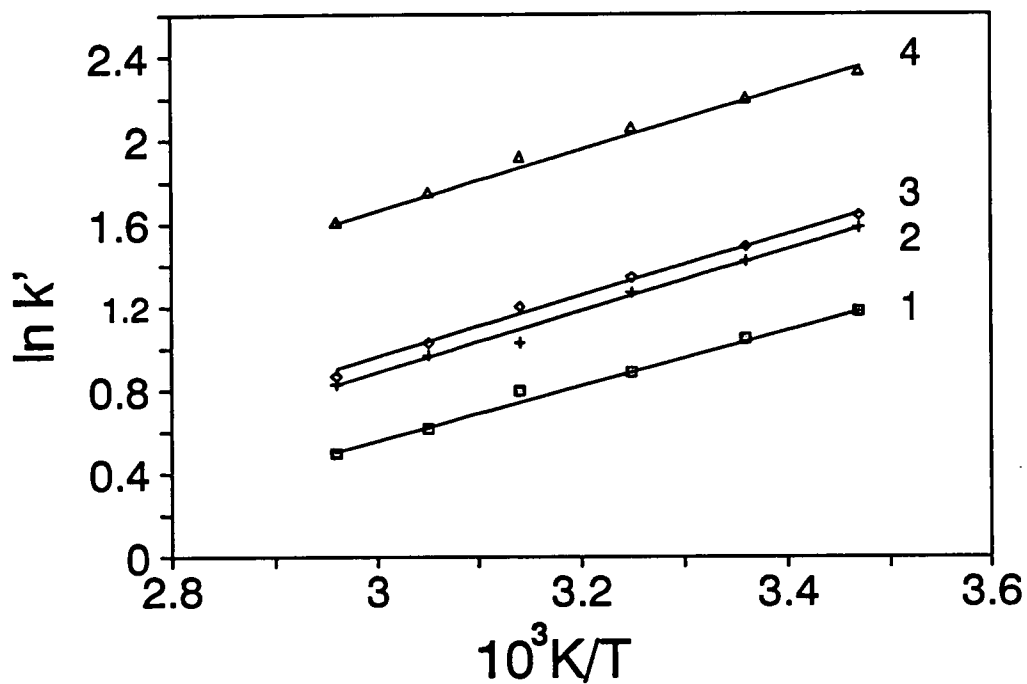
Figure 6.11. van't Hoff's plots for amino acid enantiomers. Solutes: 1 = D-threonine, 2 = L-threonine, 3 = L-proline, 4 = D-proline.
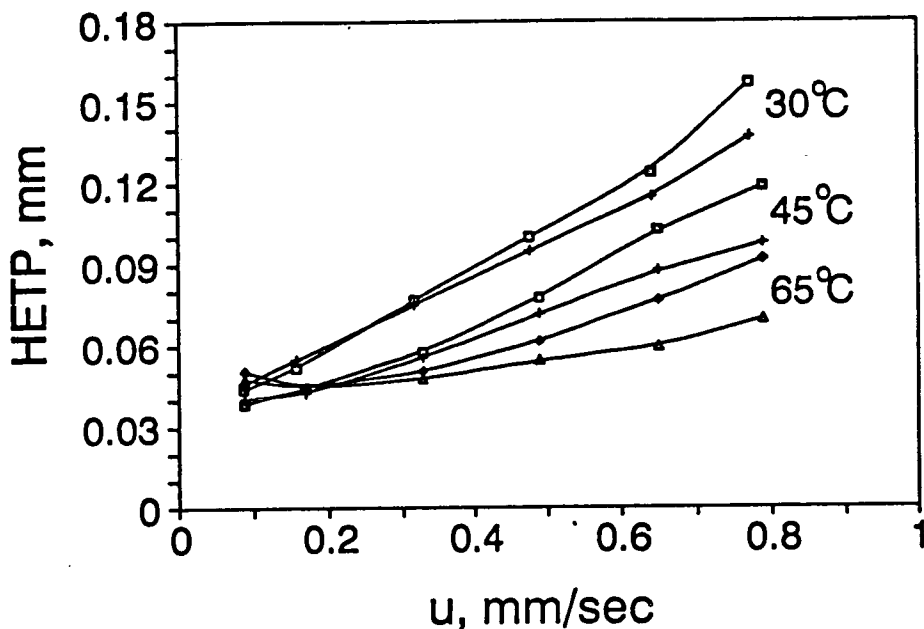
Figure 6.12. Plots of H versus u at various temperatures

recognition based on the analysis of molecular interactions. It is not surprising that negative values for entropy term are obtained in all cases since the chirally 'locked' molecules are highly restricted to move and well ordered compared to the molecules in solution. Neverthernless the degree of this ordering strongly depends upon the structure of molecule. The large difference in the entropy term for a pair of proline enantiomers, responsible for the reversal of elution order is presumably due to the rigidity of the molecules.

6.3.4 Kinetic Performance

Figure 6.12 shows plots of H versus u at different temperatures for proline enantiomers on naphthalenesulphonyl-L-phenylalanine coated graphite. The kinetic behaviour of the system is interpreted in terms of the Knox equation in slightly

Table 6.3. Kinetic characteristics of chiral chromatography

Solute	Temperature, $^\circ C$	k'	A	B	C
L-proline	30	3.86	0.026	0.0017	0.164
	45	3.49	0.017	0.0019	0.138
	65	3.36	0.015	0.0033	0.091
D-proline	30	7.84	0.053	0.0012	0.110
	45	7.09	0.038	0.0015	0.079
	65	6.46	0.046	0.0023	0.029

modified form:

$$H = \mathbf{A}\mathbf{u}^{0.33} + \frac{\mathbf{B}}{\mathbf{u}} + \mathbf{C}\mathbf{u} \tag{6.22}$$

The values of the coefficients in equation 6.22 are obtained by the curve fitting technique, using the data from Figure 6.12. The results are summarized in Table 6.3. It is noticeable that fairly large **A** and **C** terms have obtained together with negligible **B** term in all instances. The value of **C** is decreased drastically as the temperature increases while only slight change in **A** term is observed.

The theory of chromatography has indicated that C term mainly arises from slow mass transfer within the stationary zone, which comprises the stationary phase and the stagnant eluent trapped in and between the particles. There are two possible processes which govern the mass transfer term: diffusion controlled kinetics in the liquid and chemical reaction kinetics on the surface. Since liquid diffusion and exchange reaction are both activation processes with an exponential temperature dependence, the latter being superimposed onto the former in controlling the mass transfer processes, it is possible to identify which of them is predominant in some cases.

The reduced representation of column performance provides a convenient means of studying the mass transfer process. Diffusion coefficient at different
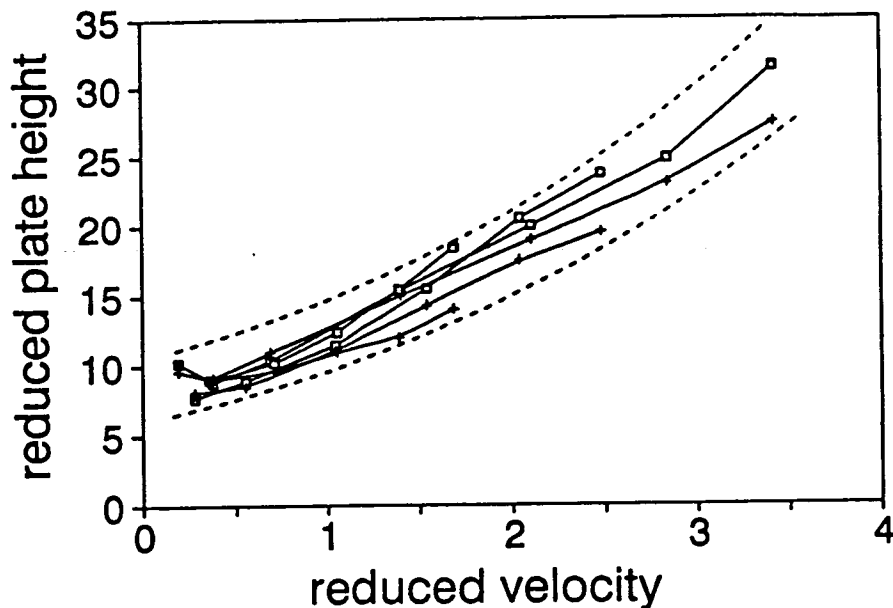
Figure 6.13. Plots of h versus ν

temperture may be estimated by the Wilke-Chang equation as given in the introduction chapter, the viscosity being taken as temperature dependence. Since the variation of diffusion coefficient with temperature is absorbed into the calculation of reduced velocity, identical curves of reduced plate height versus reduced velocity should be obtained at different temperatures if the mass transfer process is controlled only by the diffusion in the stagnant eluent. Otherwise reduction in C term is expected as the temperature is elevated.

Figure 6.13 shows the plots of h vs. ν using data from Figure 6.12 with assumption that the diffusion coefficient of proline is $1.0 \times 10^{-5} cm^2 sec^{-1}$ at $25^\circ C$ and the viscosities of the eluents are equal to those of water at corresponding temperatures [113] . Indeed, identical curves are obtained even though the column temperature is elevated from 15 to $65^\circ C$. From this study it is safe to conclude that the mass transfer process in this system is primarily controlled by the diffusion kinetics rather than the exchange kinetics.

6.4 Conclusions

Porous graphite coated with a chiral selector provides a new type of chiral stationary phase, which has excellent enantioselectivity, column efficiency and long term stability. Key to this approach is the selection of the chiral agent to be attached onto the graphite surface. For this purpose, the three- point-interaction model, initiated by Ogster, is found particularly helpful in understanding chiral recognition phenomena and hence it serves well as a general guideline.

The thermodynamic study of chiral separations based on copper complexation reveals that the elution order of enantiomers is largely controlled by the interaction of the R group on amino acid with uncovered graphite surface. However, when the entropy change involved is substantially high, the violation of this general rule may be observed. This work also establishes that the ligand exchange kinetics is not the barrier to the mass transfer process in the stationary zone. As in liquid liquid chromatography, diffusion is of decisive effect on the mass transfer properties of the chiral stationary phase using a rigid graphite as a support.

Chapter 7

Chiral Chromatography II

7.1 Introduction

When a chiral mobile phase additive is used in conjunction with an achiral solid support the situation is more complex than that with the chiral selector permanently attached onto the substrate. Two extreme cases may be observed with respect to the processes of chiral recognition. At one limit the chiral additive is considered to be adsorbed onto the solid support, which behaves as a chiral stationary phase. There is then no chiral selector in the mobile phase, and separation occurs entirely due to the difference in formation constants of transient diastereomers. At the other limit, the chiral analyte (i.e. the enantiomers to be separated) is complexed with the chiral selector in the mobile phase, and the separation occurs due to the difference in partition coefficients of diastereomers present in the eluent. In this case, the method is equivalent to the chromatographic separations of covalent diastereomers. In reality with a chiral selector added to the mobile phase giving only partial complexation of the analyte a complicated intermediate situation will exist somewhere between the two extremes.

Indirect detection based on the competitive distribution is often found of

use in chiral chromatography with chiral eluent additives. The advantage of this technique is that chiral analytes without inherent absorptivity may be transfered into detectable species without need of pre-column derivatization. It is generally accepted that the detector response is caused by the equilibrium disturbances occurring when a solute is introduced into a chromatographic system and the theoretical investigation has recently been reported [76]. It is shown that the disturbances are due to the fact that the competitive distribution of the solute relative to the eluent components in a given system is bound to occur when a common interaction such as displacement or ion-pair formation is involved.

As chiral recognition and indirect detection both originate in the molecular interactions between analyte and mobile phase additive, these two phenomena can be simultaneously studied by using a copper complex of L-phenylalanine as a chiral additive to the mobile phase and porous graphite as a solid support.

The enantiomeric resolution of free aromatic amino acids by reversed phase HPLC using eluents containing L-phenylalanine and cupric ions was first reported by Oelrich et al [108]. In selecting a desirable stationary phase they compared several reversed-phase silica gels and found LiChrosorb RP-18 gave better separations than RP-8 and RP-2 with their shorter lipophilic chain lengths. This may be interpretated as showing that a high hydrophobicity of a packing material is essential to the retention and the separation of diastereomeric complexes between cupric ion and amino acids. An attempt was made by Wernicke [109] to extend this method to the whole range of common amino acids, but only modest success was achieved. A considerable number of hydrophilic amino acids were weakly retained and eluted with k' values around 1. Neither of these studies considered the underlying mechanism of retention and separation.

The main theme of this chapter is to develop a model to account for chiral recognition and indirect detection phenomena. This model is built on the basis of

ligand exchange in the mobile phase and competitive adsorption of chiral selector and diastereomers onto the solid support.

7.2 Theoretical Considerations

In the preceding chapter, the thermodynamic basis of retention and recognition in chiral chromatography has been discussed at some length, with particular reference to the use of a chiral stationary phase where diffential stabilities of transient diastereomers are exclusively invoked to explain the chiral recognition. However, in chiral chromatography using chiral mobile phase additives an alternative process may be involved. Chiral separations are achieved at least partly via the partition of diastereomers between the mobile and the stationary phase. This type of chiral chromatography shows some analogy to the chromatography of covalently bonded diastereomers. In this case only one point interaction between chiral selector and chiral analyte is required to ensure the formation of diastereomer. As a pair of diastereomers can differ in their physical properties such as solubility and adsorbability, it is possible to separate them by means of partition chromatography provided that they have sufficient stability. In this respect partition chromatography is analogous to fractional crystallization which is based upon the differences in solubility of diastereomers, and which has been widely used to resolve acid or base enantiomers through the formation of diastereomeric salts. For example, the naturally occuring alkaloids are much utilized as resolving agents in the resolution of acids [73].

It is interseting to note that some resolving agents, though effective in crystallization or extraction techniques for optical resolution, would lose their discriminating ability when bound to a solid support. This may be understood by considering a pair of diastereomers which are free to rotate around the binding

axes without any steric hindrance. In this case the enantiomer is bound to the resolving agent through a single point to point interaction. Accordingly no difference would be expected in the formation constants for such diastereomers and therefore it would be impossible to separate them by means of chiral stationary phase. In this sense, chiral chromatography using chiral mobile phase additives is advantageous over that with chiral stationary phase as the former permits some other physical properties than stability of diastereomers to be exploited for the resolution of some particular enantiomers, for which the latter may be found incompetent.

As far as retention is concerned chiral chromatography with mobile phase additive resembles ion-pair chromatography in the way that analytes are adsorbed onto a non-polar phase mainly in ionized form. To achieve this result, they make use of the formation of ion pairs or diastereomers. In ion-pair chromatography [30] the ion pairs are formed between the analyte ion and an oppositely charged ion, which is added into the aqueous phase, this partition equilibrium can be represented by

$$A_m + P_m \rightleftharpoons AP, \tag{7.1}$$

where A is the analyte ion and P is the ion pairing agent, and the resulting ion pair will behave like a neutral molecule and therefore preferentially distributes into a non-polar phase.

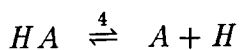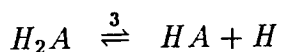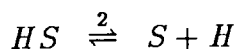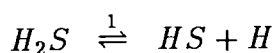A simple theory based upon the partition equilibrium shown above has been used to account for the effects observed in ion-pair chromatography. According to this theory, k' is directly proportional to the pairing ion concentration as high concentration favours the formatioon of the ion pair in the stationary phase. Alteration of the pairing ion concentration is thus a simple way of controlling retention.

As for chiral chromatography with copper diastereomer formed between the analyte ion and the chiral complexing agent in the eluent, some complications can arise in relation to ion pair chromatography because of the ligand exchange in the eluent and the displacement occuring on the surface. An alternate mechanism which takes into account these processes involved should be considered..

The formation of copper amino acid complexes in the eluent is manifested by the blue colour of the solution or, more precisely, demonstrated by UV spectra. The percentage of the acid analyte transformed into the complex can be calculated from the equilibrium constants of dissociation of the acid and of formation of the copper complex. As in ion-pair chromatography, the complexing agents are present at relatively high concentration in the aqueous phase, and mainly in the form of metal complexes whereas the analyte is usually present in rather small concentration compared to the complexing agents, it seems reasonable to assume that the analyte is predominantly in the form of ternary complex which is responsible for the retention of the analyte.

The main equilibria involved in chiral chromatography using copper complexing agents which are present in the mobile phase may be represented by the following equations (H_2S and H_2A represent the chiral selector and the analyte, respectively. M is cupric ion. The signs of the charges have been omitted for simplicity):

Dissociation of amino acids:

$$H_2S \overset{1}{\rightleftharpoons} HS + H$$

$$HS \overset{2}{\rightleftharpoons} S + H$$

$$H_2A \overset{3}{\rightleftharpoons} HA + H$$

$$HA \overset{4}{\rightleftharpoons} A + H$$

Complexation in the aqueous phase:

$$2S + M \overset{5}{\rightleftharpoons} MS_2 \tag{7.2}$$

Ligand exchange between the analyte and the complexing agents:

$$A + MS_2 \overset{6}{\rightleftharpoons} MSA + S \tag{7.3}$$

Adsorption of the selector metal complex onto the solid phase L:

$$MS_2 + L \overset{7}{\rightleftharpoons} MS_2L \tag{7.4}$$

Displacement on the surface:

$$MSA + MS_2L \overset{8}{\rightleftharpoons} MSAL + MS_2 \tag{7.5}$$

Constants for above equations may be expressed as follows:

$$K_1 = \frac{a_{HS}a_H}{a_{H_2S}}$$

$$K_2 = \frac{a_S a_H}{a_{HS}}$$

$$K_3 = \frac{a_{HA}a_H}{a_{H_2A}}$$

$$K_4 = \frac{a_A a_H}{a_{HA}}$$

$$K_5 = \frac{a_{MS_2}}{a_M a_S^2}$$

$$K_6 = \frac{a_{MSA}a_S}{a_{MS_2}a_A}$$

$$K_7 = \frac{a_{MS_2L}}{a_{MS_2}a_L}$$

$$= \frac{\theta_{MS_2}}{(1 - \theta_{MS_2})a_{MS_2}}$$

$$K_8 = \frac{a_{MASL}a_{MS_2}}{a_{MSA}a_{MS_2L}}$$

where K_7 is derived on a basis that adsorption of the metal complex obeys the Langmuir equation and the θ refers to the surface coverage.

Consider a copper complexation system in which the pH and the concentrations of the copper complexing agents are sufficiently high so that the analyte can be regarded as completely transformed into the ternary complex.

The distribution coefficient of the analyte is then given by

$$D = \frac{a_{MSAL}}{a_{MSA}} = \frac{K_7 K_8}{1 + K_7 a_{MS_2}} \tag{7.6}$$

or

$$\frac{1}{D} = \frac{1}{K_7 K_8} + \frac{K_7}{K_7 K_8} a_{MS_2} \tag{7.7}$$

Since k' is proportional to D, we observe that reciprocal of k' will be proportional to the activity of the complexing agent in the eluent. The activity in this case may be approximated by the concentration and therefore the reciprocal of k' versus the concentration of the binary complex in the eluent will produce a straight line, which may be taken as a test for the mechanism proposed above.

A further comment should be made regarding the effect of the concentration of the complexing agents in the eluent. If the concentration is kept enough low to allow linear adsorption to occur, but sufficient for the complete formation of the ternary complex, k' would reach a maximum where $D = K_7 K_8$ as $K_7 a_{MS_2}$ is negligible compared to 1. Further reduction in the concentration would cause a decrease of k' because of the dissociation of the ternary complex as shown by equilibrium 6.

Indirect detection of the ternary metal complex may be understood in terms of displacement occurring on the surface. When the column is equilibrated with a stream of eluent containing UV absorbing complexing agents, a stable backgroud absorption is observed. Upon the introduction of the analyte, a disturbance of the equilibrium occurs. In the band of the analyte, additional concentration of the complexing agents is brought in by the displacement process. With the migration of analyte band, a fraction of concentration depleted surface is left behind, which

takes the complexing agent from the eluent to retain equilibration. The change in the background absorption corresponding to this reequilibration is expected to appear as a negative band. This is so called system peak. It is not surprising that the system peaks are often found rather broad and severely tailing, largely due to the effect of nonlinearity of the adsorption isotherm.

7.3 Results and Discussion

7.3.1 Characterization

Absorption Spectra

The formation of metal complexes between cupric ions and amino acids at pH 6.8 is demonstrated by UV spectrometry. The spectra of solutions of copper-phenylalanine and copper-proline mixtures show a clear additional absorption with a maximum at 243 nm, characteristic of the known spectra of copper-amino acid complexes (Figure 7.1). The fraction of phenylalanine in the form of the complex is not deducible from the spectra but may be calculated from the known stability constants of the complex [77], which is found to be about 85%. For detection of aliphatic amino acids, UV wavelength is set at 280 nm, at which both copper complexes of aliphatic and aromatic amino acids have similar absorptivities, it is thus possible to attain a good balance between high sensitivity and low backgroud absorption.

Adsorption Isotherms

The isotherm for adsorption of the copper-L-phenylalanine complex from eluent containing 10% acetonitrile (v/v) and 5 mM phosphate buffer at pH 6.8 was determined by the breakthrough method by means of solutions of copper complex
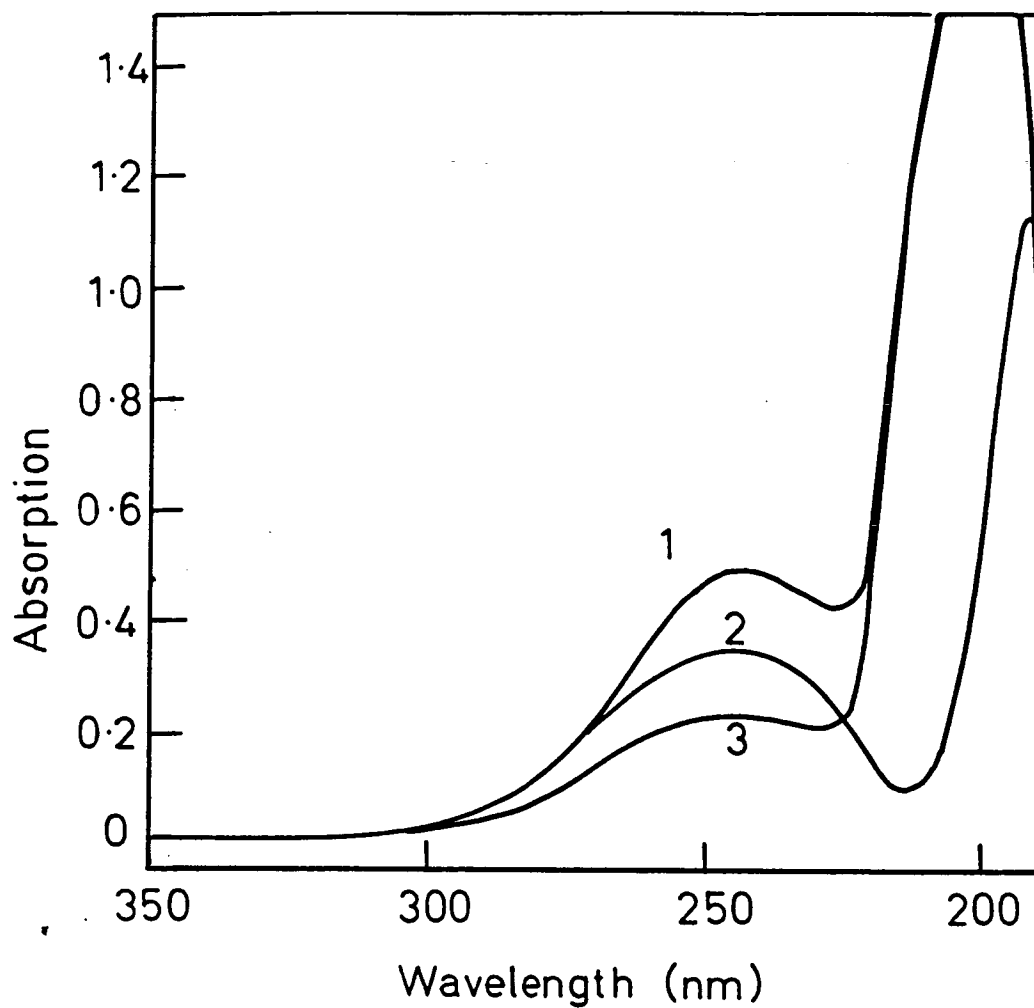
Figure 7.1. UV spectra of copper complexes. 1. 0.1 mM $CuSO_4$ + 0.2 mM L- phenylalanine. 2. 0.1 mM $CuSO_4$ + 0.2 mM L-proline. 3. 0.2 mM L-phenylalanine, pH 6.80.
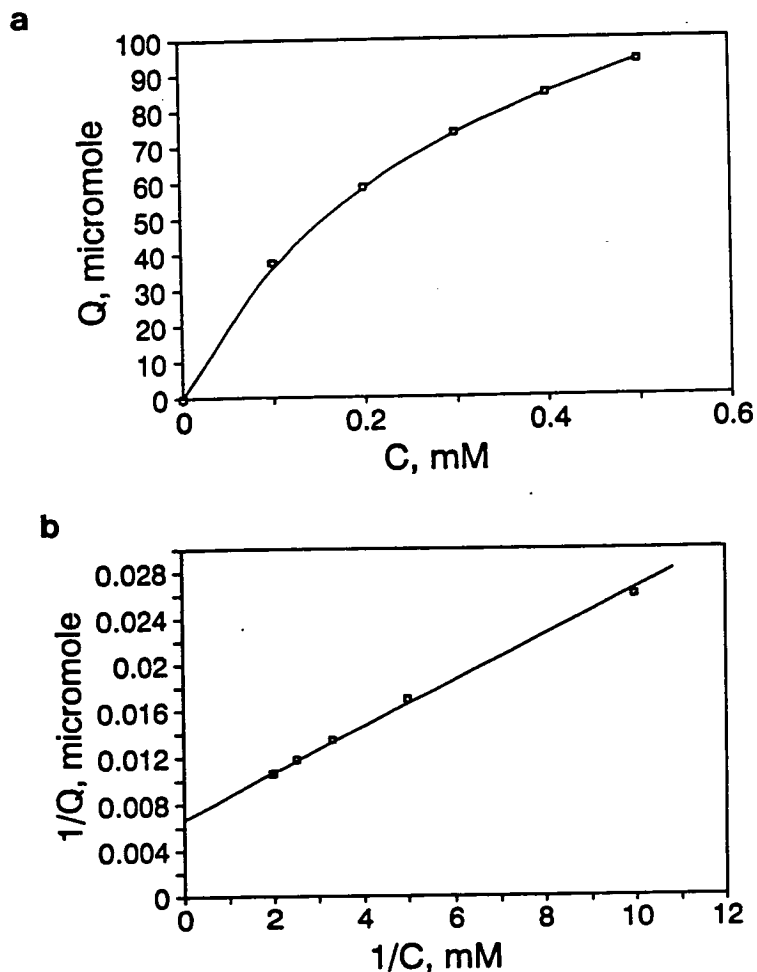
Figure 7.2. Adsorption isotherms of copper complexes. (a) Plot of Q vs. C. (b) Reciprocal plot of (a).

of different concentrations. Figure 7.2 (a) shows the isotherm plotted directly and Figure 7.2 (b) shows the isotherm plotted as $1/Q$ against $1/C$. Since a straight line is obtained it is evident that the adsorption isotherm is of the Langmuir type. Monolayer capacity for the column containing 1.0 g of graphite with S_{BET} of 107 $m^2 g^{-1}$ is calculated from the intercept of the plot to be 1.4 $\mu mol\, m^{-2}$. This value is very similar to that previously found for naphthalenesulphonyl-L-phenylalanine. The percentage of the surface coverage ranges from about 30 to 65% corresponding to the concentration varying from 0.5 to 1.5 mM.

Table 7.1. Retention and selectivity of chiral chromatography.

Amino acid	Porous graphite [a]			Reversed phase silica [b]		
	k'_D	k''_L	α	k'_D	k'_L	α
Alanine	2.67	2.67	0.40	0.48	1.20	
Aminobutyric acid	3.33	4.00	1.20	0.83	1.24	1.49
Arginine	12.67	20.83	1.64	0.15	0.52	3.47
Asparagine	5.67	4.33	0.76	1.20	1.00	0.83
Aspartic acid	4.83	3.67	0.76	-	-	-
Glutamic acid	3.33	3.33	1.00	1.23	1.33	1.08
Glutamine	2.50	2.50	1.00	-	-	-
Histidine	11.33	11.33	1.00	6.78	5.19	0.77
Leucine	7.00	9.00	1.29	10.64	16.62	1.56
Methionine	11.50	14.00	1.22	7.53	10.25	1.36
Norleucine	11.50	15.33	1.23	10.84	19.26	1.78
Norvaline	5.17	6.33	1.23	3.37	5.58	1.66
Phenylglycine	10.67	13.83	1.30	6.78	12.53	1.85
p-OH-phenyl-glycine	11.83	14.50	1.23	-	-	-
Proline	2.83	5.33	1.88	0.82	4.25	5.18
Serine	3.83	3.83	1.00	-	-	-
Threonine	4.83	3.67	0.76	1.42	1.10	0.77
Valine	3.83	5.00	1.31	2.77	4.73	1.71

[a] Chromatographic conditions as in Figure 7.3.

[b] Chromatographic conditions: column, LiChrosorb RP-18, 125 × 4 mm; eluent, 1.0 mM $Cu(OAc)_2$: 2.0 mM L-phenylalanine, pH 4.5; detection, UV 280 nm.

Chiral Separations

Figure 7.3 shows chiral separations of selected amino acids using copper-phenyl-alanine complex as the chiral selector. Most enantiomers can be resolved with D-isomers eluted first. The capacity ratios and separation factors are summarized in Table 7.1, along with the results obtained by Wernicke [109] for comparison. The enantioselectivities are similar to those observed with reversed phase silica gels but k' values are greater with graphite.
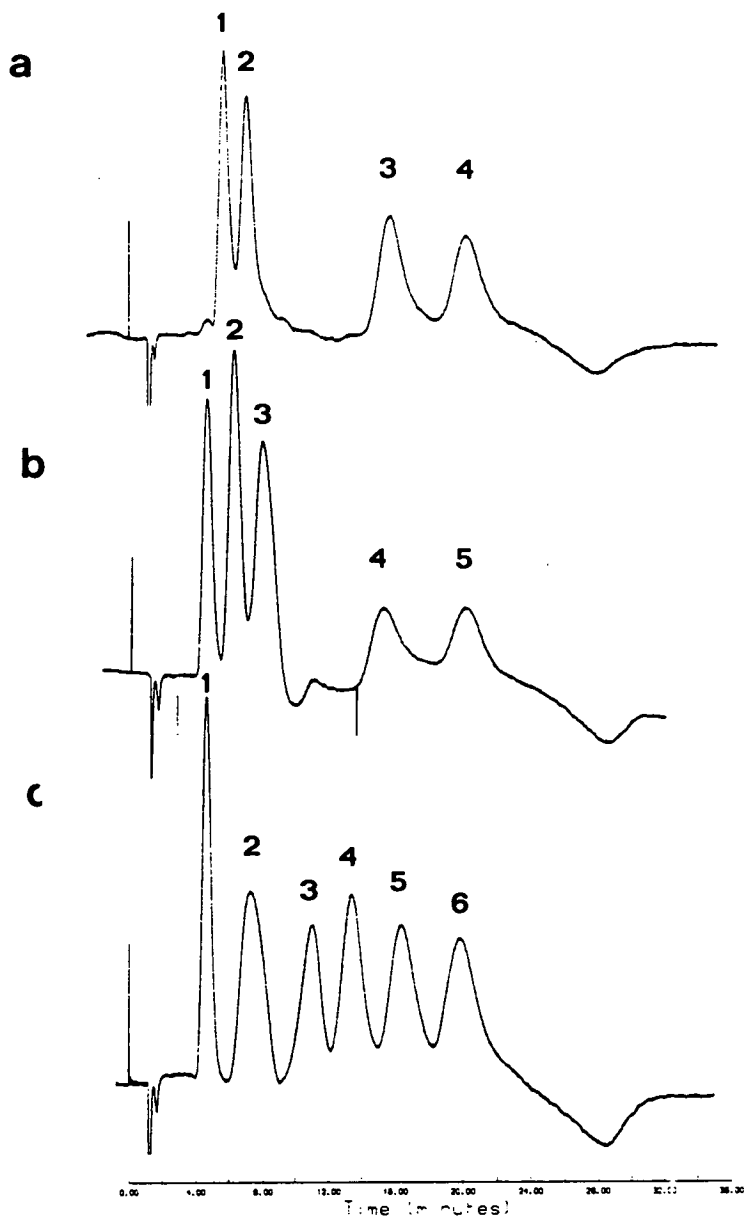
Figure 7.3. Chiral separations of amino acids. Column, PGC 94F, 100 × 4.6 *mm*; eluent, 5 *mM* phosphate buffer (pH 6.8) containing 0.5 *mM* $CuSO_4$, 1.0 *mM* L-phenylalanine and 10% acetonitrile (*v/v*); flow rate, 1 *ml/min*; detection, UV 280 *nm*. Solutes: (a) 1=L-threonine, 2=D-threonine, 3=D-phenylglycine, 4=L-phenylglycine. (b) 1=DL-alanine, 2=D-valine, 3=L-valine, 4=D-norleucine, 5=L-norleucine. (c) 1=D-proline, 2=L-proline, 3=D-leucine, 4=L-leucine, 5=D-methionine, 6=L-methionine.
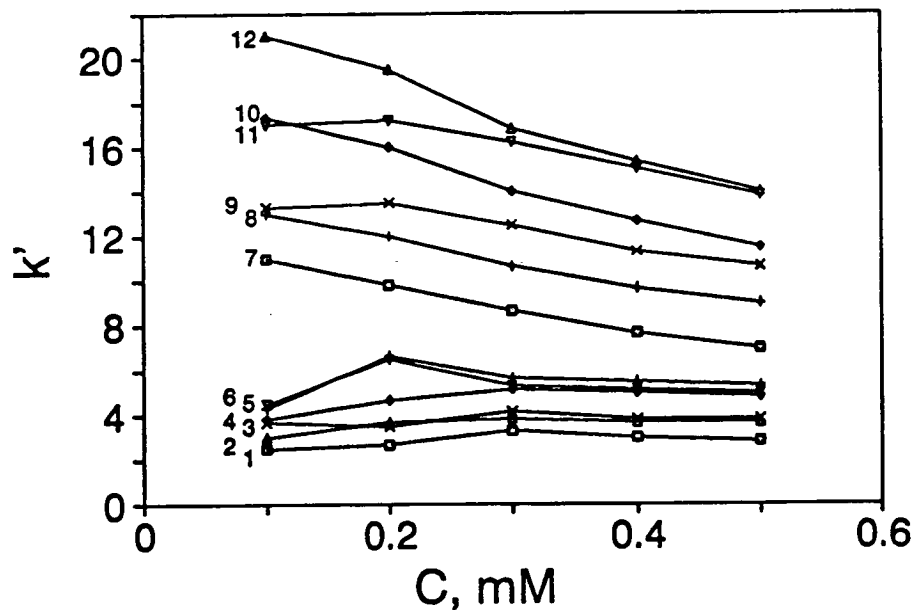
Figure 7.4. Dependence of k' upon concentration of copper complex. Solutes: 1 = D-proline, 2 = L-threonine, 3 = D-valine, 4 = D-threonine, 5 = L-proline, 6 = L-valine, 7 = D-leucine, 8 = L-leucine, 9 = D-phenylglycine, 10 = D-methionine, 11 = L-phenylglycine, 12 = L-methionine.

7.3.2 Effects of Eluent Variables upon Retention and Selectivity

Dependance of k' upon concentration of copper complexing agents

Figure 7.4 shows how the retention of amino acids is affected by alteration of the concentration of copper complex in the eluents. Two different patterns may be distinguished. For one group of amino acids which are strongly retained, k' decreases gradually with increase in concentration of the resolving agents. For the other group, particularly for the less retained species, k' increases to a maximum at about 0.2 or 0.3 mM of the resolving agents and then decreaes as for the first group.

The increase in k' with the concentration of the resolving agents is the trend expected on the basis of ligand exchange whereby a higher concentration of the resolving agents will give higher conversion of the ligand into diastereomeric

complex and thus will lead to high retention. The concentration of the resolving agents required for amino acid enantiomers to form the diastereomeric complex are different from one to another depending upon their ionization constants and stabilities of the complexes.

On the other hand the opposite trend which is observed for all the amino acids studied points to the counteracting effect on the retention of increasing concentration of the resolving agents. This can be explained in terms of the displacement equilibrium which predicts that the plot of $1/k'$ against $[MS_2]$ should yield a linear curve. However it should be noted that the theory is developed on the assumption of complete conversion of analyte acid into diastereomeric complex, it is likely that the plot of $1/k'$ vs. $[MS_2]$ exibits deviation from a straight line owing to the fact that the analyte is not entirely present in the form of diastereomer. The plots for those strongly retained species are shown in Figure 7.5. Indeed, nearly linear curves are observed in all instances. This is in agreement with predictions made by the mechanism of chiral chromatography with chiral mobile phase additives mentioned above.

Dependence of k' upon pH of eluent

Figure 7.6 shows that for all amino acids of interest retention increases as the pH of the eluent increases over the range from 5.5 to 6.8. As has been discussed in the preceding chapter, this type of effect is thought to be induced through the fraction of ionised acid, since it is this form of the acid that is responsible for the formation of the copper complex. Under our experimental conditions with phenylalanine, for instance, it was found by calculation that 61% was present as the complex $[MS_2]$ at pH 5.5, compared to 85% at pH 6.8. Decrease of $[MS_2]$ at lower pH would have positive effect upon k' according to equilibrium 7. However this positive effect is offset by the dissociation of the diastereomeric complex
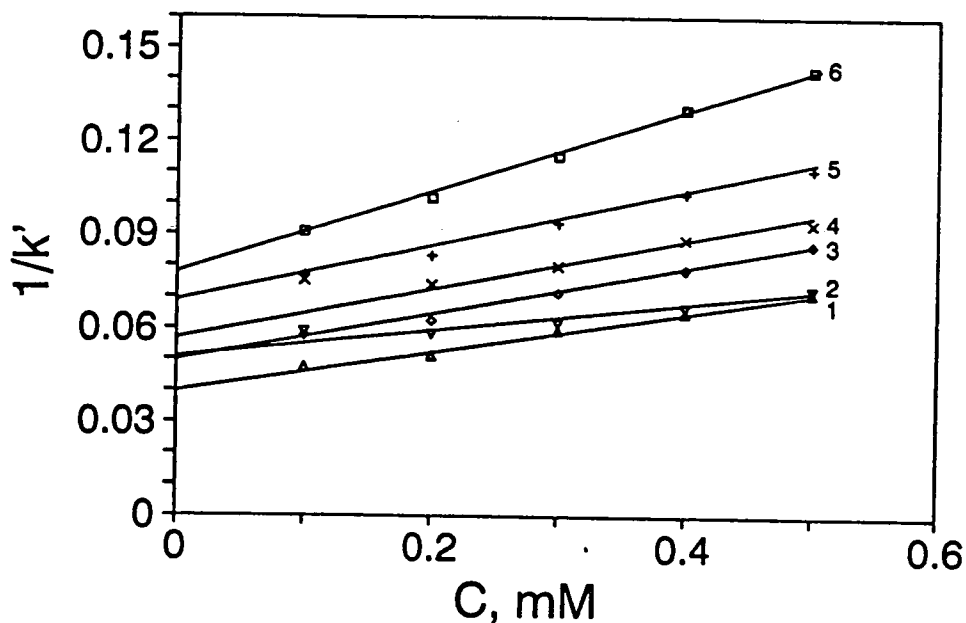
Figure 7.5. Plots of $1/k'$ vs concentration of copper complex. Solutes: 1 = L-methionine, 2 = L-phenylglycine, 3 = D-methionine, 4 = D-phenylglycine, 5 = L-leucine, 6 = D-leucine.
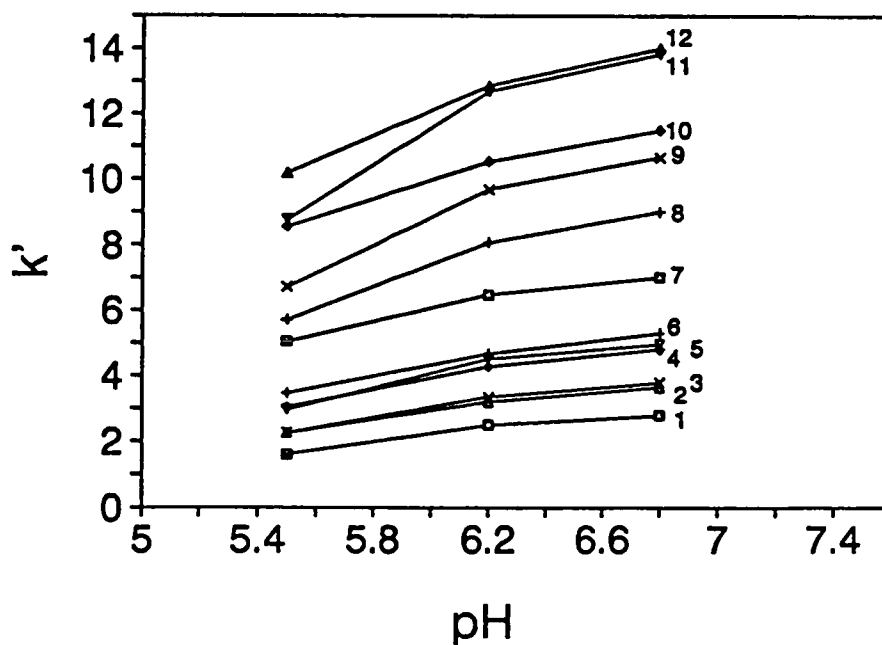
Figure 7.6. Dependence of k' upon pH of eluent. Solutes as for Figure 7.4
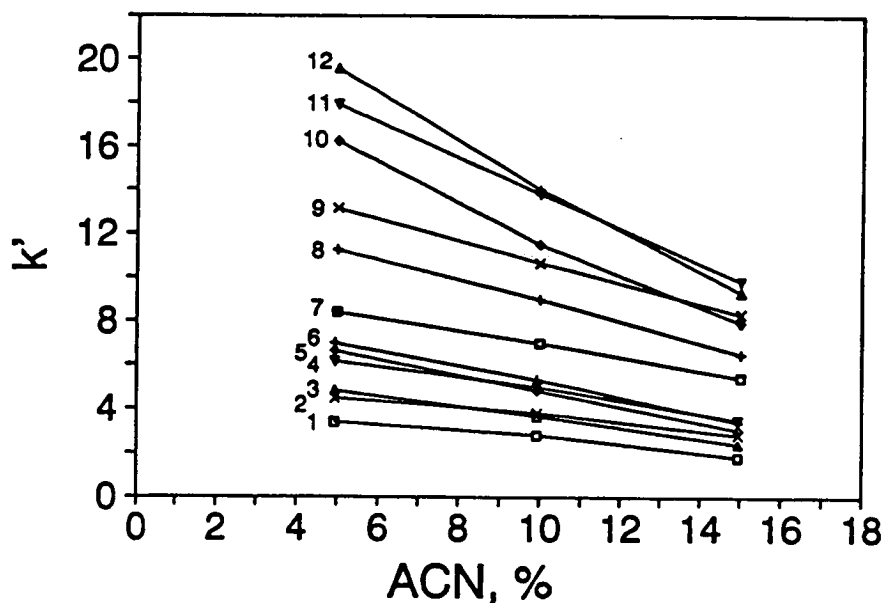
Figure 7.7. Dependence of k' upon percentage of acetonitrile. Solutes as for Figure 7.4

which has a more profound effect on retention. This may be understood from two respects. First, the fraction of [A] is inversely proportional to $[H_3O^+]$ and so therefore is k'. Second, additional amount of the resolving ligand in the eluent brought in by the dissociation of $[MS_2]$ shifts the ligand exchange equilibrium in a direction unfavourable for the formation of the diastereomer and hence decreases retention .

Dependence of k' upon Concentration of Acetonitrile

Figure 7.7 shows, as expected, that an increase in the percentage of acetonitrile in the eluent decreases retention. This is considered to be due to improved solubility of the neutral copper amino acid complexes in eluents with higher percentage of acetonitrile.

7.3.3 Kinetic Performance and Fronted System Peak

Kinetic Performance

As has been seen from the representative separations shown in Figure 7.3, the chromatographic bands of the analytes are generally symmetric but rather broad. Reduced plate heights, as with ODS silicas, are of the order of 20 at linear velocity of 1.2 $mm\ sec^{-1}$. These values are about twice those for simple test solutes such as phenol and aniline under the same conditions.

One would suspect that the poor efficiency of the system might be due to the volume overloading effect [110]. An experiment was carried out to examine the possible effect of sample size accordingly. With methionine enantiomers, the plate height values and capacity ratios were found almost independent of the amount of sample injected. A linear relationship between the peak height and the sample volume provides additional support for the preclusion of this possibility (see Figure 7.8).

The extra band spreading is thus ascribed to the chemistry of copper complexation. A single analyte band can actually contain more than one species, each of which has distinct distribution coefficient. Since these complexes interact with one another to attain equilibrium during the migration of the band they may not be able to separate but contribute to the overall band spreading owing to the fact that they have different migration rates. This type of band spreading has been studied in detail by Knox and Shibukawa [111].

Fronted System Peak

Three negative system peaks have been seen in all chromatograms shown in Figure 7.3. The first and the last were shown to correspond to copper ion and its neutral complex with phenylalanine, respectively. As the broad, unsymmetric
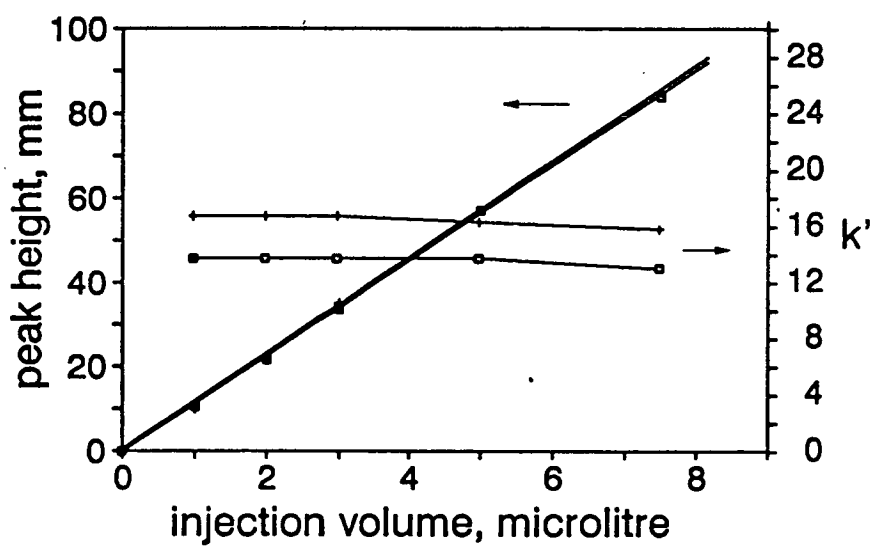
Figure 7.8. Plots of peak height and k' vs sample volume. Solutes: lower, D-methionine; upper, L-methionine.

peak of the copper complex may interfere with detection of other amino acids, it would be desirable to control the retention of the system peak so as to reduce its detrimental effect. To achieve this, an understanding of the origin of the system peak is essential.

In the present system the adsorbed complexing agents, mainly in the form of neutral copper complex, are maintained at equilibrium dynamically with those in the eluent. When an injection of analyte solution, which is short of the complexing agents, is made, a perturbation of the equilibrium occurs, leading to the desorption of the complex from the solid surface. Thus the analyte appears as a positive band which is actually composed of desorbed complexing agents. This analyte band is always accompanied by a number of negative bands corresponding to the species being displaced.

The retention of desplaced species is mainly determined by its distribution coefficient, however, it is also affected by the type of adsorption isotherm, as shown by de Vault's theory. If the desorption process can be covered by the Langmuir equation, recalling de Vault equation,

$$u_{band} = \frac{u_{solvent}}{1 + \phi f'(C)} \tag{7.8}$$

we may find that average migration rate of the negative band decreases when nonlinearity of the isotherm increases since $f''(C)$ in this case is positive, corresponding to the desorption process. This sharply contrasts to the trend observed with tailed peak in adsorption chromatography. Figure 7.9 illustrates the elution curves with respect to some typical values of $f''(C)$, where Langmuir adsorption is assumed in all instanses.

As noted above, in nonlinear system the average retention time of the negative band decreases with increase in surface coverage while increases with the sample size. Thus the negative band will become more fronted when large quantity of
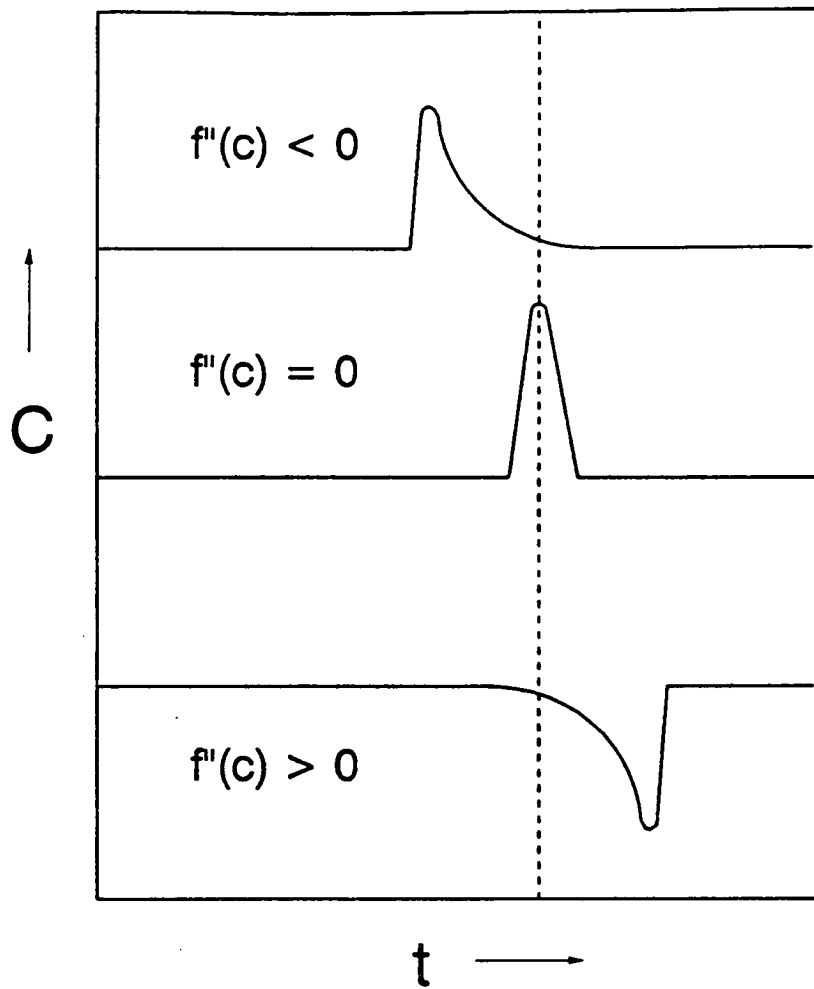
Figure 7.9. Elution curves for different values of $f''(C)$.

analyte is injected. The system peaks therefore impose a limit on the sample size and peak capacity of the chromatographic system. This limitation may be alleviated to some extent by judicial selection of complexing agents. In addition to the requirement of high enantioselectivity and absorbtivity, a chiral selector should have appropriate adsorbability so that its position in the chromatogram is arranged in such a way to avoid interference with bands of analyte. Control of surface coverage provides additional option to optimize the separatiom system.

7.4 Conclusions

A model which combines the ion-pair mechanism and the ion-exchange mechanism is developed to account for the retention behaviour of enantiomers on porous graphite when used with copper amino acid complexes as mobile phase additives. In the range of low concentrations of the additives, k' increases with the concentration, indicating the complex-formation equilibrium operating. However, after reaching a maximum, k' decreases with further increase in the concentration, pointing to a predominance of competitive adsorption .

In indirect detection system, system peak is the consequence of equilibrium disturbance occurring upon sample injection. The peak shape is thus related to the type of equilibrium isotherm in exactly the same way as in adsorption chromatography.

Chapter 8

Exclusion Chromatography

8.1 Introduction

Exclusion chromatography or gel chromatography is a technique for separation of high molecular weight substances primarily on the basis of molecular size. In contrast to all forms of retentive chromatography, the separation of solutes is achieved through differential permeabilities into a porous matrix and no interactions between the solutes and the surface of the matrix should occur in an ideal exclusion system. The technique may come under different names but they all refer to the same process. For example, gel filtration was first introduce by Poroth and Flodin [78] in 1959,referring to the separation of water-soluble polymers carried out in aqueous eluents whereas gel permeation, coined by Moore [79], designates the separation of hydrophobic synthetic polymers in organic solvents.

A variety of packing materials have been used to effect separation by exclusion chromatography. According to their bulk composition, these packings may be grouped into organic and silica based types. Representative of the first type are cross linked agarose and cross linked polystyrene. Both products have relatively uniform surfaces, adsorption being virtually avoided by selection of compatible

150

eluents. True exclusion chromatography is often attained with these packings. However, the organic gels do not allow the application of high pressures because of their high porosity due to swelling and consequently lack of rigidity. Silica based packings maintain premier position owing to their mechanical stability and rigid pore structure. High efficiency has been demonstrated with unmodified silica in conjunction with organic solvents for the separation of polystyrene samples [30]. However in the case of separation of biopolymers, protective functional groups such as diols must be bonded onto the silica surface to reduce ionic or hydrophobic interactions with solutes [80]. Bonded silicas, unfortunately, are not completely satisfactory because they are susceptible to dissolution at pH > 8. Coating the silica with hydrophilic polymers can enhance its resistance to some extent but cannot prevent the support being eroded eventually [103].

In an effort to combine a rigid pore structure with chemical stability in a single packing for size exclusion chromatography of water soluble polymers, we have examined the feasibility of coating porous graphite with hydrophilic polymers. Although a variety of such compounds as polysaccharides may be considered for this purpose, polyvinylalcohol (PVA) has become our choice of testing material owing to the fact that PVA shows strong tendency to adsorb on the graphite surface. Cross linked PVA beads have been obtained by controlled methanolysis of polyvinyl acetate suspension and followed by cross linking with epichlorohydrin [101]. Being essentially same as with other hydrophilic gels this material alone is useless in HPLC unless supported by a rigid matrix.

8.2   Theory of Size Exclusion

Retention behaviour of analytes in size exclusion is unique in that all sample molecules elute within a well defined narrow volume, based on the column geometry and packing characteristics. The definitions of retention parameters widely used in retentive chromatography are therefore inappropriate in this connection. Accordingly the elution volume (V_e) of a solute in exclusion chromatography is defined by the equation

$$V_e = V_o + K V_p \qquad (8.1)$$

where V_o is the interstitial volume outside the particles and V_p is the pore volume within the particles; K is the permeation ratio, whose values vary between zero and unity, corresponding to the total exclusion and total permeation limits of the column, respectively.

The retention mechanism based on geometrical considerations have been generally accepted [99, 100]. The essense of this model is that the centre of a spherical molecule of radius r cannot approach closer than r to any part of the internal surface of the matrix. Thus the pore volume can be divided into two regions: the molecules can explore freely in one region but are completely excluded from the other. The permeation ratio K is then the fraction of the pore volume accessible to the centre of the gravity of the solute molecules.

The solute size in exclusion chromatography is determined by the hydrodynamic radius or the molecular radius of gyration. The effective size of a solute is therefore governed by various factors such as geometrical shape (hard sphere, random coil, or rigid rod), intramolecular interactions. Several geometrical theories have been developed to relate K to the molecular size in quantitative way [100].
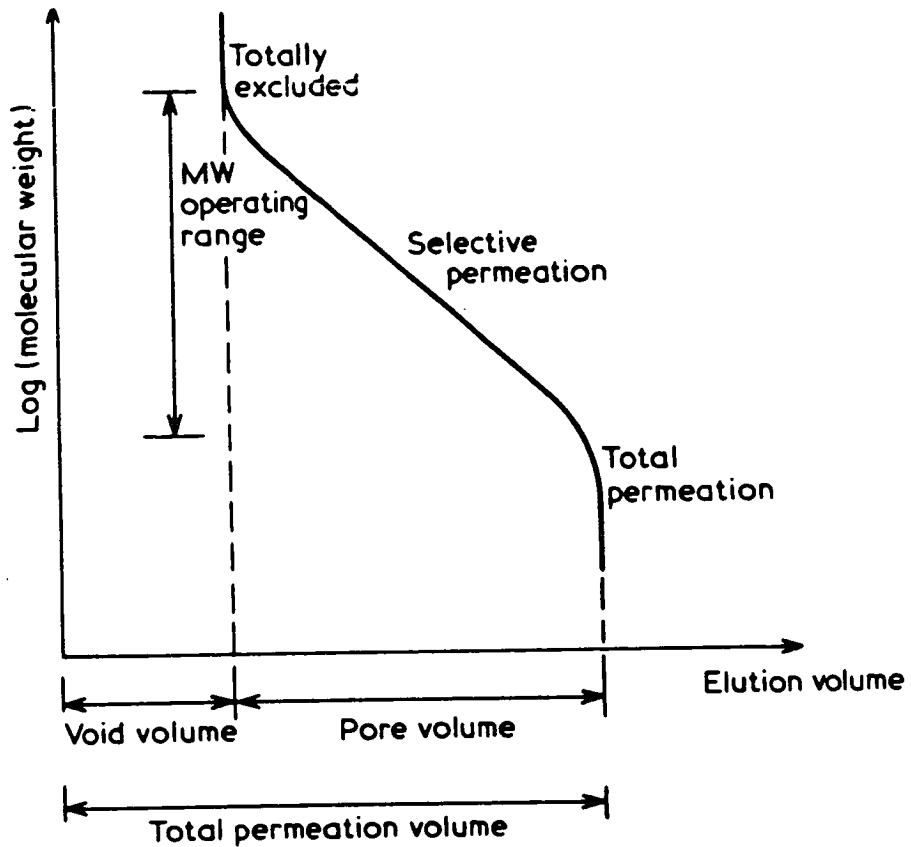
Figure 8.1. Idealized calibration curve for exclusion chromatography

The normal way of plotting exclusion data is in the form of a semi-logarithmic calibration curve relating molecular weight to either V_e or K and a typical curve is shown in Figure 8.1. Such calibration curves normally have a fairly sharp exclusion limit at the high molecular weight end, a more or less linear intermediate portion and a gradual curve away from the linear towards the region of tatal permeation.

8.3 Results and Discussion

Graphite is well known for its strong hydrophobicity as it is wetted by water only in the presence of organic modifiers or surfactants. In order for porous graphite to be useful in separation of water-soluble polymers, the primary requirement is to mask the hydrophobicity. The simplest way to do this is to adsorb polyvinyl alcohol onto the graphite surface from an aqueous solution and then stabilize it by cross-linking. In this way a monolayer coating of PVA is obtained, which gives about 4 $\mu mol\, m^{-2}$ of hydroxy group. Unfortunately, proteins tested on graphite coated with a monolayer of PVA in this way were all irreversibly adsorbed. Repeated treatment of porous graphite with a solution of PVA cannot eliminate adsorption completely. Given no ionic functional groups on the graphite surface, excessive retention is primarily attributed to hydrophobic interactions. This may be regarded as indictive of the incomplete coverage by hydrophilic coating.

It became clear that extra PVA should be added in order to promote the formation of a thicker layer. By the evaporation method a multilayer coating was attached onto the surface of graphite which gives about 10 $\mu mol\, m^{-2}$ of hydroxy group. With phosphate buffer as an eluent, most proteins were then eluted within the elution volume of acetone. A separation of thyroglobulin and myogolbin is shown in Fig. 8.2.

In order to determine K, the interstitial volume and the totally permeation volume of the column should be known. It is therefore necessary to identify a high molecular weight species such as Blue Dextrin that is totally excluted from the mesopores of particles, and then to measure its elution volume accurately. With coated graphite a Blue Dextrin of two million dalton was found unsuitable to serve this purpose as it was adsorbed so strongly that no elution is possible. This type of problem was also reported with silica based materials [81]. Unfortunitely
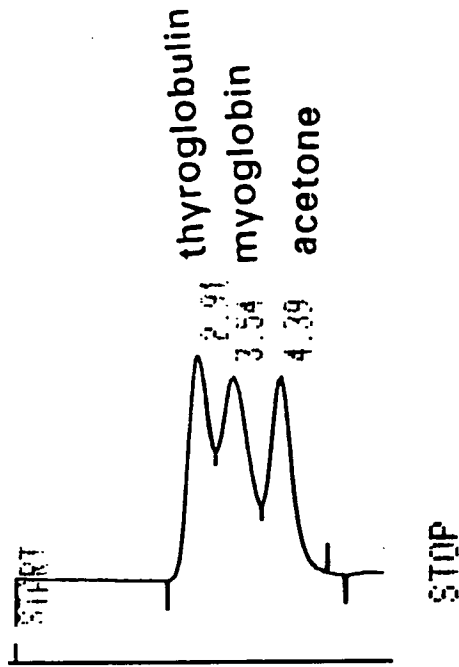
Figure 8.2. Separation of thyroglobulin and myoglobin on PVA coated graphite. Column, PGC 94F coated with PVA, 50 × 4.6 *mm*; eluent, 0.02 *M* phosphate, pH 7.0; detection, UV 280 *nm*.
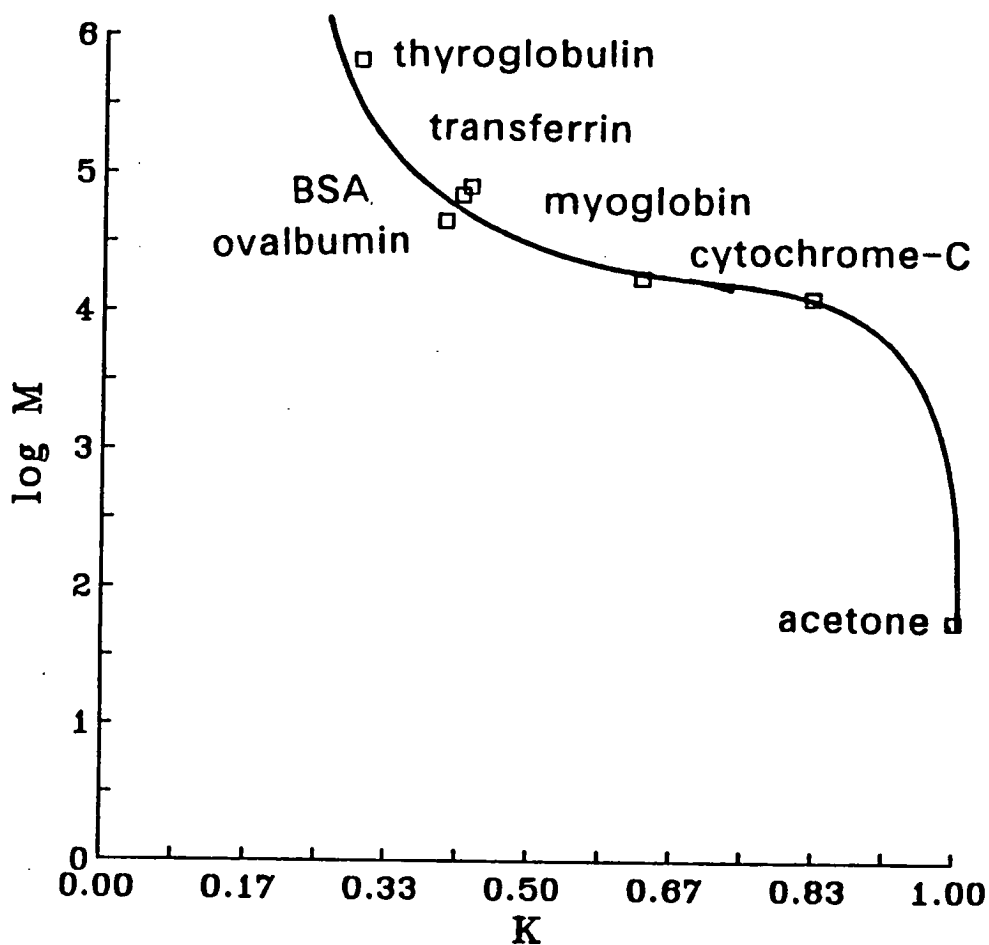
Figure 8.3. Calibration curve for proteins separated on PVA coated graphite

no macromolecular probes were immediately available in the laboratory, and the interstitial porosity was therefore estimated to be about 0.36 for the column of dimensions of 50 × 4.6 mm, in which the elution volume of acetone was taken as the sum of the interstitial and the pore volume. The particle porosity was assumed to be 0.65.

Fig. 8.3 plots log protein molecular weight against permeation ratio K. Proteins including thyroglobulin, transferrin, BSA, ovalbumin, myoglobin and

cytochrome-c were eluted in roughly reverse order of molecular weight, indicationg the predominant size exclusion mechanism. However, even with a multilayer coating more hydrophobic proteins such as trypsin and lysozyme were somewhat adsorbed. There is no doubt that the adsorption effect is due to small portion of the graphite surface left intact and thus accessible to solutes. This may be caused by cracks and defects in the coating, but more likely, by swelling of loosely cross-linked PVA in aqueous media. Highly restriced diffusion of solutes in the swollen polymeric coating is manifested by noticeably low efficiency as observed in Fig. 8.2.

8.4   Conclusions

A neutral hydrophilic coating enables some proteins to be separated on porous graphite in the order of molecular size. Unfortunately, this size exclusion mechanism cannot be generalized to a wide range of proteins because of adsorption effect. The strong non-polar nature of graphite makes it less promising to use in exclusion chromatography of biopolymers.

Appendix A

Glossary of symbols

A, B, b, C, c Constants.

a	Activity.
A_m	Cross-sectional area of molecule.
B_o	Specific permeablity.
C	Molar concentration.
C_m, C_s	Solute concentration in stationary and mobile phases, respectively.
D	Distribution coefficient.
D	Diffusion coefficient.
D_{col}	Diffusion coefficient in a column.
D_i	Diffusion coefficient in region i.
D_m, D_s	Diffusion coefficients for mobile and stationary phases, respectively.
D_{mz}, D_{sz}	Diffusion coefficients for mobile and stationary zones, respectively.
d	Distance from the charged surface within Helmhotz layer.
d_c	Column diameter.
d_f	Thickness of the bulk stationary phase.
d_p	Mean particle diameter.
E	Interaction energy.

e	Elementary charge.
F	Faraday constant.
ΔG	Free energy change of mass transfer or activation.
H	Plate height.
ΔH	Enthalpy change of transfer or activation.
h	Reduced plate height, H/d_p.
I	Ionization potential.
K^o	Thermodynamic distribution coefficient.
K_c	Concentration distribution coefficient.
k	Boltzman constant.
k', k''	Phase and zone capacity ratios, respectively.
L	Column length or length migrated if the latter is less.
l	Random walk step length.
M	Constant proportional to solute mass.
M_2	Molecular weight of solvent.
N	Plate number, H/L.
N	Avogadro's number.
n	Number of random walk steps.
n	Empirical factor.
P	Equilibrium gas pressure.
P_o	Vapour pressure.
ΔP	Pressure drop along the column.
Q	Amount of solute adsorbed.
Q^o	Monolayer adsorption capacity.
R	Retention ratio or, equivalently, the fraction of solute in the mobile phase.

R	Radius of hydrated molecule.
r	Separation between two molecules under interaction.
r	Radial coordinate, i.e., distance from centre.
S	Persistence of path distance for molecular migration.
S_{BET}	BET surface area.
S_e	Persistence of path distance for molecular migration in extreme velocity.
ΔS	Entropy change of transfer or activation.
T	Absolute temperature.
t	Time spent during migration or retention time.
t_e	Exchange time between flow paths.
t_m, t_s	Time spent in mobile and stationary phases, respectively.
t_{mz}, t_{sz}	Time spent in mobile and stationary zones, respectively.
U	Interaction potential.
u	Mean linear velocity.
Δu	Differential velocity between mean and extreme velocities.
V	Retention volume.
V_1	Molar volume of solute.
V_m, V_s	Volumes of mobile phase and stationary phase, respectively.
w	Interaction energy of adsorbed molecules between neibouring sites.
X_i	Fraction of solute in phase i.
Z	Charge number.
z	Distance along column axis.
α	Polarizability.
α	Separation factor.
α_E	Enantioselectivity.

γ	Obstruction factor for molecular diffusion.
ϵ	Interparticle porosity.
$\varepsilon_o, \varepsilon_r$	Permittivities in vacuum and in medium, respectively.
ϵ_m, ϵ_s	Overall departure term for mobile and stationary phases, respectively.
η	Viscosity.
θ	Fractional surface coverage.
κ	Reciprocal of electric double layer thickness.
λ	Eddy diffusion coefficient.
$\bar{\mu}$	Electrochemical potential.
μ	Chemical potential.
μ	Dipole moment.
ν	Reduced velocity, $d_p u / D_m$.
σ	Standard deviation.
σ_o	Charge density at the surface.
Φ	Ratio of interparticle free volume to total (interparticle plus intraparticle) free volume.
Φ	Electric potential in membrane model.
ϕ	Phase ratio, V_s / V_m.
φ	Ratio of stagnant mobile phase to total mobile phase.
Ψ	Electric potential in Stern model.
Ψ_2	Association factor for liquid diffusion.
ω_α	Ratio of exchange distance (i.e., between velocity extremes) to d_p.
ω_β	Ratio of differential velocity to mean velocity, $\Delta u / u$.
ω_λ	Ratio of persistence of path, S, to d_p.

Appendix B

Courses and conferences attended

In accordance with the University of Edinburgh regulations the following lecture courses and conferences were attended throughout the period of study.

1. EMAS Scribe Course
2. Medicinal Chemistry
3. Surface Chemistry
4. Spectroscopy and kinetics
5. Electrochemistry
6. Chromatography
7. Recent Advances in Physical Chemistry
8. Surfaces and Interfaces
9. Meetings of the East of Scotland HPLC Users Group
10. 18th International Symposium on Chromatography, 1990
11. 15th International Symposium on Column Chromatography, 1991

Bibliography

[1] Tswett, M. S., *Warsaw Soc. Nat. Sci., Biol. Sec.*, 6(1903)14.

[2] Heftmann, E., in *Chromatography*, Heftemann, E., Ed, Reinhold, New York, 1975.

[3] Kuhn, R., Winsterstein, A. and Lederer, E., *Hoppe Seyler's Z. Physiol. Chem.*, 197(1931)141.

[4] James, A. T. and Martin, A. J. P., *Analyst*, 77(1952)915.

[5] Hamilton, P. B., Bogue, D. C. and Anderson, R. A., *Anal. Chem.*, 32(1960)1782.

[6] Giddings, J. C., *Anal. Chem.*, 35(1963)2215.

[7] Davies, M., *Some Electrical and Optical Aspects of Molecular Behaviour*, Pergamon Press, Oxford, 1965.

[8] Wilke, C. R. and Chang, P., *Am. Inst. Chem. Engr. J.*, 1(1955)264.

[9] Carman, P. C., *Flow of Gases through Porous Media*, Butterworths, London, 1956.

[10] Golay, M. J. E., in *Gas Chromatography 1958*, Desty, D. H. Ed., Butterworths, London, 1958.

[11] Kennedy, G. J. and Knox, J. H., *J. Chromatogr. Sci.*, 10(1972)549.

[12] Bristow, P. A. and Knox, J. H., *Chromatographia*, 10(1977)279.

[13] Knox, J. H. and Scott, H. P., *J. Chromatogr.*, 282(1983)297.

[14] Done, J. D. and Knox, J. H., *J. Chromatogr. Sci.*, 10(1972)606.

[15] Knox, J. H. and McLaren, L., *Anal. Chem.*, 36(1964) 1477.

[16] Knox, J. H. and Vasvari, G., *J. Chromatogr.*, 83(1973)181.

[17] Hawkes, S. J., *J. Chromatogr.*, 68(1972)1.

[18] Knox, J. H. and Parcher, J. F., *Anal. Chem.*, 41(1969)1599.

[19] Rigby, M., Smith, E. B., Wakeham, W. A. and Maitland, G. C., *The Forces between Molecules*, Clarendon, Oxford, 1986.

[20] Glueckauf, E., *Disc. Faraday Soc.*, 7(1949)12, 202.

[21] Glueckauf, E., *Analyst*, 77(1952)903.

[22] Horvath, C., Preiss, B. and Lipsky, S. R., *Anal. Chem.*, 39(1967)1422.

[23] Huber, J. F. K. and Hulsman, J. A. R. J., *Anal. Chim. Acta*, 38(1967)305.

[24] Kirkland, J. J., *J. Chromatogr. Sci.*, 7(1969)7.

[25] Martin, A. J. P. and Synge, R. L. M., *Biochem. J.*, 35(1941)1358.

[26] Van Deemter, J. J., Zuiderweg, F. J. and Klinkenberg, A., *Chem. Eng. Sci.*, 5(1956)271.

[27] Giddings, J. C., *Dynamics of Chromatography*, Marcel Dekker, New York, 1965

[28] Grushka, E., Snyder, L. R. and Knox, J. H., *J. Chromatogr. Sci.*, 13(1975)25.

[29] Tswett, M., *Ber. der Deut. Botan. Ges.*, 24(1906)316.

[30] Knox, J. H., *High-Performance Liquid Chromatography*, Edinburgh University Press, Edinburgh, 1978.

[31] Gilbert, M. T., Knox, J. H. and Kaur, B., Chromatographia, 16(1982)138.

[32] Unger, K., Roumeliotis, P., Mueller, H. and Goetz, H., *J. Chromatogr.*, 202(1980)3.

[33] Unger, K., *Anal. Chem.*, 55(1983)361A.

[34] Knox, J. H. and Kaur, B., *Euro. Chromatogr. News*, 1(1987)12.

[35] Bassler, B. J., Kaliszen, R. and Hartwick, R. A., *J. Chromatogr.*, 461(1989)139.

[36] Colin, H., Eon, C. and Guiochon, G., *J. Chromatogr.* , 119(1976)41.

[37] Colin, H., Eon, C. and Guiochon, G., *J. Chromatogr.*, 122(1976)223.

[38] Colin, H. and Guiochon, G., *J. Chromatogr.*, 137(1977)19.

[39] Knox, J. H. and Gilbert, M. T., U. K. patent 7939449, 1979.

[40] Bernal, J. D., *Proc. Roy. Soc. (London)*, A100(1924)749.

[41] Ciccioli, P., Tappa, R., Di Corcia, A. and Liberti, A., *J. Chromatogr.*, 206(1981)35.

[42] Millard, B., Caswell, E. G., Leger, E. E. and Mills, D. R., *J. Phys. Chem.*, 59(1955)876.

[43] Knox, J. H. and Kaur, B., in *High Performance Liquid Chromatography*, Brown, P. R. and Hartwick, R. A. Eds, J. Wiley, New York, 1989.

[44] Application Notes, Shandon Scientific Ltd., Runcorn, 1990.

[45] Wheeler, A., in *Catalysis*, Emmet, P. H. Ed., Vol. 2, Reinhold, New York, 1955.

[46] Bassler, B. and Hartwick, R. A., *J. Chromatogr. Sci.*, 27(1989)162.

[47] Graham, D., *J. Phys. Chem.*, 61(1957)1310.

[48] Di Corcia, A. and Samperi, R., *J. Chromatogr.*, 77(1973)277.

[49] Di Corcia, A. and Samperi, R., *J. Phys. Chem.*, 77(1973)1301.

[50] Di Corcia, A. and Bruner, F., *Anal. Chem.*, 43(1971)1634.

[51] Knox, J. H., Kaur, B. and Millward, G. R., *J. Chromatogr.*, 352(1986)3.

[52] Knox, J. H., Unger, K. K. and Mueller, H., *J. Liquid Chromatogr.*, 6(1983)1.

[53] Kiselev, A. V., Yashin, Y. I., *Gas Adsorption Chromatography*, Plenum, New York, London, 1969.

[54] Tee, P. A. H. and Tonge, B. L., *J. Chem. Educ.*, 40(1963)117.

[55] Hummers, W. S., Jr. and Offeman, R., *J. Amer. Chem. Soc.*, (1958)1339.

[56] McChesney, E. W. and Swann, W. K., Jr., *J. Amer. Chem. Soc.*, 59(1937)1116.

[57] Brunaner, S., Emmett, P. H. and Teller, E., *J. Am. Chem. Soc.*, 60(1938)309.

[58] Ruthven, D. H., *Principles of Adsorption and Adsorption Processes*, John Wiley & Sons, New York, 1984.

[59] James, D. H. and Phillips, C. S. G., *J. Chem. Soc.*, (1954)1066.

[60] Glueckauf, E., *Trans. Faraday Soc.*, 51(1955)1540.

[61] Cremer, E. and Huber, J. R. K., *Angew. Chem.*, 73(1961)461.

[62] Ritchie, H. J., PhD thesis, University of Edinburgh, 1986.

[63] Ajie, H., Alvarez, M. M., Anz, S. J., Beck, R. D., Diederich, F., Fostiropoulos, K., Huffman, D. R., Kratschmer, W., Rubin, Y., Schriver, K. E., Sensharma, D. and Whetten, L., *J. Phys. Chem.*, 94(1990)8630.

[64] Unger, K. K., *Porous Silica*, Elsevier, Amsterdam, 1979.

[65] Langmuir, I., *J. Am. Chem. Soc.*, 40(1918)1361.

[66] Fowler, R. H. and Guggenheim, E. A., *Statistical Thermodynamics*, Cambridge University Press, Cambridge, 1939.

[67] Sternberg, J. C. in *Ad. in Chromatography*, Giddings, J. C. and Keller, R. A. Eds., Vol. 2, Marcel Dekker, New York, 1966.

[68] Colin, H., Guiochon, G. and Jandera, P., *Chromatographia*, 15(1982)133.

[69] Kielland, J., *J. Am. Chem. Soc.*, 59(1937)1675.

[70] Hiemenz, P. C., *Principles of Colloid and Surface Chemistry*, Marcel Detter, New York, 1977.

[71] Helfferich, F., *Ion Exchange*, McGraw-Hill, New York, 1962.

[72] Atkins, P. W., *Physical Chemistry*, Oxford University Press, Oxford, 1986.

[73] Lliel, E. L., *Stereochemistry of Carbon Compounds*, McGraw-Hill, New York, 1962.

[74] Pirkle, W. H. and Pockapsky, T. C., *Chem. Rev.*, 89(1989) 347.

[75] Katoh, H., Ishida, T., Baba, Y. and Kiniwa, H., *J. Chromatogr.*, 473(1989)241.

[76] Poppe, H., *J. Chromatogr.*, 506(1990)45.

[77] Laurie, S. H., in *Comprehensive Coodination Chemistry*, Wilkinson, G. Ed., Vol. 2, Pergamon, Oxford, 1987.

[78] Porath, J. and Flodin, *Nature (London)*, 183(1959)1657.

[79] Moore, J. C., *J. Polym. Sci.*, A2(1964)835.

[80] Schmidt, D. E. Jr., Giese, R. W., Conron, D. and Karger, B. L.,*Anal. Chem.*, 52(1980)177.

[81] Pfeiffer, E., Lu, K. C., Regnier, F. E. and Barth, H. G., *J. Chromatogr. Sci.*, 18(1980)430.

[82] Fischer, E. and Bergell, P., *Ber.*, 35(1902)3779.

[83] Rudorf, W., in *Advances in Inorganic Chemistry and Radiochemistry*, Vol. 1, Academic, New York, 1959.

[84] Hennig, G. R., in *Progress in Inorganic Chemistry*, Vol. 1, Interscience, New York, 1959.

[85] DeVault, D., *J. Am. Chem. Soc.*, 65(1943)532.

[86] Snyder, L. R., *Principles of Adsorption Chromatography*, Dekker, New York, 1963.

[87] Bockris, J. O'M. and Reddy, A. K. N., *Modern Electrochemistry*, Vol. 2, Plenum, New York, 1970.

[88] Grahame, D. C., *Chem. Rev.*, 41(1947)441.

[89] Ogster, A. G., *Nature*, 162(1948)963.

[90] Salem, L., Chapuisat, X., Segal, G., Hiberty, P. C., Minot, C., Leforrestier, C. and Sautet, P., *J. Am. Chem. Soc.*, 109(1987).

[91] Dalgliesh, C. E., *J. Chem. Soc.*, (1952)3940.

[92] Baczuk, R. J., Landram, G. K., Dubois, R. J. and Dehm, H. C., *J. Chromatogr.*, 60(1971)351.

[93] Davankov, V. A., in *Advances in Chromatography*, Giddings, J. C., Ed.,Vol. 18, Marcel Dekker, New York, 1980.

[94] Davankov, V. A., in *Advances in Chromatography*, Giddings, J. C., Ed., Vol. 22, Marcel Dekker, New York, 1983.

[95] Rogozhin, S. V. and Davankov, V. A., *Chem. Commun.*, (1971)490.

[96] Ihrig, H. K. and Porter, C. W., *J. Am. Chem. Soc.*, 45 (1923)1990.

[97] Adams, R. and Ingersoll, A. W., *J. Am. Chem. Soc.*, 44(1922)2930.

[98] Armani, E., Barazzoni, L., Dossena, A. and Marchelli, R., *J. Chromatogr.*, 441(1988)287.

[99] Giddings, J. C., Kucera, E., Russell, C. P. and Myers, M., *J. Phys. Chem.*, 72(1968)4397.

[100] Casassa, E. F., *J. Phys. Chem.*, 75(1971)3929.

[101] Dimonie, M., Schell, H. D., Hubca, G., Mateescu, M. A., Oprescu, C. G., Todireanu, S., Maior, O., Languri, J. and Iosif, M., *J. Macromol. Sci.-Chem.*, A22(1985)729.

[102] Porath, J., Janson, J. and Laas, T., *J. Chromatgr.*, 6(1971)167.

[103] Schomburg, A., Deege, A., Kohler, J. and Brien-Vogelsang, U., *J. Chromatogr.*, 282(1983)27.

[104] Davankov, V. A., Kurganov, A. A. and Ponomareva, T. M., *J. Chromatogr.*, 452(1988)309.

[105] Saunders, K. J., *Organic Polymer Chemistry*, Chapman and Hall, London, 1973, pp. 450-451.

[106] Rothbart, H. L., in *An Introduction to Separation Science*, Karger, B. L., Snyder, L. R. and Horvath, Cs., Eds., John Wiley & Sons, Inc., New York, 1973.

[107] Purnell, H., *Gas Chromatography*, John Wiley & Sons, Inc., New York, 1967.

[108] Oelrich, E., Preusch, H. and Wilhelm, E., *J. High Resolution Chromatogr. & Chromatogr. Communications*, 3(1980)269.

[109] Wernicke, *J. Chromatogr. Sci.*, 23(1985)39.

[110] Knox, J. H. and Pyper, H. M., *J. Chromatogr.*, 363(1986)1.

[111] Knox, J. H. and Shibukawa, M., *J. Chromatogr.*, 545(1991)123.

[112] Kiniwa, H., Baba, Y., Ishida, T. and Katoh, H., *J. Chromatogr.*, 461(1989)397.

[113] Weast, R. C. (Ed.), *Handbook of Chemistry & Physics*, 64th edition, CRC press, Inc., Florida, 1985.